UNIVERSITÀ DEGLI STUDI DI SASSARI

FACOLTÀ DI ARCHITETTURA
Dipartimento di Architettura e Pianificazione

Scuola di Dottorato di Ricerca
Architettura e Pianificazione
Indirizzo: scienza dei materiali e fisica tecnica ed ambientale
XXII CICLO

HYBRID ORGANIC-INORGANIC MATERIALS: FROM SELF-ORGANIZATION TO NANOCRYSTALS

Relatore:
Ch.mo prof. Plinio Innocenzi

Dottoranda
Cristiana Figus

Correlatore:
Ch.mo prof. Masahide Takahashi

Coordinatore della Scuola:
Ch.mo prof. Giovanni Maciocco

A. A. 2008-2009

TABLE OF CONTENTS

ABSTRACT

The advantage of inorganic–organic hybrids is that they can combine the properties of organic and inorganic components in one material; this provides the opportunity to invent new materials with a large spectrum properties. The synthesis of hybrid materials through the precise structure control from the molecular to the macroscopic level is a key point for a variety of applications.

3-Glycidoxypropyltrimethoxysilane (GPTMS) is one of the most common precursors for the preparation of hybrid materials. Important applications have been reported for these materials, for instance as protective layers, antiscratch coatings, anticorrosion coatings and restoration materials; in the photonic field, as optical waveguides, or second order non-linear optical materials.

Hybrids materials commonly synthesized as amorphous, only in few cases hybrid crystals can be obtained; but the practical application as photonics, require optically transparent films.

In the present work we have extended the formation of hybrid crystals to thin films. This represents an important result, several requirements have to be fulfilled, such as optical transparency, and controlling of the properties that are added by nanocrystals.

We have investigated the reactions in highly basic conditions of GPTMS by different techniques. We have presented the possible reaction pathways whose control is necessary to obtain a hybrid material of tunable properties. We have varied some key processing parameters such as aging time and aging temperature, and we have studied how they affect the self-organization process, the silica condensation and epoxy opening reactions.

Finally we have demonstrate that the hybrid films prepared by sol-gel method employed GPTMS as precursors in basic condition can be used for the microfabrication and this open the route to develop new functional materials.

ABSTRACT

Il vantaggio dei materiali ibridi organici-inorganici è che essi combinano in uno stesso materiale le proprietà di un materiale organico e inorganico; questo fornisce l'opportunità di realizzare nuovi materiali con differenti proprietà. La sintesi dei materiali ibridi attraverso un preciso controllo della struttura dal livello molecolare a quello macroscopico, è l'elemento chiave per una varietà di applicazioni.

Il 3-Glycidoxypropyltrimethoxysilane (GPTMS) è uno dei più noti precursori impiegati nella preparazione di materiali ibridi. Sono riportate numerose applicazioni: rivestimenti protettivi, antiscratch, anticorrosione, nel campo del restauro, nel campo della fotonica (guide d'onda o materiali per l'ottica non lineare).

I materiali ibridi solitamente sintetizzati sono amorfi, in alcuni casi però sono stati ottenuti cristalli ibridi in bulk; tuttavia per una loro applicazione, quale in fotonica, sono richiesti su film otticamente trasparenti.

Nel presente lavoro si è ottenuto la formazione di cristalli ibridi su film sottili. Questo rappresenta un importante risultato, diversi requisiti sono stati ottenuti, come la trasparenza ottica e il controllo delle proprietà aggiunte dai nanocristalli ibridi.

E' stata studiata la reazione del GPTMS in condizioni basiche mediante diverse tecniche. Si è descritto il meccanismo di reazione, la cui conoscenza è importante per ottenere un materiale ibrido con proprietà modulabili. Sono stati variati alcuni parametri come temperature e tempo d'invecchiamento, ed è stato studiato come questi incidano sul sulle reazioni di condensazione inorganica e apertura dell'epossido, e sul processo di auto-organizzazione.

Si è infine dimostrato che i film ibridi preparati mediante processo sol-gel dal GPTMS in condizioni basiche, possono essere impiegati nella microfabbricazione e questo apre la strada allo sviluppo di nuovi materiali funzionali.

CHAPTER I

ORGANIC-INORGANIC HYBRID MATERIALS: AN INTRODUCTION

1.1. Introduction

Hybrid materials represent one of the most fascinating developments in materials chemistry in recent years. However, the basic science is sometimes still not understood, therefore investigations in this field in particular to understand the structure–property relationships are crucial[1-9]. Different building blocks and approaches can be used for their preparation and these have to be adapted to bridge the differences of inorganic and organic materials[1]; beside the preparation of hybrid materials, their nano- and microstructure formation, processing and analysis is important.

Recent technological innovation and the request for new functions generate an enormous demand for novel materials. Many of the traditional materials, such as metals, ceramics or organic polymers cannot fulfill all technological requirements for the various new applications. The group of composites[10-17] which are formed by the incorporation of a basic structural material into a second substance, the matrix, show interesting properties. Usually the systems incorporated are in the form of particles, whiskers, fibers, lamellae, or a mesh. Most of the resulting materials show improved mechanical properties and a well-known example is inorganic fiber-reinforced polymers.

The structural building blocks[18-25] in these materials which are incorporated into the matrix are predominantly inorganic in nature and show a size range from the lower micrometer to the millimeter range. Decreasing the size of the inorganic units to the same level as the organic building blocks could lead to more homogeneous materials that allow a further fine tuning of materials' properties on the molecular and nanoscale level, generating novel materials that either show characteristics in between the two original phases or even new properties.

The concepts of bonding and structure in the hybrid materials are intensively studied by many scientists to understand the fundamental processes of their formation and to realize

news and exiting ideas. Different levels of complexity are reached by soft chemical self-assembly mechanisms over a large dimension, which is one of the major challenges of modern materials chemistry.

1.2. Definition of Hybrid Materials

The term hybrid materials[1] is used for many different systems on the wide area of different materials, such as crystalline highly ordered coordination polymers, amorphous sol–gel compounds, materials with and without interactions between the inorganic and organic units. Is possible try to delimit this term by taking into account various concepts of composition and structure[1-9]. We have different possibilities of composition[10-17] and structure of hybrid materials: the matrix can be crystalline or amorphous and organic or inorganic with the building blocks[18-25] as molecule, macromolecules or particle fibers, moreover the nature of the interaction of the components can be strong or weak.

Usually we define one material a hybrid material when two moieties includes are blended on the molecular scale. Commonly one of these compounds is inorganic and the other one organic in nature. A more detailed definition distinguishes between the possible interactions connecting the inorganic and organic species[1]. Class I hybrid materials are those that show weak interactions between the two phases, such as van der Waals, hydrogen bonding or weak electrostatic interactions[1-9]. Class II hybrid materials are those that show strong chemical interactions like a covalent bonding between the components[1-9]. But because of the gradual change in the strength of chemical interactions there is a transition between weak and strong interactions (Figure 1.1)[1].

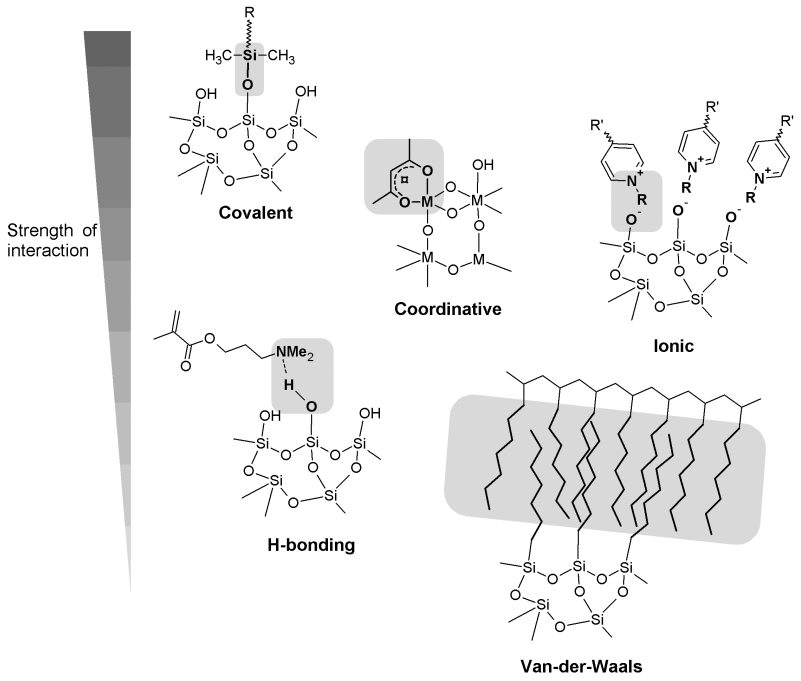

Figure 1.1- Selected interactions typically applied in hybrid materials and their relative strength[1].

In addition to the bonding characteristics structural properties can also be used to distinguish between various hybrid materials. An organic moiety containing a functional group that allows the attachment to an inorganic network, e.g. a trialkoxysilane group, can act as a network modifying compound because in the final structure the inorganic network is only modified by the organic group[1].

Phenyltrialkoxysilanes for example modify the silica network in the sol–gel process via the reaction of the trialkoxysilane group without place additional functional groups designed to produce further chemical reactions to the material formed. If a reactive functional group is incorporated the system is called a network functionalizer (Scheme 1.1c)[1]. If two or three of such anchor groups modify an organic segment we obtain materials in which the inorganic group become an integral part of the hybrid network (Scheme 1.1b)[1].

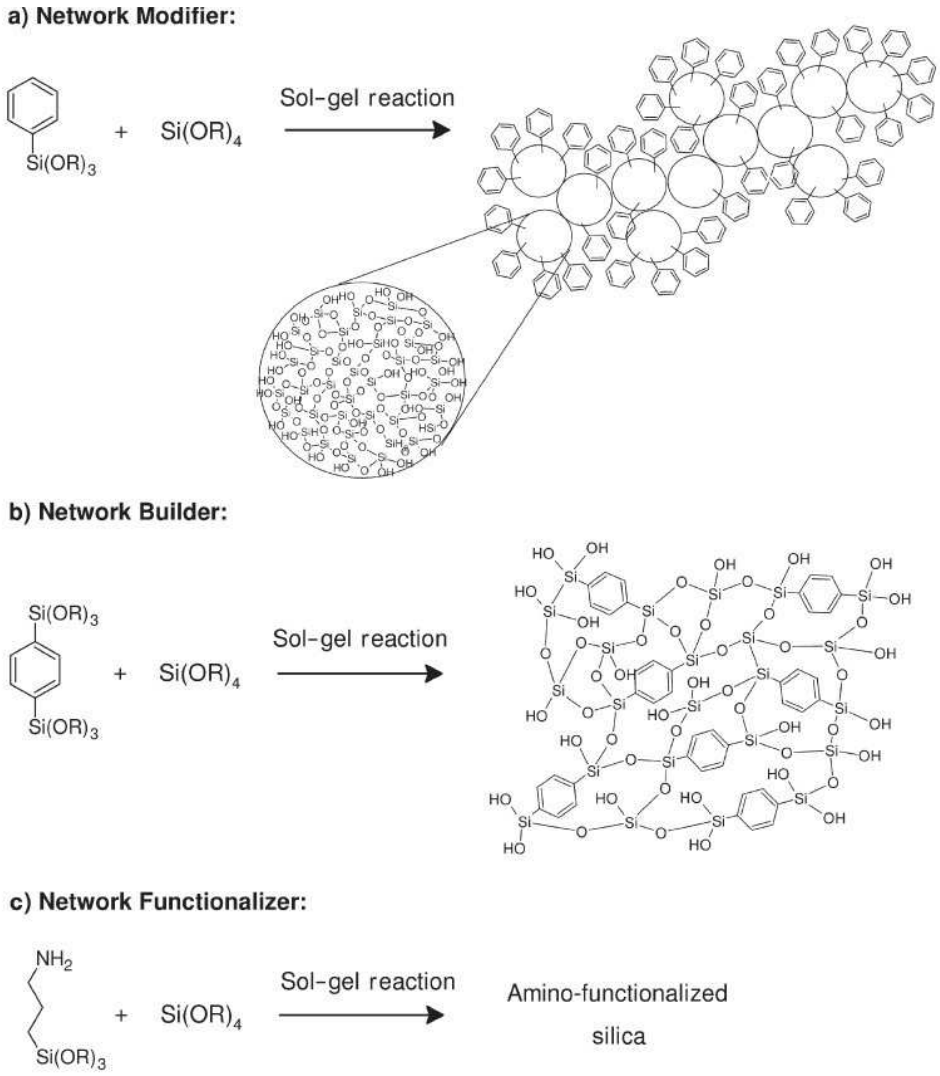

Scheme 1.1 Different role of organically functionalized trialkoxysilanes in the silicon-based sol–gel process[1].

Blends are formed if no strong chemical interactions exist between the inorganic and organic building blocks, for example combination of inorganic clusters or particles with organic polymers (Scheme 1.2a)[1]. If an inorganic and an organic network interpenetrate each other without strong chemical interactions, so called interpenetrating networks are formed (Scheme 1.2b)[1], which is for example the case if a sol–gel material is formed in

presence of an organic polymer or vice versa. Both these materials belong to *class I* hybrids[1-9].

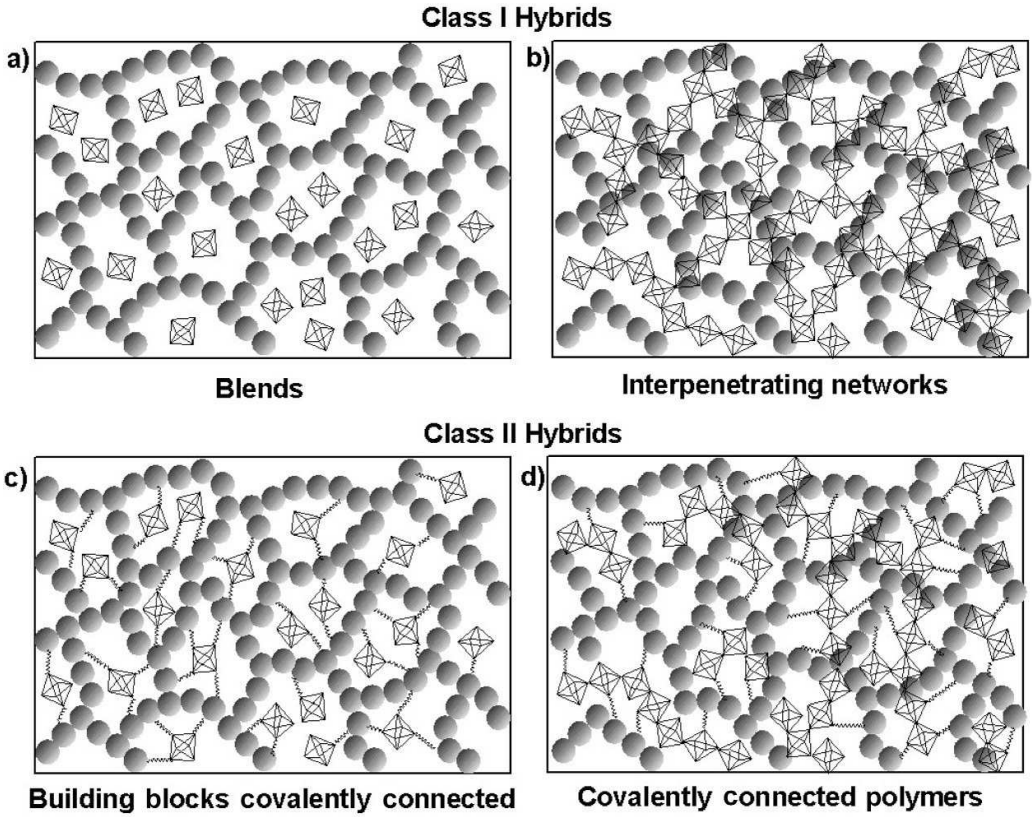

Scheme 1.2 The different types of hybrid materials of the class I and II (Kickelbick 2007).

Class II hybrids are formed when the inorganic components are covalently bonded to the organic polymers (Scheme 1.2c)[1] or inorganic and organic polymers are covalently connected with each other (Scheme 1.2d)[1].

There is a gradual transition between hybrid materials and nanocomposites[10-17] because large molecular building blocks[18-25] for hybrid materials, such as large inorganic clusters, can already be of the nanometer length scale. In fact there is no clear borderline between these materials. The term nanocomposite is used if one of the structural units, either the organic or the inorganic, is in a defined size range of 1–100nm[18-25].

Commonly the term nanocomposites[1] is used if discrete structural units in the respective size regime are used and the term hybrid materials is more often used if the inorganic units are formed *in situ* by molecular precursors, for example applying sol–gel reactions[26-28]. Examples of discrete inorganic units for nanocomposites are nanoparticles, nanorods, carbon nanotubes and galleries of clay minerals[10-17]. Usually a nanocomposite is formed from these building blocks by their incorporation in organic polymers[1].

The transition from the macroscopic world to microscopic, nanoscopic and molecular objects leads, beside the change of physical properties of the material itself, i.e. the so called quantum size effects, to the change of the surface area of the objects[10-17]. While in macroscopic materials the majority of the atoms is hidden in the bulk of the material it becomes vice versa in very small objects; the surface becomes when objects become very small. In small nanoparticles (<10nm) nearly every atom is a surface atom that can interact with the environment[1]. One very important feature of hybrid materials or nanocomposites is their inner interface, which has a direct impact on the properties of the different building blocks and therefore on the materials properties[18-25]. As already explained the nature of the interface has been used to divide the materials in two classes dependent on the strength of interaction between the moieties. If the two phases have opposite properties, such as different polarity, the system would thermodynamically phase separate. The same can happen on the molecular or nanometer level, leading to microphase separation.

1.3. Advantage of organic-inorganic hybrid materials

The most advantage of inorganic–organic hybrids is that they can combine the often properties of organic and inorganic components in one material[1]. Because of the many possible combinations of components this field is very creative, since it provides the opportunity to invent an almost unlimited set of new materials with a large spectrum of known and as yet unknown properties[1-9]. Another driving force in the area of hybrid materials is the possibility to create multifunctional materials. Examples are the incorporation of inorganic clusters or nanoparticles with specific optical, electronic or magnetic properties in organic polymer matrices[1-9].

Another important property of hybrid materials that makes this material class interesting for many applications is their processing[1]. In the case of solid state inorganic materials is required a high temperature treatment for their processing, on the other hand the hybrid materials show a more polymer-like handling, either because of their large organic content or because of the formation of crosslinked inorganic networks from small molecular precursors just like in polymerization reactions. Then these materials can be shaped in any form in bulk and in films; the possibility of their processing as thin films can lead to property improvements of cheaper materials by a simple surface treatment, e.g. scratch resistant coatings[1-9].

Dependent on the composition used the resulting hybrid materials and nanocomposites can shows optical transparency; this makes these materials ideal candidates for many optical applications[9]. Furthermore, the materials building blocks can also deliver an internal structure to the material which can be regularly ordered[29-37]. While in most cases phase separation is avoided, phase separation of organic and inorganic components is used for the formation of porous materials[29-37].

Table 1-Comparison of general properties of typical inorganic and organic materials[1]

Properties	*Organics (polymers)*	*Inorganics (SiO_2, transition metal oxides (TMO))*
Nature of bonds	covalent [C—C], van der Waals, H-bonding	ionic or iono-covalent [M—O]
T_g	low (–120 °C to 200 °C)	high (≫200 °C)
Thermal stability	low (<350 °C–450 °C)	high (≫100 °C)
Density	0.9–1.2	2.0–4.0
Refractive index	1.2–1.6	1.15–2.7
Mechanical properties	elasticity plasticity rubbery (depending on T_g)	hardness strength fragility
Hydrophobicity	hydrophilic	hydrophilic
Permeability	hydrophobic ±permeable to gases	low permeability to gases
Electronic properties	insulating to conductive redox properties	insulating to semiconductors (SiO_2, TMO) redox properties (TMO) magnetic properties
Processability	high (molding, casting, film formation, control of viscosity)	low for powders high for sol–gel coatings

The many possibilities of the hybrid materials allow to design a smart materials such as materials that react to environmental changes or switchable systems. This open routes to novel technologies[1-9], for example electroactive materials, electrochromic materials, sensors and membranes, biohybrid materials, etc. The desired function can be delivered from the organic or inorganic or from both components. One of the advantages of hybrid materials in this context is that functional organic molecules as well as biomolecules often show better stability and performance if introduced in an inorganic matrix.

1.4. Formation of hybrid materials by different approaches

Usually two different approaches[1] can be used for the formation of hybrid materials, the building block[18-25] approach and the in situ formation of hybrid materials starting from a precursors[26-28]; both this methodologies have their advantages and disadvantages. Either well-defined preformed building blocks are applied that react with each other to form the final hybrid material in which the precursors still at least partially keep their original integrity or one or both structural units are formed from the precursors that are transformed into a new network[26-28]; which means that structural units that are present in these sources for materials formation can also be found in the final material. At the same time typical properties of these building blocks usually survive the matrix formation[18-25], which is not the case if material precursors are transferred into novel materials. Examples of such well-defined building blocks are modified inorganic clusters or nanoparticles with attached reactive organic groups[18-25]. Depending on the number of groups that can interact, these building blocks are able to modify an organic matrix (one functional group) or form partially or fully crosslinked materials (more than one group)[1].

Beside the molecular building blocks mentioned, nanosized building blocks, such as particles or nanorods, can also be used to form nanocomposites[10-17]. The advantage of the building block approach is that the building block is well-defined and usually does not undergo significant structural changes during the matrix formation[1], better structure–property predictions are possible; and the building blocks can be designed in such a way to give the best performance in the materials formation, for example good solubility of inorganic compounds in organic monomers by surface groups showing a similar polarity as the monomers.

The *in situ* formation of the hybrid materials[26-28] is based on the chemical transformation of the precursors used throughout materials' preparation. Typically this is the case if organic polymers are formed but also if the sol–gel process[26-28] is applied to produce the inorganic component. In these cases well-defined discrete molecules are transformed to

multidimensional structures, which often show totally different properties from the original precursors. Generally simple, commercially available molecules are applied and the internal structure of the final material is determined by the composition of these precursors but also by the reaction conditions[26-28]. Therefore control over the latter is a crucial step in this process. Changing one parameter can often lead to two very different materials. If, the inorganic species is for example, a silica derivative formed by the sol–gel process, the change from base to acid catalysis makes a large difference because base catalysis leads to a more particle-like microstructure while acid catalysis leads to a polymer-like microstructure[1-9]. Hence, the final performance of the derived materials is strongly dependent on their processing and its optimization.

Many of the classical inorganic solid state materials are formed using solid precursors and high temperature processes, which are often not compatible with the presence of organic groups because they are decomposed at elevated temperatures[1-9]. Hence, these high temperature processes are not suitable for the *in situ* formation of hybrid materials. Reactions that are employed should have more the character of classical covalent bond formation in solutions. One of the most prominent processes which fulfill these demands is the sol–gel process[26-28]. However, such rather low temperature processes often do not lead to the thermodynamically most stable structure but to kinetic products, which has some implications for the structures obtained. For example low temperature derived inorganic materials are often amorphous or crystallinity is only observed on a very small length scale, i.e. the nanometer range[1-9].

1.5. The sol-gel process

This process is chemically related to an organic polycondensation reaction in which small molecules form polymeric structures by the loss of substituents. Usually the reaction results in a three-dimensional (3-D) crosslinked network[1,26-28]. The fact that small molecules are used as precursors for the formation of the crosslinked materials implies several advantages, for example a high control of the purity and composition of the final

materials and the use of a solvent based chemistry which offers many advantages for the processing of the materials formed.

The silicon-based sol–gel process is probably the one that has been most investigated[26-28]; therefore the fundamental reaction principles are discussed using this process as a model system. One important fact also makes the silicon-based sol–gel processes a predominant process in the formation of hybrid materials, which is the simple incorporation of organic groups using organically modified silanes.

Si—C bonds have enhanced stability against hydrolysis in the aqueous media usually used, which is not the case for many metal–carbon bonds, so it is possible to easily incorporate a large variety of organic groups in the network formed[1]. Principally $R_{4-n}SiX_n$ compounds (n = 1–4, X = OR', halogen) are used as molecular precursors, in which the Si—X bond is labile towards hydrolysis reactions forming unstable silanols (Si—OH) that condensate leading to Si—O—Si bonds[1,26-28]. In the first steps of this reaction oligo- and polymers as well as cyclics are formed subsequently resulting in colloids that define the sol. Solid particles in the sol afterwards undergo crosslinking reactions and form the gel (Scheme 1.3)[1].

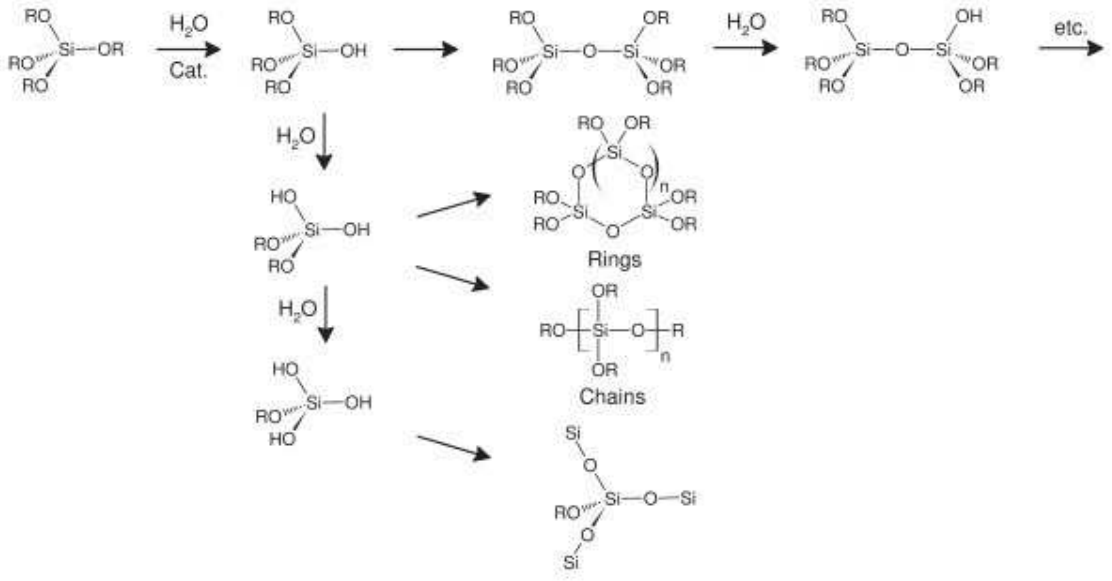

Scheme 1.3 Fundamental reaction steps in the sol–gel process based on tetrialkoxysilanes[1].

The process is catalyzed by acids or bases resulting in different reaction mechanisms by the velocity of the condensation reaction (Scheme 1.4)[1]. The pH used therefore has an effect on the kinetics which is usually expressed by the gel point

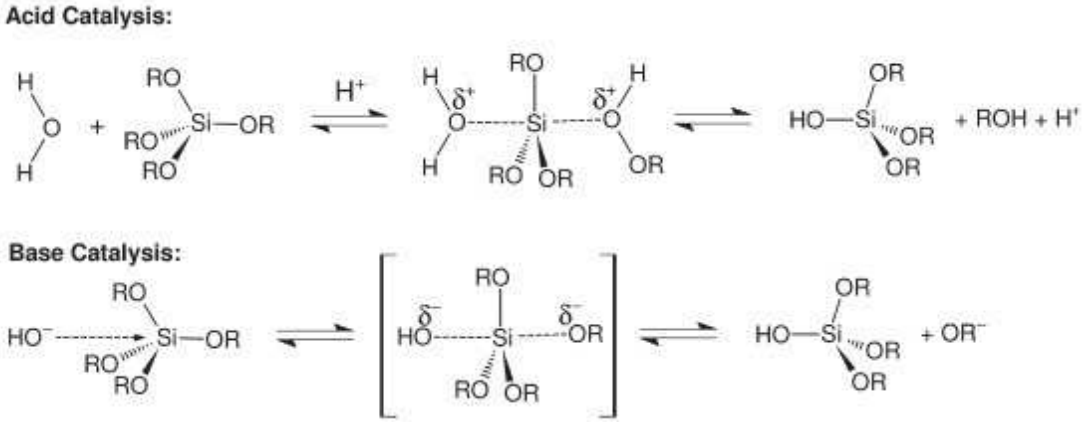

Scheme 1.4 Differences in mechanism depending on the type of catalyst used in the silicon-based sol–gel process[1].

of the sol–gel reaction. The reaction is slowest at the isoelectric point of silica (between 2.5 and 4.5 depending on different parameters) and the speed increases rapidly on changing the pH[1,26-28]. Not only do the reaction conditions have a strong influence on the kinetics of the reaction but also the structure of the precursors. Generally, larger substituents decrease the reaction time due to steric hindrance.

In addition, the substituents play a mature role in the solubility of the precursor in the solvent. Water is required for the reaction and if the organic substituents are quite large usually the precursor becomes immiscible in the solvent. By changing the solvent one has to take into account that it can interfere in the hydrolysis reaction, for example alcohols can undergo *trans*-esterification reactions leading to quite complicated equilibria in the mixture[1]. Then for a well-defined material the reaction conditions have to be fine-tuned.

The pH not only plays a major role in the mechanism but also for the microstructure of the final material[26-28]. Applying acid-catalyzed reactions an open network structure is formed in the first steps of the reaction leading to condensation of small clusters afterwards. Contrarily, the base-catalyzed reaction leads to highly crosslinked sol

particles already in the first steps. This can lead to variations in the homogeneity of the final hybrid materials. Commonly used catalysts are HCl, NaOH or NH4OH, but fluorides can be also used as catalysts leading to fast reaction times.

The transition from a sol to a gel is defined as the gelation point[1,26-28], which is the point when links between the sol particles are formed to such an extent that a solid material is obtained containing internal pores that incorporate the released alcohol. However at this point the reaction has not finished, but condensation reactions can go on for a long time until a final stage is reached. This process is called ageing[1,26-28]. During this reaction the material shrinks and stiffens. This process is carried on in the drying process, where the material acquires a more compact structure and the associated crosslinking leads to an increased stiffness. During the drying process the large capillary forces of the evaporating liquids in the porous structure take place which can lead to cracking of the materials[1]. Reaction parameters such as drying rate, gelation time, pH, etc. can have a major influence on the cracking of the gels and have therefore to be optimized[1,26-28]. Under some circumstances the destruction of the gel network can lead to the formation of powders instead of monoliths during materials formation.

Stress during the drying process can be avoided if the liquid in the pores is exchanged under supercritical conditions where the distinction between liquid and vapor no longer exists. This process leads to so-called highly porous aerogels compared with the conventionally dried xerogels[1].

Because many parameters influence the speed of the sol–gel reaction[26-28]; if a homogeneous material is required all parameters must be optimized. This is particularly true if hybrid materials are the target, because undesired phase separations of organic and inorganic species in the materials or between the network and unreacted precursors weaken the materials' properties. The water to precursor ratio is also a major parameter in the sol–gel process[1]. If tetraalkoxysilanes are used as precursors, two water molecules per starting compound are necessary to form completely condensed SiO_2. Applying a lower H_2O/Si ratio, would lead to an alkoxide containing final material[1].

In the nonhydrolytic sol-gel process the reaction between metal halides and alkoxides is used for the formation of the products. The alkoxides can be formed during the process by various reactions. Usually this process is carried out in sealed tubes at elevated temperature but it can also be employed in unsealed systems under an inert gas atmosphere.

Metal and transition-metal alkoxides are generally more reactive towards hydrolysis and condensation reactions compared with silicon. The metals in the alkoxides are usually in their highest oxidation state surrounded by electronegative –OR ligands which render them susceptible to nucleophilic attack[1]. Transition metal alkoxides show a lower electronegativity compared with silicon which causes them to be more electrophilic and therefore less stable towards hydrolysis in the sol–gel reactions[26-28].

More sterically demanding alkoxides, such as isopropoxides, lead to a lower degree of aggregation and smaller alkoxides, such as ethoxides or *n*-propoxides, to a larger degree of aggregation[1]. In addition, the length of the alkyl group in the metal alkoxides also influences their solubility in organic solvents, for example ethoxides often show a much lower solubility as their longer alkyl chain containing homologs.

The M—C bonds in metal alkoxides[1,26-28] are in most cases not stable enough to survive the sol–gel conditions. Therefore, contrary to the silica route, other mechanisms have to be employed if it is desired that hybrid inorganic–organic metal oxide materials be formed in a one-step approach, for example the use of organically functionalized bi- and multidentate ligands[1] that show a higher bonding stability during the sol–gel reaction and, reduce the speed of the reaction by blocking coordination sites.

1.6. The hybrid materials by sol-gel process

Organic molecules other than the solvent can be added to the sol and become physically entrapped in the cavities of the formed network upon gelation. For this purpose the molecules have to endure the reaction conditions of the sol–gel process, namely the aqueous conditions and the pH of the environment. Hence, functional organic groups that

can be hydrolyzed are not tolerated, but a partial tolerance for the pH can be obtained if the sol–gel reaction is carried out in a buffer solution. This is particularly necessary if biological molecules, such as enzymes, are to be entrapped in the gel[1]. Physical entrapment has the disadvantage that sometimes the materials obtained are not stable towards phase separation or leaching because of differences in polarity. Chemical modification of organic compounds with trialkoxysilane groups can partially avoid such problems due to co-condensation during the formation of the sol–gel network and thus development of covalent linkages to the network[1].

While the formation of homogeneous materials with a chemical link between the inorganic and organic component is in many cases the preferred route, there are cases where a controlled phase separation between the entrapped organic molecules and the sol–gel material is compulsory for the formation of the material, for example in the preparation of mesoporous materials[29-37].

Besides the entrapment of organic systems, precursors with hydrolytically stable Si—C bonds can also be used for co-condensation reactions with tetraalkoxysilanes[1-9].

In addition, organically functionalized trialkoxysilanes can also be used for the formation of 3-D networks alone forming so called silsesquioxanes (general formula R-$SiO_{1.5}$) materials[1]. Generally a 3-D network can only be obtained if three or more hydrolyzable bonds are present in a molecule. Two such bonds generally result in linear products and one bond leads only to dimers or allows a modification of a preformed network by the attachment to reactive groups on the surface of the inorganic network (Figure 2)[1]. Depending on the reaction conditions in the sol–gel process smaller species are also formed in the organo-trialkoxysilane based sol–gel process, for example cage structures or ladder-like polymers (Figure 2)[1-9]. Because of the stable Si—C bond the organic unit can be included within the silica matrix without transformation[1]. There are only a few Si—C bonds that are not stable against hydrolysis, for example the Si—C ≡ C bond where the Si— C bond can be cleaved by H_2O if fluoride ions are present. Some typical examples

for trialkoxysilane compounds used in the formation of hybrid materials are shown in Scheme 1.5. Usually the organic functionalizations have a large influence on the properties of the final hybrid material. First of all the degree of condensation of a hybrid material prepared by trialkoxysilanes is generally smaller than in the case of tetraalkoxysilanes and thus the network density is also reduced.

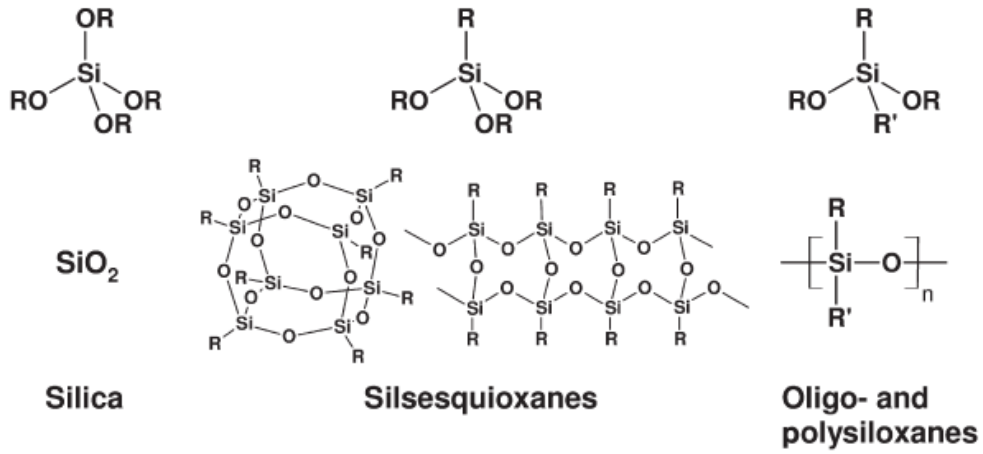

Figure 1.2 Formation of different structures during hydrolysis in dependence of the number of organic substituents compared to labile substituents at the silicon atom[1].

In addition, the functional group incorporated changes the properties of the final material, for example fluoro-substituted compounds can create hydrophobic and lipophobic materials, additional reactive functional groups can be introduced to allow further reactions such as amino, epoxy or vinyl groups (Scheme 1.5)[1]. Beside molecules with a single trialkoxysilane group also multifunctional organic molecules can be used.

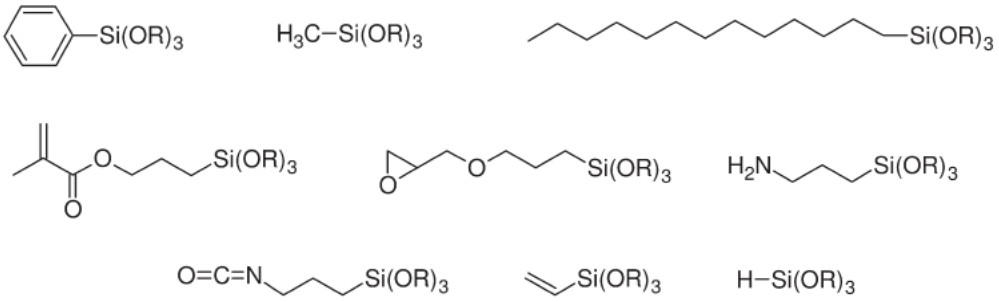

Scheme 1.5 Trialkoxysilane precursors often used in the sol–gel process[1].

Compared with other inorganic network forming reactions, the sol–gel processes show mild reaction conditions and a broad solvent compatibility[1,26-28]. These two characteristics offer the possibility to carry out the inorganic network forming process in presence of a preformed organic polymer or to carry out the organic polymerization before, during or after the sol–gel process. The properties of the final hybrid materials are not only determined by the properties of the inorganic and organic component, but also by the phase morphology and the interfacial region between the two components. The often dissimilar reaction mechanisms of the sol–gel process and typical organic polymerizations, such as free radical polymerizations, allow the temporal separation of the two polymerization reactions which offers many advantages in the material formation.
If a porous 3-D inorganic network is used as the inorganic component for the formation of the hybrid material a different approach has to be employed depending on the pore size[29-37], the surface functionalization of the pores and the stiffness of the inorganic framework. In many cases intercalation of organic components into the cavities is difficult because of diffusion limits. Several porous or layered inorganic materials have already been used to prepare hybrid materials and nanocomposites[10-17]. Probably the most studied materials, class in this respect is that of two-dimensional (2-D) layered inorganic materials that can intercalate organic molecules and if polymerization between the layers occurs even exfoliate, producing nanocomposites. Contrary to intercalated systems the exfoliated hybrids only contain a small weight percentage of host layers with no structural order.
Contrary to the layered materials, which are able to completely delaminate if the forces produced by the intercalated polymers overcome the attracting energy of the single layers, this is not possible in the case of the stable 3-D framework structures, such as zeolites, molecular sieves and M41S-materials[1]. The composites obtained can be viewed as host–guest hybrid materials[10-17].
Simultaneous formation of the inorganic and organic polymers can result in the most homogeneous type of interpenetrating networks. Usually the precursors for the sol–gel process are mixed with monomers for the organic polymerization and both processes are

carried out at the same time with or without solvent. Applying this method, three processes are competing with each other[1]: (a) the kinetics of the hydrolysis and condensation forming the inorganic phase, (b) the kinetics of the polymerization of the organic phase, and (c) the thermodynamics of the phase separation between the two phases. Tailoring the kinetics of the two polymerizations in such a way that they occur simultaneously and rapidly enough, phase separation is avoided or minimized.

One problem that also arises from the simultaneous formation of both networks is the sensitivity of many organic polymerization processes for sol–gel conditions or the composition of the materials formed.

It is often also necessary to optimize the catalytic conditions of the sol–gel process[1,26-28]. It is known, for example, that if the silicon sol–gel process is used basic catalysis leads to opaque final materials while the transparency can be improved if acidic conditions are used. This is most probably due to the different structures of the silica species obtained by the different approaches. While base catalysis leads to more particle-like networks that scatter light quite easily, acid catalysis leads to more polymer-like structures. Of course not only these parameters play a role for the transparency of the materials but also others such as the refractive index difference between organic polymer and inorganic species.

1.7. Organic alkoxide precursors

A very clever route towards hybrid materials by the sol–gel process is the use of precursors that contain alkoxides (figure 1.5)[1] which also can act as monomers in the organic polymerization. The released alkoxides are incorporated in the polymers as the corresponding alcohol while the sol–gel process is carried out (Scheme 1.3 and 1.4)[1]. This leads to hybrid materials and nanocomposites with reduced shrinkage and high homogeneity.

1.8. Example of chemical design

In recent years many building blocks[18-25] have been synthesized and used for the preparation of hybrid materials. Chemists can design these compounds on a molecular

scale with highly sophisticated methods and the resulting systems are used for the formation of functional hybrid materials. Many future applications, in particular in nanotechnology, focus on a bottom-up approach in which complex structures are hierarchically formed by these small building blocks[1].

Two methods are used for the synthesis of such surface-functionalized molecular building blocks[1]: either the surface groups are grafted to a pre-formed cluster ("post-synthesis modification" method) or they are introduced during the cluster synthesis ("*in-situ*" method).

Beside pure metal clusters and nanoparticles an interesting class of materials are metal oxides, because they have interesting magnetic and electronic properties often paired with low toxicity[1]. Simple easy-to-synthesize oxidic compounds are silicon-based systems such as silica particles or spherosilicate clusters, therefore these systems are often used as model compounds for the class of metal oxides, although they do not really represent the class of transition metal oxides that are probably more often used in technological relevant areas. Silica particles or spherosilicate clusters both have in common that the surface contains reactive oxygen groups that can be used for further functionalization (Figure 4)[1]. Mono-functional polyhedral silsesquioxane (POSS) derivatives of the type $R R7Si_8O_{12}$ (R = functional group, R = nonfunctional group) are prepared by reacting the incompletely condensed molecule $R7Si_7O_9(OH)_3$ with $RSiCl_3$. The eighth corner of the cubic closo structure is inserted by this reaction, and a variety of functional organic groups R can be introduced, such as vinyl, allyl, styryl, norbornadienyl, 3-propyl methacrylate, etc (Figure 1.3a). The incompletely condensed compounds $R_7Si_7O_9(OH)_3$ are obtained when certain bulky groups R (e.g. cyclopentyl, cyclohexyl, *tert*.-butyl) prevent the formation of the closo structures from $RSiX_3$ precursors and lead to the precipitation of open-framework POSS. These bulky substituents not only lead to open framework structures but also increase the solubility of the inorganic units in organic solvents. The closed cubic systems still show the high solubility whichmaterials.

Beside pure metal clusters and nanoparticles an interesting class of materials

are metal oxides, because they have interesting magnetic and electronic properties often paired with low toxicity

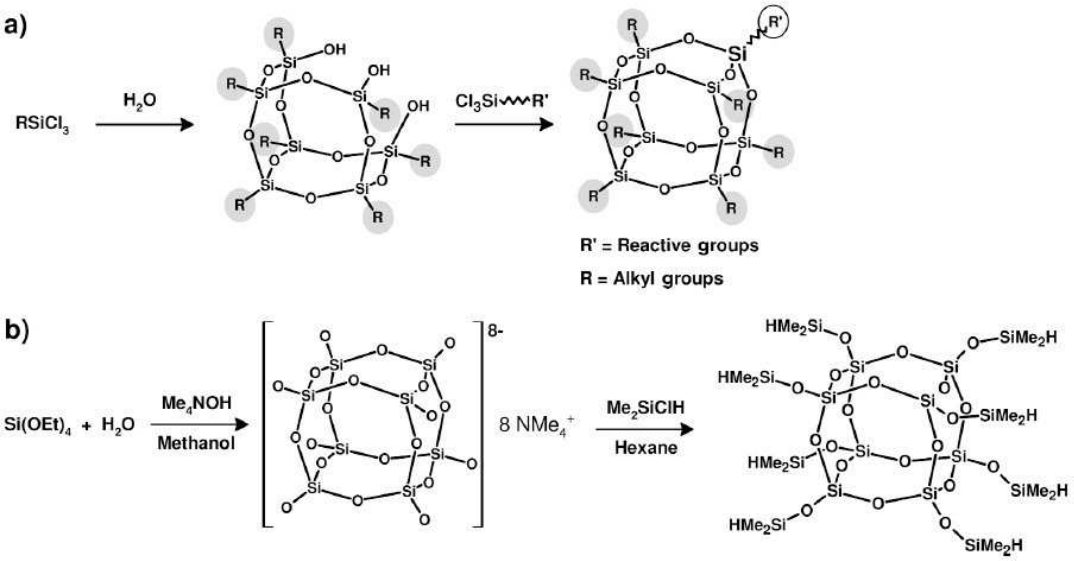

Figure 1.3 Preparation of various well-defined silicon-based building blocks[1].

is necessary if the inorganic building blocks are to be incorporated in an organic environment for the functionalization of organic materials. The simple handling of these systems caused their boom in the preparation of hybrid materials. Other popular silsesquioxanes that have been prepared are the octahydrido- or the octavinyl-substituted molecules, which offer eight reactive sites[18-25]. While the preparation of these systems is still very costly not least because of the low yields of the targeted products, another building block is much easier to obtain, namely spherosilicates. The polyhedral silicate species [O-SiO3/2]n n− are commonly prepared by hydrolysis of Si(OR)4 in the presence of quaternary ammonium hydroxide (Figure 1.3b). The best investigated compound is the cubic octamer (n = 8, "double fourring", D4R). Spherosilicates are obtained from inorganic silica sources and can be considered the smallest piece of silica. The length of a Si—O—Si edge in the D4R structure is approximately 0.3nm and the diameter of the cluster (Si—Si distance) 0.9nm. Therefore the molecules can be considered sub-nanometer particles or – including the organic groups – particles in the low nanometer range. The anionic oxidic surface of the species $[SiO_{5/2}]n\ n-$ mimics the surfaces of

larger silica particles, and therefore the polyhedral silicate clusters are also model systems for (nano)particles. After functionalization usually eight reaction sites are attached to these silica cores. Some typical reactions lead to the attachment of initiating or polymerizable groups at the corners and therefore the resulting clusters can be used as multifunctional initiators for polymerizations or as crosslinking monomers.

In the case of silica-based building blocks typically surface OH-groups are reacted with so-called silane coupling agents of the general composition $R_4 – nSiXn$ (n = 1–3; R = functional or nonfunctional organic group; X = halide or OR') to form stable covalent bonds .These molecules contain reactive Si—Cl or Si— OR groups that react with surface Si—OH groups to form stable Si—O—Si bonds[1].

Another way to attach functional groups to the surface of a preformed building block is the exchange of surface groups similar to the above mentioned ligand exchange on gold clusters.

Silsesquioxanes with only one substitution pattern at each silicon atom are typical examples for the *in situ* formation of functionalized building blocks[18-25]. As mentioned above they are prepared by the hydrolysis and condensation of trialkoxy- or trichlorosilanes, thus they contain inherently one functional group that is also present in the final material. Depending on the reaction procedure either ladderlike polymers or polyhedral silsesquioxanes (POSS) are obtained. The polyhedral compounds [RSiO3/2]n can be considered silicon oxide clusters capped by the organic groups R.

Polyhedral silsesquioxanes $[RSiO_{3/2}]n$ are obtained by controlled hydrolytic condensation of $RSiX_3$ (X = Cl, OR') in an organic solvent. There is a high driving force for the formation of polyhedral rather than polymeric compounds, particularly if the precursor concentration in the employed solvent is low (when the concentration is increased, increasing portions of network polymers may be formed).

Which oligomers are produced and at which rate, depends on the reaction conditions, such as solvent, concentration of the monomer, temperature, pH and the nature of the organic group R. The main parameter[1] that controls the mutual arrangement of the $[SiO_4]$ and $[RSiO_{3/2}]$ building blocks[18-25] is the pH. It was shown that upon sol–gel processing of

$RSi(OR')_3$ / $Si(OR')_4$ mixtures (with nonbasic groups R) under basic conditions Si(OR')4 reacts first and forms a gel network of agglomerated spherical nanoparticles. The $RSi(OR')_3$ precursor reacts in a later stage and condenses to the surface of the pre-formed silica nanoparticulate network[1].

1.9. Hybrid materials by templating approach

Templates for the synthesis of hybrid materials can be preformed structures such as dendrimers or nanoparticles that form 2-D or 3-D ordered structures[29-37]. Furthermore the supramolecular self-organization of single molecules into larger 2-D and 3-D structures can also be employed as a template.

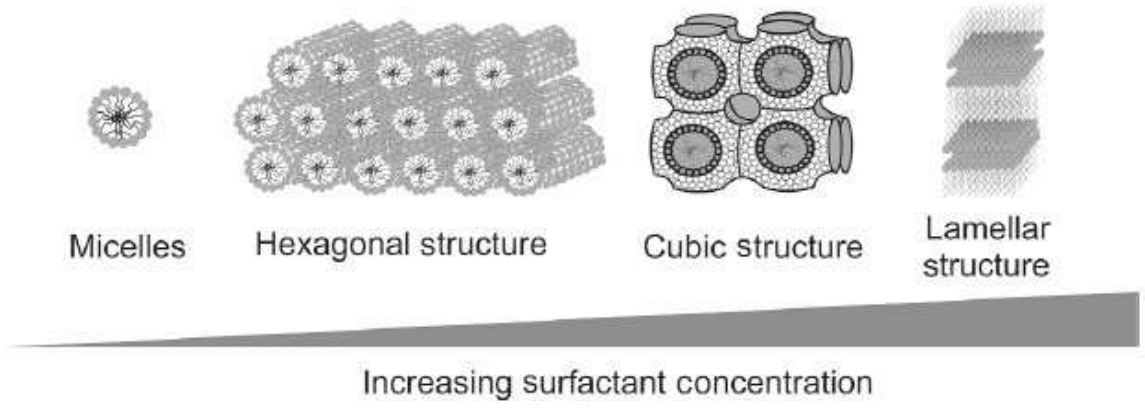

Figure 1.4 Examples of ordered 3-D structures obtained by supramolecular self-assembly of surfactant molecules[1].

One example is the application of amphiphilic surfactants that organize into micelles and more complicated 3-D arrangements such as hexagonal arranged rod-like structure, cubic interpenetrating networks or lamellar structures (Figure 1.4)[1]. The latter are notusually used for structural engineering because they collapse after removal of the template[29-37]. The structures formed, that are dependent on parameters such as the concentration of the surfactants in the solvent, the temperature and sometimes the pH, consist of hydrophobic and hydrophilic regions and the interfaces between them which are applied in the

formation of solid materials, primarily by sol–gel process (Fig. 1.16)[1]. As long as the organic surfactants are still incorporated in the formed inorganic matrix the materials can be considered as inorganic–organic hybrid materials. After removal of the template which commonly occurs by calcinations at temperatures above 450°C, the materials are purely inorganic in nature[29-37]. Probably the most prominent example of the use of single organic (macro)molecules and their 3-D assembly as templates for inorganic and hybrid materials is the use of surfactants in the formation of nano- and mesostructured materials porous materials[1]. The silicate or metal oxide walls of the mesoporous materials were substituted by hybrid materials formed by bridged silsesquioxanes and so-called periodically mesoporous organosilicas(PMOs) were formed [1,29-37]. Colloids with narrow size distributions can order in 3-D objects so-called colloidal crystals. Most of the time latex or silica colloids are used for the preparation of such 3-D objects, because they can be prepared quite easily over different length scales and with the desired size distribution[1]. They are crystallized in structurally well-ordered three-dimensional colloidal crystals that resemble the packing of atoms on a smaller scale. Because similar spheres can only fill the room by a close packing up to 74% the voids can be infiltrated by inorganic or organic reactive

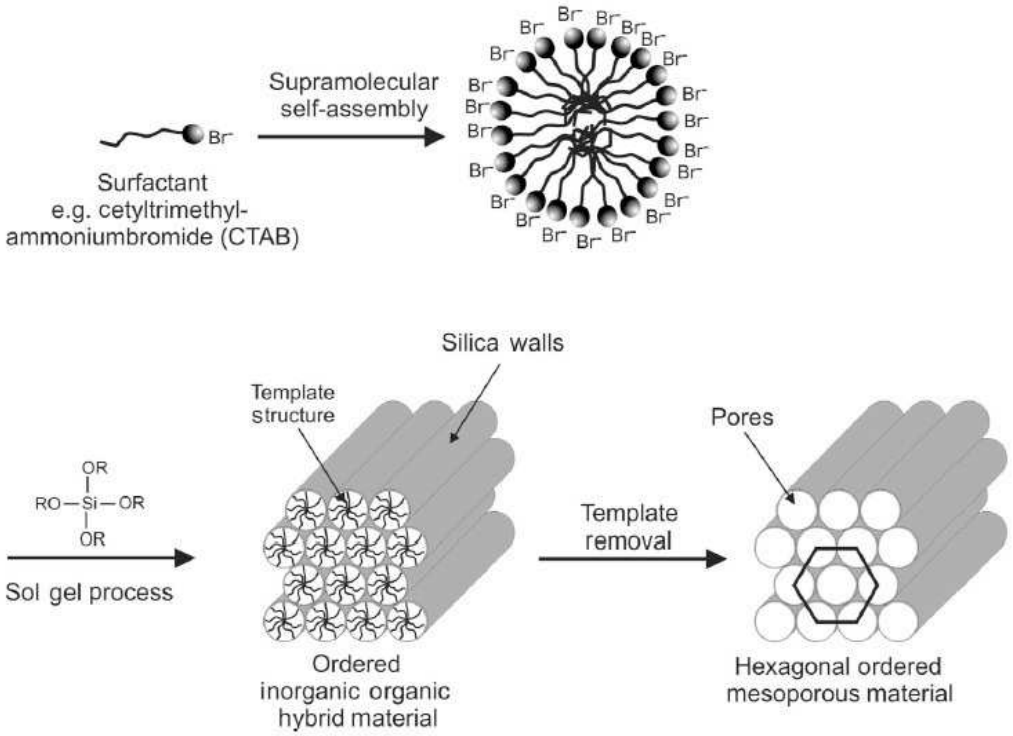

Figure 1.5 Formation of well-ordered mesoporous materials by a templating approach[1].

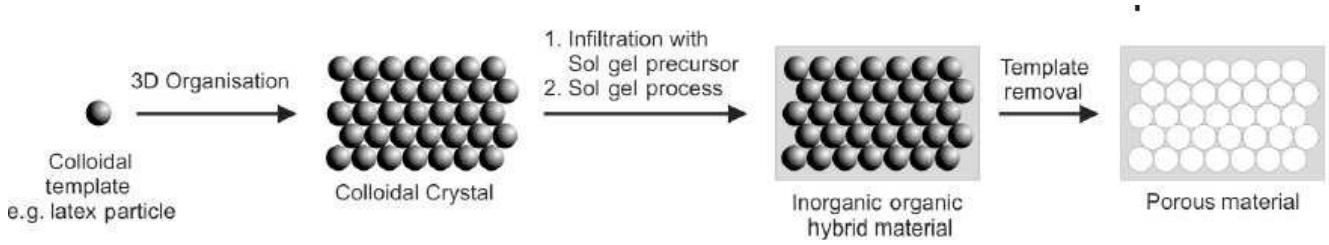

Figure 1.5 Colloidal crystal templating[1].

species, such as materials precursors, clusters or smaller nanoparticles and a hybrid material is formed. Generally the templates are afterwards removed and porous materials are formed (Figures 1.4, 1.5)[1]. Many other methods can be used for the controlled

preparation of nanometer structures such as soft lithography, the use of nanoscale pores, for example in anodic alumina membranes, etc.

1.10. Structural control by top-down and bottom-up approach

Two different techniques can be identified for a structural control on the nanometer length scale: the top-down and the bottom-up approach[1]. The top-down approach forms the nanostructures from larger objects by physical or chemical methods and is more engineering-related, while the bottom-up approach relies on self-organization (also called self-assembly) of molecules or nanometer sized compounds[1-9]. The latter process is for many scientists the more elegant way to form large complex hierarchical structures. Think about the possibilities, for example if you have a liquid that contains your precursors and if you paint a support, it forms a hierarchical structure form the molecular over the nanometer to the macroscopic level over several hundred of square meters. This requires a detailed insight into many fundamental chemical and physico–chemical properties of the building blocks that should self assemble. In a bottom-up approach many reaction details have to be understood and controlled[1,18-28]. Therefore, this process, although very promising, is yet only understood for quite small molecules and there are only some promising techniques that can already be applied for large scale technological applications[1-9].

One of them is definitely the self-organization of block copolymers and their use in creating specific reaction environments. Self-assembly is the major principle of the controlled formation of structural building blocks[18-25]. It means nothing other than the spontaneous organization of unorganized systems to a complex structure, which is first of all an art to break and generate specific interactions and to work against entropy[1]. There are several basic principles that have to be taken into account for a self-assembly process: the structure and shape of the building blocks, their interactions like the attractive and repulsive forces, their interactions with solvents, the environment where the reaction is carried out and diffusion processes. The balance between these principles is something

which has to be set to create the desired structures[1]. Two principles are employed in the synthesis of hybrid materials, the self-assembly of the building blocks[18-25] of the material itself and the use of templates[29-37] that can self-assemble and form a shape which is applied in the preparation of a material. Such templates are used in technology since a long time, for example as porogenes but it was only recently that they found a widespread use in the formation of hybrid materials[1].

1.11 Film formation

An important area with respect to potential applications of hybrid materials[1-9] and nanocomposites[10-17] is the ability to design these materials on several length scales, from the molecular to the macroscopic scale. Because the processing of hybrid materials is more similar to that of organic polymers than to classical inorganic materials, such as ceramic or metal powders, based on the solvent-based chemistry behind the materials there is a variety of methods that can be adapted for their processing on the macroscopic scale. One has to distinguish between different applications to identify the best processing strategies. Thin films and coatings are generally formed by dip or spin coating[26-28], fibers are formed by spinning techniques and bulk materials are usually obtained if the often liquid precursors are simply poured into forms and curing is carried out. These techniques are used for the macroscopic processing of the materials, the molecular and microstructuring is obtained by a variety of other techniques.

One problem that has to be addressed in many of the macroscopic processing techniques in particular if the materials, such as the sol–gel network or the organic polymer in a hybrid are formed during the processing, is the problem of shrinkage. While in bulk materials this problem can be handled, it is more serious when films are applied on surfaces. At the interface between the coating and the support that does not follow the shrinkage considerable forces can appear that lead to inhomogeneities and cracks in the materials[1]. As already mentioned this problem is particularly observed when the polymers or networks are formed during the processing, therefore often hybrid materials or nanocomposites are formed using preformed building blocks such as oligo- or

polymers and clusters or nanoparticles to reduce this effect. However in many cases shrinkage can not totally avoided because the materials processing is usually based on solvents that are evaporated during processing.

Besides the macroscopic processing and the tailoring of the materials on a molecular scale, control of the nanometer structures is one of the major issues in the preparation of hybrid materials and nanocomposites. Many future technologies rely on hierarchically well-ordered materials from the micro- to the nanoscale[1]. Applying the building block approach the structure of course is already engineered by the shape and distribution of the building blocks in the matrix[1]. For example a homogeneous distribution of nanoparticles in an organic polymer has different properties than a material where the particles are agglomerated or where nanorods instead of nanoparticles are used. In addition to this building block based structural engineering the microstructure can often be influenced in hybrid materials similar to organic polymers, for example using lithographic techniques.

References

1 G. Kickelbick, *Hybrid Materials. Synthesis, Characterization, and Applications*. Wiley-VCH, 2007

2 Special issue of *J. Mater. Chem.* 2005, *15*, 3543–3986.

3 P. Gómez-Romero, C. Sanchez , *Functional Hybrid Materials*, Wiley-VCH, Weinheim, 2004.

4 G. Schottner,. *Chem. Mater.* 2001, *13*, 3422–3435.

5 C. Sanchez, G. J. de A.A. Soler –Illia, F.Ribot, T. Lalot, C.R. Mayer, V. Cabuil, *Chem. Mat*. 2001, 13, 3061-3083.

6 G. Kickelbick, U. Schubert, *Monatsh. Chem.* 2001, *132*, 13.

7 K.-H. Haas, *Adv. Eng. Mater.* 2000, *2*, 571–582.

8 C. Sanchez, F. Ribot, B. Lebeau,. *J. Mater. Chem.* 1999, *9*, 35–44.

9 K. G. Sharp,. *Adv. Mater.* 1998, *10*, 1243–1248.

10 Special issue of *J. Nanosci. and Nanotechn.* 2006, *6*, 265–572.

11 R. M. Laine, *J. Mater. Chem.* 2005, *15*, 3725–3744.

12 A. Usuki, N. Hasegawa, M. Kato. *Adv. Polym. Sci.* 2005, *179*, 135–195

13 B. C. Sih, M. O. Wolf, *Chem. Comm.*2005, *3375-3384.*

14 C. Sanchez, B. Julian, P. Belleville, M. Popall, *J. Mater. Chem*. 2005, *15*, 3559–3592.

15 P. Gómez-Romero, K. Cuentas-Gallegos, M. Lira-Cantu, N. Casan-Pastor, *J. Mater. Sci.* 2005, *40*, 1423–1428.

16 G. Kickelbick. *Progr. Polym. Sci.* 2003, *28*, 83–114.

17 Special issue of *Chem. Mater.* 2001, *13*, 3059–3910.

18 D. Y. Godovsky, *Adv. Polym. Sci.* 2000, *153*, 163–205.

19 J. Wen, G. L. Wilkes, Garth L. *Chem. Mater.* 1996, *8*, 1667–1681.

20 G. J. de A. A. Soler-Illia, L. Rozes, M. K. Boggiano, C. Sanchez, C.-O. Turrin, A.-M. Caminade, J.-P. Majoral, *Angew. Chem. Int. Ed.* 2000, *39*, 4249–4254.

21 J. L. Hedrick, T. Magbitang, E. F. Connor, T. Glauser, W. Volksen, C. J. Hawker, V. Y. Lee, R. D. Miller,. *Chem. – Europ. J.* 2002, *8*, 3308–3319.

22 J. W. Kriesel, T. D. Tilley, *Adv. Mater.* 2001, *13*, 1645–1648

23 P. R. Dvornic, C. Hartmann-Thompson, S. E. Keinath, E. J. Hill, *Macromolecules* 2004, *37*, 7818–7831.

24 R. W. J. Scott, O. M. Wilson, R. M. Crooks, *J. Phys. Chem. B* 2005, *109*, 692–704.

25 V. Castelvetro, C. De Vita, Cinzia. *Adv. Coll. Interf. Sci.* 2004, *108–109*, 167–185. Ranch, 2004.

26 C. J. Brinker, G. W. Scherer, *Sol-Gel Science: The Physics and Chemistry of Sol-Gel Processing*, Academic Press, London, 1990.U. Schubert, N. Hüsing , A. Lorenz, *Chem. Mater.*1995, 7, 2010-2027.

27 U. Schubert, N. Hüsing , A. Lorenz, *Chem. Mater.*1995, 7, 2010-2027.

28 A.Varshneya, *Fundamentals of Inorganic Glasses,* Accademic Press. Inc. 1994

29 A. Sayari, S. Hamoudi. *Chem. Mater.* 2001, *13*, 3151–3168.

39 F. Hoffmann, M. Cornelius, J. Morell, M. Fröba, *J. Nanosci. Nanotechnol.* 2006, *6*, 265 288.

31 J-L. Shi, Z.-L. Hua, L.-X. Zhang, *J. Mater. Chem.* 2004, *14*, 795–806.

32 R. Gangopadhyay, A. De,. *Chem.Mater.* 2000, *12*, 608–622.

33 C. J. Brinker, Y. Lu, A. Sellinger, H. Fan, *Adv. Mater.* 1999,*11*, 579–585.

34 N. Hüsing, U. Schubert. *Angew. Chem. Int. Ed.* 1998, *37*, 22–45.

35 A. Sayari, S. Hamoundi. *Chem. Mat.*2001, 13, 3151-3168.

36 F. Hoffmann, M. Cornelius, J. Morell, M. Froba, *J. Nanosci. Nanotechnol.*2006, 6, 265-288.

37 B. Hatton, K. Landskron, W. Whitnall, D. Perovic, G.A. Ozin, *Acc. Chem. Res*.2005, 38, 305-312.

CHAPTER II

APPLICATIONS OF HYBRID MATERIALS

2.1. Introduction

There is almost no limit to the combinations of inorganic and organic components in the formation of hybrid materials. Therefore materials with novel composition– property relationships can be generated that have not yet been possible, and many of the properties and applications are dependent on the properties of the precursors. Based on the increased importance of optical data transmission and storage, optical properties of materials play a major role in many high-tech applications. The materials used can reveal passive optical properties, which do not change by environmental excitation, or active optical properties such as photochromic (change of color during light exposure) or electrochromic (change of color if electrical current is applied) materials. Both properties can be incorporated by building blocks with the specific properties, in many cases organic compounds, which are incorporated in a matrix. Hybrid materials based on silicates prepared by the sol–gel process and such building blocks reveal many advantages compared with other types of materials because silica is transparent and if the building blocks are small enough, does not scatter light, and on the other hand organic materials are often more stable in an inorganic matrix. One of the most prominent passive features of hybrid materials already used in industry are decorative coatings obtained for example, by the embedment of organic dyes in hybrid coatings. Another advantage of hybrid materials is the increased mechanical strength based on the inorganic structures. Scratch-resistant coatings for plastic glasses are based on this principle. One of the major advantages of hybrid materials is that it is possible to include more than one function into a material by simply incorporating a second component with another property into the material formulation. In the case of scratch-resistant coatings, for example, additional hydrophobic or antifogging properties can be introduced. One of the advantages of hybrid materials, namely, their quite simple processing into coatings and thin films, applying such coatings to cheaper supports can be advantageous. Silica is preferred as the inorganic component in such

applications because of its low optical loss. Other inorganic components, for example zirconia, can incorporate high refractive index properties, or titania in its rutile phase can be applied for UV absorbers. Functional organic molecules can add third order nonlinear optical (NLO) properties and conjugated polymers, conductive polymers can add interesting electrical properties. Nanocomposite based devices for electronic and optoelectronic applications include light-emitting diodes, photodiodes, solar cells, gas sensors and field effect transistors. While most of these devices can also be produced as fully organic polymer-based systems, the composites with inorganic moieties have important advantages such as the improvement of longterm stability, the improvement of electronic properties by doping with functionalized particles and the tailoring of the band gap by changing the size of the particles. The enhancement of mechanical and thermal properties of polymers by the inclusion of inorganic moieties, especially in the form of nanocomposites, offers the possibility for these materials to substitute classical compounds based on metals or on traditional composites in the transportation industry or as fire retardant materials for construction industry. Medical materials are also one typical application area of hybrid materials, as their mechanical properties can be tailored in combination with their biocompatibility, for example nanocomposites for dental filling materials.

Composite electrolyte materials for applications such as solid-state lithium batteries or supercapacitors are produced using organic–inorganic polymeric systems formed by the mixture of organic polymers and inorganic moieties prepared by sol–gel techniques. In these systems at least one of the network-forming species should contain components that allow an interaction with the conducting ions. This is often realized using organic polymers which allow an interaction with the ions, for example via coordinative or by electrostatic interactions. One typical example is proton conducting membranes which are important for the production of fuel cells. The application of hybrid composites is interesting for these systems because this membrane is stable at high temperatures compared with pure organic systems. The advantages of sol-gel-derived hybrid materials and the steady improvement of knowledge with respect to their mechanical, electrical, and optical properties have already been demonstrated by several well-established

industrial application[1] and numerous application oriented research activities all over the world. Meanwhile an increasing number of industrial research groups and startup companies dealing with hybrid materials seem to indicate a major breakthrough of the technology.

2.2. Properties and applications of hybrid materials

2.2.1. Mechanical properties

Hybrid materials can be employed as abrasion Resistant Coatings for Plastics. Hard poly(methylsiloxane)s and related colloidal silica containing coating formulations have been developed several decades ago and still find industrial application in improving the wear and abrasion resistance of engineering plastics, e.g. on top of headlights of cars made from polycarbonate (PC) or side windows in busses made from poly(methyl methacrylate) (PMMA). The nanostructural character of many sol-gel-derived hybrids can be described by the term nanocomposite, whereby the filler is transparent (<100 nm). The latter constituents are either formed in situ by cohydrolysis of slowly reacting organo(alkoxy)- silanes in the presence of main group or transition metal alkoxides as described above or incorporated during sol-gel processing[2,3]

Due to their highly cross-linked nature, these components are hard and, therefore, improve the scratch and abrasion resistance of hybrid coatings to a level well above the typical values of purely organic materials These outstanding mechanical properties together with the high transparency of these hybrids and their processability at low temperatures are the background for their industrial use in protecting soft materials like transparent plastics. Most of the industrial companies involved in the ophthalmic lens business worldwide nowadays are used to produce thermosetting films on top of polymeric lenses (CR 39, polycarbonate, poly(methyl methacrylate) etc.) by wet chemical techniques[4,5].

The lenses are coated via spin- or dip-coating in large quantities.

One of the first hybrid sol-gel systems developed for CR 39 (n_D = 1.498) was developed by sol-gel processing of GPTMS, TMOS, and titaniumtetraethylate (Ti(OEt)4, incorporation of the titanium alkoxideprecursor (20 mol %) resulted in a higher refractive index (n_D = 1.533) of the coating and in a fast curing behavior even for polymeric lenses of low thermal stability[1,6,7].

The improved mechanical stability of the hybrid coatings vs the noncoated hard resin lens can be visualized by semiquantitative, application-oriented standard test procedures.

Similar results have been achieved on polycarbonate (PC) substrates equipped with UV-curable hybrid coatings and were correlated with indentation methods[8]. The transparent PC showed microhardness values of 125 (±3) MPa, whereas the coatings demonstrated microhardnesses up to 220 (±10) MPa.

The correlation of these data with composition and microstructural features of the hybrid nanocomposites presents one major task for further optimization and application of such coatings on plastics[9].

The ophthalmic lens market is innovative and highly competitive. In recent years polymer lenses showing high refractive indices (n_D =1.56, 1.60, 1.67) have been commercialized, and therefore, high index coatings are necessary to avoid interference strings appearing with thin coatings and insufficient index matching between coating and substrate. Here, the hybrid sol-gel coatings based on transition metals offer good prospects to develop adhesive, abrasion resistant, transparent, and index-matched materials[10].

A limiting factor in the application of thermally curing hybrids or poly(methylsiloxanes) is the long curing time (several hours) necessary to fully exploit their mechanical properties. Highly promising activities are, therefore, concerned with UV-curable systems and have led to the successful development of a hard coating for plastic substrates made from poly(methyl methacrylate) (PMMA). The hybrid coating material in this case has been derived from vinyltriethoxysilane (VTES,) and (3-mercaptopropyl)triethoxysilane (MPTES,) by cohydrolysis and cocondensation[1,11]

Other developments on polymer lenses concern antireflective and hydrophobic or “easy-to-clean” coatings also derived from hybrid sol-gel type polymers[12].

2.2.2. Barrier properties

The development of hybrid, colored coatings for lead crystal glasses has also shown that the leaching of lead ions out of the glass surface is drastically reduced due to the highly crosslinked nature of the coating material. This results both in a low solubility and a slow diffusion coefficient for the mobile lead ions with respect to the hybrid layer[13]. It is obvious from these experimental results that hybrid sol-gel coatings might be able to protect metals from corrosive stresses, especially if the corrosion is initiated by chemical reagents, e.g., chlorine ions in salt spray test facilities. Comparatively few reports have appeared describing the application of sol-gel-derived inorganic and hybrid coatings on top of metals, such as stainless steel[14], aluminum alloys[15], bronze,[16] and brass[1].

Figure 2.1- Stainless steel substrate coated by spraying of an abrasion resistant, fluorinated hybrid coating (lower part), demonstrating the "easy-to-clean" aspect[18].

There have been preliminary results concerning structure- property relationships in the anticorrosive behavior of the coatings[17], but the research field of sol-gel coatings on metals seems to be still in its infancy, despite the fact that the application on brass has already been commercialized[1]. The perspectives for industrial use might be higher, if thin hybrid sol-gel coatings are used as an interlayer between the metal surface and

conventional protective coatings resulting in higher layer thicknesses and less corrosive stress implied directly onto the hybrid sol-gel film. For reasons of cost, the hybrid film has to combine several functions that cannot be achieved with conventional organic or inorganic coatings alone. Figure 2.1 shows a fully transparent, abrasion resistant and oleophobic hybrid sol-gel coating on top of stainless steel that is equipped with a fluorinated silane to achieve water repellent and easy-to-clean properties on this mechanically and chemically very sensitive metal surface.

The low-temperature processing conditions of the solgel hybrids and their fast curing behavior enables one to perform coil coating processes and to apply thin films on metal sheets or polymeric foils. These properties are necessary prerequisites to commercialize hybrid barrier coatings[18]. The barrier effect of thin (5-10 μm) hybrid layers with respect to the permeation of hydrocarbons through high-density polyethylene (HDPE) substrates has been described long ago[1]. Very low permeability values have been recognized and were attributed to the synergistic cooperation of the inorganic and organic moieties present in the coatings derived from GPTMS or MAPTMS and ASB.

Thin hybrid sol-gel coatings in combination with SiOx layers produced by vacuum coating techniques on polymeric packaging materials, such as poly(ethylene terephthalate) (PET), have been successfully developed to reduce the permeation rate of oxygen to very low values (<0.05 cm3/m2 d bar)[19]. The structural requirements for low permeation rates of oxygen are a high condensation degree of the inorganic part of the hybrid material and also a high degree of polymerization of the epoxy moieties of the GPTMS present in the coating material[20]. Despite the fact that several sometimes conflicting parameters have to be controlled to achieve high barrier effects against oxygen and water, the hybrid polymers offer a very good chance to realize transparent, abrasion resistant, fast curing, and impermeable coatings for food packaging applications.

2.2.3. Electrical properties.

Most hybrids are highly isolating materials due to the nonionic nature of the individual precursors and the neutral reaction conditions of the sol-gel process. Typically, specific

bulk electrical resistivities of 10^{13}-10^{16} Ω•cm can be achieved. This insulating behavior, together with the high adhesion to various surfaces via Si-OH groups and the possibility to use conventional photoresist technologies to form microstructural patterns, is the basis for their use as passivation and dielectric layers in microelectronic applications[1,21].

Nevertheless, the selection of appropriate organo- (alkoxy)silane precursors also allows to reduce the high bulk or surface resistivities to about 10^8 Ω•cm[22] . Coatings exhibiting surface resistivities in this range are useful to reduce electrostatic charging of transparent plastics, e.g., on windows or touch panels integrated in heavy duty industrial machinery. The easy removal of electrostatic charges prevents the plastic sheets from soiling and consequently reduces cleaning and maintenance intervals, thereby increasing the lifetime of the soft plastic sheets. The APTES is one precursor used in coatings for this application. The coatings have to meet the additional requirements of scratch and abrasion resistance as well as perfect transparency, functions that can hardly be achieved with organic materials.

A further increase in the conductivity of hybrids can be realized by reducing the glass transition temperature of the material to values far below room temperature.

Hybrids derived from TMOS and poly(ethylene glycol)s (PEG) of low molecular weight (200-600) have been used as constituents for hosting Li+ ions, which were introduced by addition of LiClO4 during sol-gel processing[23]. The Tg values ranged from -74 (PEG200) to -50 °C (PEG600); i.e., they increased with higher molecular weight of the organic polymer. Concurrently, the ionic conductivity decreased from 5.3 × 10-5 to 1.8 × 10-5 S/cm at room temperature, thus demonstrating the influence of the mobility of the polymeric chains, which are bonded to an inorganic backbone and with their freely dangling ends serve to solubilize and transport the metal cations.

Were realized interesting work by incorporating Li+- salts in hybrid inorganic-organic polymers based on GPTMS and MAPTMS copolymerized with epoxy functional polyethers[24].[25]

2.2.4. Optical properties

Decorative and functional coatings for glasses.

The glasslike transparency of many sol-gel-based inorganic or hybrid materials has rendered them candidates to modify glasses by applying thin coatings. The proper adhesion of the above-described molecular hybrids or nanocomposites to plastic substrates is a critical aspect. Sometimes, especially on nonpolar substrates like polycarbonate or polyolefins, a primer layer or physical

pretreatment is required. On glass surfaces the situation is completely different due to the presence of SiOH groups[26], which can react with their counterparts in the sol-gel-based materials. Figure 2.2 visualizes the idealized model of modifying a silicate-based inorganic material with a hybrid sol-gel coating[1]. This situation, in most cases, precludes adhesion problems and has stimulated intense research and development efforts to modify glasses by transparent, functional inorganic or hybrid sol-gel coatings[27].

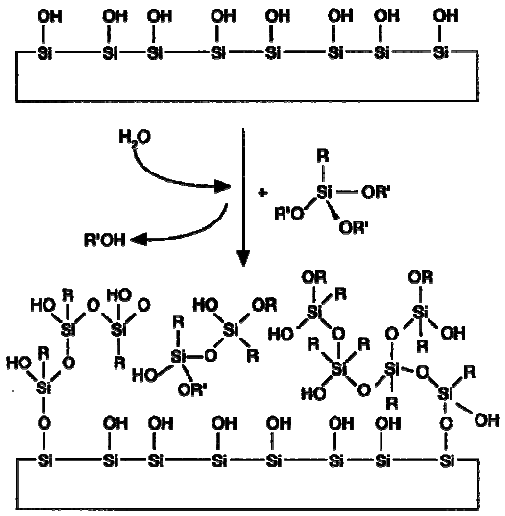

Figure 2.2. Schematic drawing visualizing the adhesion mechanism of hybrid sol-gel coatings on glass surfaces[1].

Thereby, the mechanical (good adhesion to glass and plastics, abrasion resistance), optical (high transparency), and processing advantages (stepwise transformation of a thermoforming resinous matrix to a thermoset, fairly hard matrix) of sol-gel-derived

hybrid polymeric resins have been combined with a topographical modification to create novel optical features (refractive index gradient, antireflective surface).

One more traditional aspect is the coloration of glasses via hybrid coatings. On glass surfaces a coating derived from GPTMS, ASB, and PhTMS has shown excellent adhesion, abrasion resistance, and chemical stability[28]. Commercially available organic dyes can be dissolved in the respective sols, and colored coatings are obtained by spraying the sol onto the glass[1] The incorporation of hydrophobic organic epoxy resins copolymerizing with the functional groups present as substituents in the GPTMS improves the chemical stability of the cured coating against alkaline media, thereby imposing on the coating sufficient stability in dishwashing machines. Figure 2.3gives an impression of the high optical quality of coated glassware[1,30]. The method is highly flexible, either enabling the partial coating of objects or complete coloration. The broad color range of organic dyes is now available to achieve fashionable and new articles, which cannot be manufactured by traditional means. The procedure is environmentally friendly and also cost-effective in comparison to the laborious traditional coloration techniques via molten glass batches containing toxic transition metal oxides. Dye-doped transparent hybrid sol-gel coatings containing organic dyes, in particular their silylated derivatives, are also in use on container glasses[1].

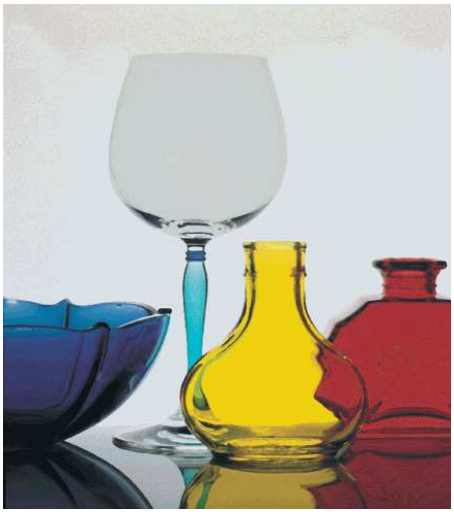

Figure 2.3-Glassware demonstrating the high quality optical appearance of crystal glass and other types of glasses after being spray coated with colored, sol-gel-derived hybrids[1].

Colored glass bottles have been commercially available in Japan since 1999.[1] They are coated via a combined dipping and rotating process by sols consisting of co-condensates of TMOS, titanium tetraisopropylate, VTES, and MAPTMS. Intense coloration is achieved by entrapping of nanosized organic pigments. A two-step UV and thermal curing process is performed in a special coating plant[1] .One major advantage of the coloration by organic dyes or pigments is the recyclability of the glass containers due to complete degradation of the organic constituents at high temperatures.

Figure 2.4-Easy to recycle colored glass bottles coated by hybrid organic-inorganic materials[1].

These hybrid coatings (figure 2.4)[1,29,30] can not only give access to a wide variety of colors, thus enhancing the consumer appeal, but also allow an improvement of the mechanical properties of glass bottles. Moreover, these dye-colored bottles are easy to recycle as

uncolored glass (these materials do not need color-classifcation recycling), because, unlike conventional glass bottles, their coloration does not arise from transition metals that are very difficult to remove on remelting.

Photoactive coatings and systems.

Hybrid nanocomposites present a paramount advantage for facilitating integration, miniaturization, and multifunctionalization of devices, opening a land of opportunities for

applications in the field known as *nanophotonics*[31]. A consequence, there is widespread agreement in the scientific community that active optical applications of hybrid nanocomposites might present the most attractive field to realize applications for the 21st century. Indeed, the exploitation of active optical properties of photoactive coatings and systems is a strong emerging field. For example, hybrid materials with an excellent laser efficiency and good photostability[32], very fast photochromic response[33], very high and stable secondorder nonlinear optical response[34], or acting as original pH sensors[35], electroluminescent diodes[36], or hybrid liquid crystals[37] have been reported in the past five years.

Many examples of functional hybrids exhibiting emission properties (solid-state dye lasers, rare-earth-doped hybrids, electroluminescent devices), absorption properties (photochromic), nonlinear optical (NLO) properties (second-order NLO, photochemical hole burning (PHB), photorefractivity), sensing properties, as well some examples of hybrid-based integrated optical devices are presented.

The hybrid materials show interesting active optical applications[38] .The possible application are in several research areas. The first important property is nonlinear optically active materials and their dynamical behavior[39]; meanwhile, high second order NLO coefficients have been realized[40,41]

Other intresting example of application are cheap, new photoelectrochemical cell based on a chelatingmetal-complex dye and doped TiO_2 nanoparticles has been developed for solar energy conversion[1].

Luminescing hybrids doped with rare earth metal ions or quantum dots have been intensively studied and the structural properties of the host matrix adjusted to achieve large fluorescence quantum yields[42] Hybrid optical switching and data storage devices have been described based on photochromic dyes or photochemical hole burning[42,43]. Sol-gel-based hybrid coatings have been used to detect various species via fiber-optic sensors[44].

The availability of novel methods to generate the required asymmetry (both structural as well as electronic asymmetry) in hybrid inorganic–organic compounds, along with their thermal stability and optical transparency, render them to be candidates for nonlinear

optical (NLO) materials. Structural asymmetry can be easily generated in hybrid frameworks by using acentric or chiral centers (asymmetric linkers, nodes, polar H-bonds, head-to-tail alignment of dipolar guests confined in channels etc) to create structures with polar or chiral space groups. The use of polarizable ligands and metals with efficient donor– acceptor charge transfer (LMCT or MLCT), or 'hard' and 'soft' ligands trans to one another at the metal center, can ensure electronic asymmetry.

2.3. Application to Architecture

Organosilica hybrids, especially in the form of water-based formulations which abate the VOC-content of traditional coating paints, have emerged in the last few years as a broad class of new covering materials capable of serving both traditional requirements of the industry, namely the versatility of organic polymers and the strength and durability typical of inorganic polymers. For instance, the facade of a building painted with one of these new paints containing the sol–gel hybrid formulation (Figure 2.5) recently commercialized by BASF will now retain its fresh aspect for y

Figure 2.5- The new nanobinder Col.9 combines in one product the different advantages of conventional coating types in terms of low dirt pick-up, chalking and rack resistance, and color retention. (www.col9.com)

Indeed there is purpose in using silica-based hybrid coatings as multifunctional coatings that are finding applications in fields ranging from cultural heritage to aircraft protection. These coatings are of special interest since their properties, intermediate between those of polymers and glasses, can deliver specific and unique requirements not afforded by organic polymers and glasses alone. Alternative coating methods such as chemical vapor deposition (CVD, especially used for barrier coatings) are generally energy- and capital-intensive requiring the use of dedicated plants and deposition processes. Silica and organosilica coatings, instead, are obtained under very mild conditions in liquid phase by sol–gel process.

One of the most important drawbacks of classical and new advanced functional materials for outdoor applications, namely in environments with high ultraviolet (UV) irradiation, is the light induced damage that reduces drastically their effective operational lifetime or durability. UV light, either natural or artificial, causes organic compounds to decompose and degrade, because the energy of the photons in UV light is high enough to break chemical bonds.

A thin film, for example, of phenylsilica doped with rhodamine dye obtained from a precursor solution consisting of mixtures of TEOS and PhTES (phenyltriethoxysilane) and ethanol in a 0.7:0.3:1 molar ratio, reduces the UV light reaching the substrate to less than seven per cent of the incident light, whereas the degradation of 20% of the dye molecules is 14 times slower in coated samples, making such a protective coating very attractive for commercial applications[45].

Similarly, the first ORMOSIL-based facade coating on the market (trademarked Col.9 by BASF)[45] is a formulation whose half content is a dispersion of organic plastic polymer particles in which nanoscale particles of silica are incorporated and evenly distributed. Thanks to this combination of elastic organic material and hard mineral, coatings based on this novel nanobinder combine in one product the different advantages of conventional coating types in terms of low dirt pick-up, chalking and crack resistance, and color retention (Figure 2.6)[46]

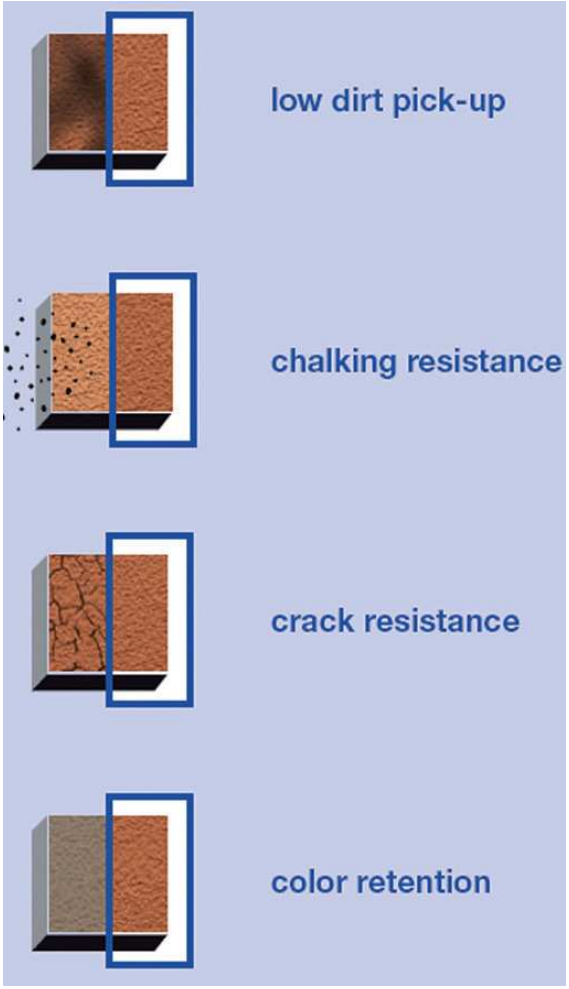

Figure 2.6- Multifunctional properties of surfaces treated with the nanobinder Col.9. (www.col9.com.)

Decorative hybrid coatings are increasingly used on glass, mineral and metal surface sheets. For example, a series of industrial coatings (SC from Hybrid Glass Technologies)[45] are based on ethanol solutions of various silica or alumino-silica based formulations, made available as clear liquids or colored formulations. Spin-, dip- or flow-coating techniques are then used to apply these formulations to flat windows or sandblastedglass substrates (Figure 2.7) to achieve hard 1–10 mm protective coatings for glass that exhibit superior protective anti-staining properties and water repellency when compared to several existing commercial products. Indeed, they form strong chemical bonding with the

Figure 2.7- Decorative hybrid coatings used on glass surface sheets (www.hybridglass.com).

Other application of the hybrid like protective coatiting. In spite of its toxicity carcinogenic Cr(VI) unfortunately remains an essential ingredient in the metal finishing industry for corrosion control[45, 47] Thus its replacement with doped hybrid sol–gel coatings also offers an enormous environmental benefit. Epoxysilica hybrids are well known for their abrasion resistance and low thermal expansion due to the presence of nanostructured bicontinuous domains[45,48] Most recently Safe Marine Nanotechnologies started commercialization of these self-healing anticorrosives for yachts and for large metal vessels. In general, the silicon alkoxides adhere to steel surfaces by chemical binding to iron surface hydroxyls (Fe–OH) formed upon iron oxidation in water (corrosion) resulting in strong adhesion to a ballast paint[45].

Typically, these paints are epoxy-silica hybrids doped with molybdate ions which, taking part in the sol–gel condensation reactions, become part of the inorganic network to be later slowly released as a corrosion inhibitor[45].

In another approach, ZrO_2 nanoparticles are used as a reservoir for the storage and prolonged release of a corrosion inhibitor for aluminium alloys such as cerium ions. The resulting nanostructured doped sol–gel material can be proposed as a potential candidate for substitution of the chromate pretreatments for aluminium alloy AA2024-T3[49]. The films are made from TEOS and GPTMS (3-glycidoxypropyltrimethoxysilane) precursors, doping the hybrid nanosol with ZrO_2 nanoparticles and cerium nitrate as the corrosion inhibitor.

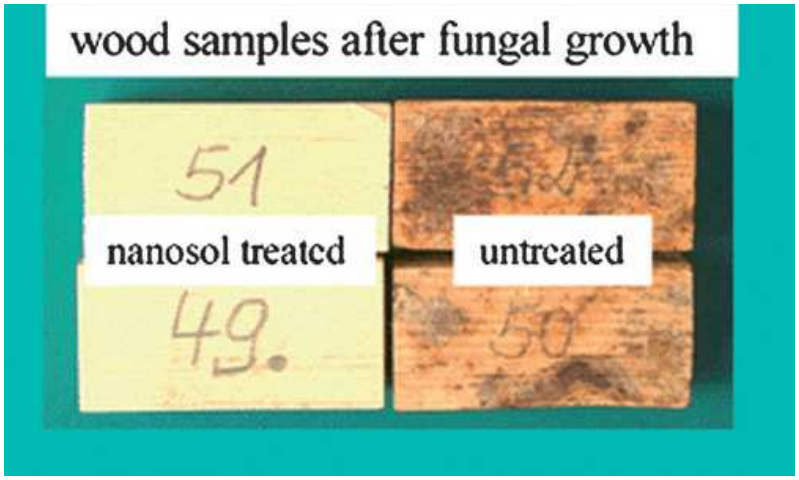

Figure 2.8- Organosilane-based coatings form an almost invisible protective layer on untreated wood surfaces and on weathered and varnished wood surfaces. Dynasylan SIVO 121 produces a strong hydrophobic and oleophobic effect (bottom)[1].

Hydrophobic silane formulations such as those of the waterbased organosilanes line are good surface protection agents for wood[1] (Figure2. 8) as the resulting coating repels both oil (dirt) and water, protects the surface from the effects of weathering, and reduces the growth of microorganisms. The silane formulation does not affect the expansion and contraction behavior of the wood and is therefore particularly suitable for outdoor objects without ground contact. The resulting coating features many relevant properties. The mechanical properties of wood are improved and at the same time the modified silica coating imparts flame retardant, water repellent and antimicrobial properties[50].

The properties of silane-based wood coatings are based on covalent chemical reactions between the silanes and the hydroxyl groups at the wood surface (Figure 2.9)[1]. For the reaction to occur under mild outdoor conditions, the silica has to be modified by using reactive organic groups like epoxysilanes.

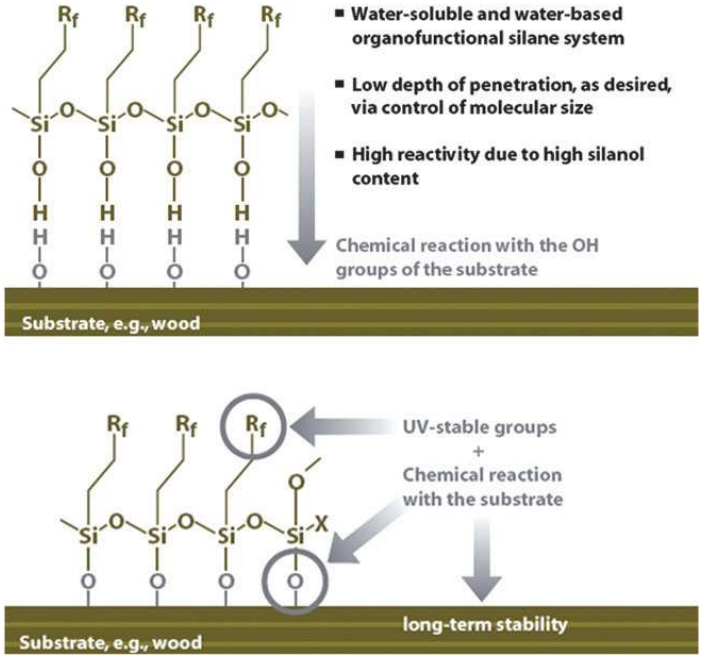

Figure 2.9 Covalent bonding of silanes to the wood's surface ensures durable protectability for all wood surfaces. Optimal treatment of 1 m2 requires 0.1 L Dynasilan, ensuring 3 years protection. (www.specialchem4coatings.com)

With careful selection of the combination of starting alkoxides and appropriate synthesis conditions, the sol–gel technology is now widely applied to the conservation of art objects and cultural heritage.

Sol-gel derived hybrid coatings are also used in art conservation. One of the most striking examples concerns the long-term protection of the 14th century Last Judgment Mosaic situated above the gates of the St. Vitus cathedral in Prague castle[51].

a)

b)

Figure 2.10- The Mosaic of Prague Castle a) Before, b) after hybrid coating [51].

The Last Judgment Mosaic in Prague is a large outdoor panel made from 1 million multicolored glasses, or tesserae, embedded in mortar. This high potassium glass is chemically unstable and since the glass is exposed to harsh weather conditions (high SO2 levels, rain, temperatures varying between -30 ^{o}C and +65 ^{o}C), the alkali reacts with the atmosphere and water to form salt deposits that blurs and corrodes the masterpiece. All organic polymers used in the previous protection attempts have failed to stop corrosion because of their poor durability, poor adhesion to the glass, and large diffusion coefficient for SO2 and water. After reviewing many possible choices the most efficient coating was made from a combination of a hybrid nanocomposite and a fluoropolymer.
The selected coating for treatment of the entire 13 m x 10 m mosaic is a multilayer system composed of a hybrid organic-inorganic functional layer made from organo alkoxysilanes and oxide nanoparticles, placed between the multicolored glass substrate and a fluoropolymer coating (Figure 2.11). This coating combination is a transparent efficient anti-corrosion barrier, much better than all the tested organic polymers[52].

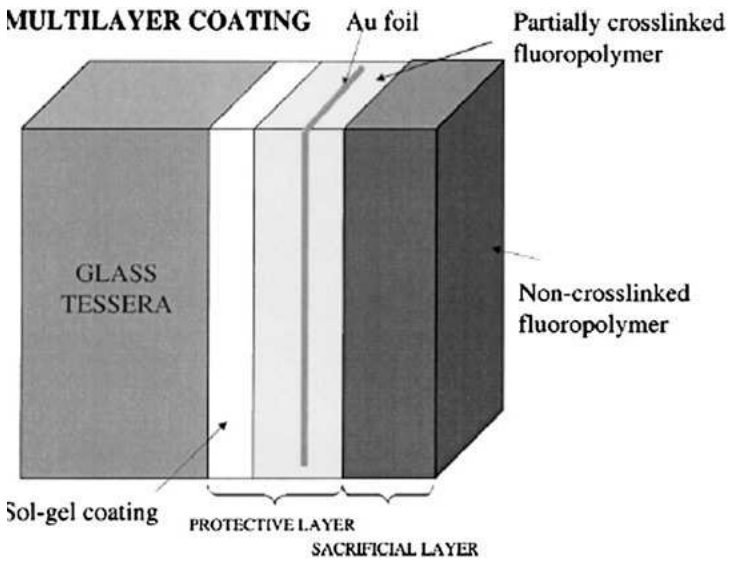

FIGURE 2.11-Schematic cross section of the multi-layer coating used in the long-term protection of the mosaic. The mosaic was originally gilded; therefore, a tiny gold foil is inserted into each tessera[51].

It consists of a protective coating (one sol–gel layer derived from epoxy silanes and methyl silanes, coated with a partially crosslinked functionalized fluoropolymer) and a

sacrificial, removable coating consisting of the same fluoropolymer, non-crosslinked, which is removed and re-applied periodically. The sol–gel layers underneath the top polymer layer are estimated to last for 25 years. Beyond the long term stability under severe ageing conditions, the advantage of such materials compared to polymers lies in their ability to adhere to many substrates, the possibility of making thicker coatings than with purely inorganic sol–gel systems, and their ease of application using a brush (by hand in order to avoid coating the interstitial spaces between tesserae) followed by curing at 90 ^{o}C for twohours using large infrared lamps.

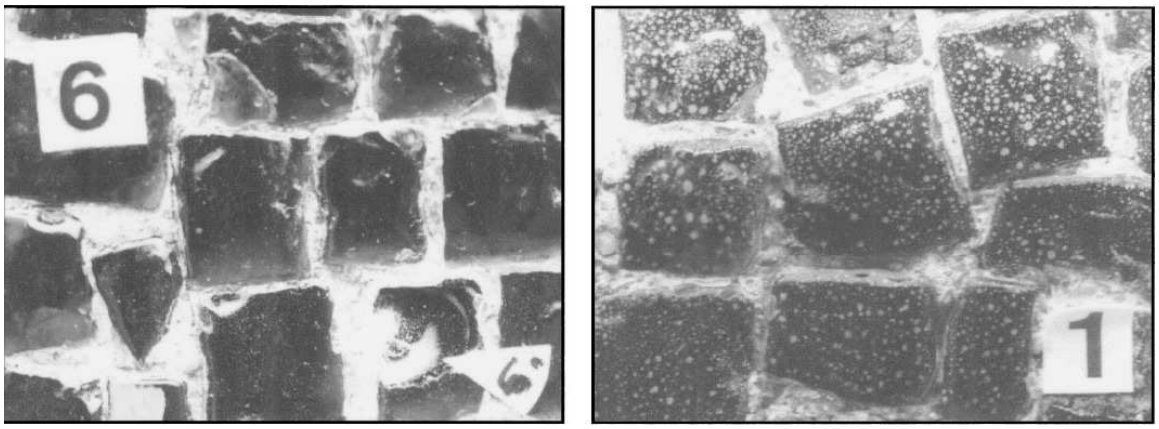

Figure 2.12- On site testing after 2 years of outdoors exposure. Left is the sol-gel/functionalized fluoropolymer coating combination. Right is an epoxy polymer exhibiting onset of delamination[51].

Figure 2.12 shows the difference in test field appearance between an epoxy polymer coating and the sol-gel/fluoropolymer coating after two years of outdoors exposure.

References

1 M. Pagliaro, R. Ciriminna, G. Palmisano, *J. Mat. Chem*., 2009, 19, 31 16-3126; G. Schotter, *Chem. Mater*. 2001, 13, 3422-3435;

2 Schmidt, H. K.; E. Geiter,; M. Mennig,; H. Krug,; C. Becker,; R.-P Winkler,. *J. Sol-Gel Sci. Technol.* 1998, 13, 397.

3 M. Templin, U. Wiesner, H. Spiess, W. *Adv. Mater*. 1997, 9, 814.

4 M. Pagliaro, R. Ciriminna, G. Palmisano, *J. Mat. Chem*., 2009, 19, 31 16-3126.

5 Chaffin, R. *Opt. World* 1997, 8

6 H. Schmidt, B. Seiferling, G. Philipp, K Deichmann,. *In Ultrastructure Processing of Advanced Ceramics*; Mackenzie, J.D., Ulrich, D. R., Eds.;Wiley: Chichester, England, 1988; p 651.

7 G. Philipp, H. Schmidt, *J. Non-Cryst. Solids* 1986, 82, 31

8 J. M. Urreaga, M. C., Matias, V. Lorenzo, M. U. de la Orden, *Mater. Lett*. 2000, 45, 293.

9 J. Wen, V. J. Vasudevan, G. L Wilkes,. *J. Sol-Gel Sci. Technol*. 1995, 5, 115.

10 B. Wang, G. L. Wilkes, J. C. Hedrick, S. C. Liptak, McGrath, *J. E. Macromolecules* 1991, 24, 3449.

11 M. Pagliaro, R. Ciriminna, G. Palmisano, *J. Mat. Chem*., 2009, 19, 31 16-3126;

K. Rose,. *InOrganosilicon Chemistry II*; Auner, N.,Weis, J., Eds.; VCH: Weinheim, Germany, 1995; p 649.

12 G. Schotter *Chem. Mater*. 2001, 13, 3422-3435.

13 G. Schottner, J. Kron, K.-J. Deichmann, *J. Sol-Gel Sci. Technol*.1998, 13, 183.

14 Mennig,M.; Schelle, C.; Duran, A.; Damborenea, J. J.; Guglielmi, M.; Brusatin, G. *J. Sol-Gel Sci. Technol.* 1998, 13, 717.

15 M. Pagliaro, R. Ciriminna, G. Palmisano, *J. Mat. Chem*., 2009, 19, 31 16-3126; T. L.. Metroke, , R. L. Parkhill, E. T. Knobbe, *Mater. Res. Soc. Symp*. Proc. 1999, 576, 293.

16 M. Pilz, H. Romich, *J. Sol-Gel Sci. Technol*. 1997, 8, 1071

17 T. L. Metroke, R. L. Parkhill, Knobbe, E. T. *Mater. Res. Soc. Symp*. Proc. 1999, 576, 293.

18 S. Amberg-Schwab, H. Katschorek, U. Weber, M. Hoffmann, A. Burger, *J. Sol-Gel Sci. Technol.* 2000, 19, 125.

19 S. Amberg-Schwab, M. Hoffmann, H. Bader, M. Gessler, *J. Sol-Gel Sci. Technol*. 1998, 2, 141.

20 S. Amberg-Schwab, H. Katschorek, U. Weber, M. Hoffmann, A Burger,. *J. Sol-Gel Sci. Technol.* 2000, 19, 125.

21 M. Pagliaro, R. Ciriminna, G. Palmisano, *J. Mat. Chem*., 2009, 19, 31 16-3126K. Rose, S. Amberg-Schwab, M. Heinrich, *In Organosilicon Chemistry IV*; Auner, N., Weis, J., Eds.; VCH: Weinheim, Germany, 1999; p 613.

22 K. Nishio, K. Okubo, Y. Watanabe, T. Tsuchiya,. *J. Sol-Gel Sci. Technol*. 2000, 19, 187.

23 K. Nishio, K. Okubo, Y. Watanabe, T. Tsuchiya,. *J. Sol-Gel Sci. Technol*. 2000, 19, 187.

24 M. Popall, M. Andrei, J. Kappel, J. Kron, K. Olma, B. Olsowski, *Electrochim. Acta* 1998, 43, 1155.

25 L. Depre´, Kappel, J.; Popall, M. *Electrochim. Acta* 1998, 43,1301.

26 J. GrobeStoppek-Langner, K. Nachr. *Chem. Tech. Lab*. 1993,41, 1233.

27 H. Schmidt, *J. Non-Cryst. Solids* 1994, 178, 302.

28 J. Kron, K.-J. Deichmann, G. Schottner, Glastech. Ber., *GlassSci. Technol*. 1995, 68C1, 378.

29 T.Minami, J. *sol-Gel Sci. Technol*. 2000, 18, 290

30 C. Sanchez, B Lebeau, F. Chaput, J.P Boilot, *Adv. Mater*. 2003, 15, 1969.

31 C. Sanchez, B Lebeau, F. Chaput, J.P Boilot, *Adv. Mater*. 2003, 15, 1969.

32 M. Faloss, M. Canva, P. Georges, A. Brun, F. Chaput, J.-P. Boilot, *Appl. Opt.* 1997, 36, 6760

33 B. Schaudel, C. Guermeur, C. Sanchez, K. Nakatani, J. Delaire, *J. Mater. Chem*. 1997, 7, 61.

34 B. Lebeau, C. Sanchez, S. Brasselet, J. Zyss, Chem. Mater. 1997, 9, 1012.

35 C. Rottman, G. Grader, Y DeHazan, S. Melchior, D. Avnir, *J. Am. Chem. Soc*. 1999, 121, 8533.

36 T. Dantas de Morais, F. Chaput, J.-P. Boilot, K. Lahlil, B. Darracq, Y. Levy, *Adv. Mater*. 1999, 11, 107

37 a) D. Levy, J. M. S. Pena, C. J. Serna, J. M. Oton, L. Esquivias, J. Non- Cryst. Solids 1992, 147-148, 646. b) J. M. Oton, J. M. S. Pena, A. Serrano, D. Levy, *Appl. Phys. Lett*. 1995, 66, 929

38 D. R. Uhlmann, G. Teowee, *J. Sol-Gel Sci. Technol*. 1998, 13, 153; J. D. Mackenzie, E. P. Bescher, *J. Sol-Gel Sci. Technol*. 1998, 13, 371.

39 B. Lebeau, J. Maquet, C. Sanchez, F. Beaume, F. Laupreˆtre, *J. Mater. Chem*. 1997, 7, 989.

40 B.Lebeau, S. Brasselet, J. Zyss, C. Sanchez, *Chem. Mater*.1997, 9, 1012.

41 C.N.R. Rao, A.K. Cheetham, A. Thirumurugam *J. Phys.: Condens. Matter* **20** (2008)

42 V. Ptatschek, B. Schreder, K. Herz, U. Hilbert, W.Ossau, G. Schottner, O. Raha¨user, T. Bischof, G. Lermann, A. Materny, W. Kiefer, G. Bacher, A. Forchel, D. Su, M. Giersig, G. Mu¨ller, L. Spanhel, *J. Phys. Chem*. B 1997, 101, 44.

43 G. Schottner, W. Grond, L. Ku¨mmerl, D. Haarer, *J. Sol-GelSci. Technol*. 1994, 2, 657.

44 C. M. McDonagh, A. M. Shields, A. K. McEvoy, B.D.; MacCraith, Gouin, J. F. *J. Sol-Gel Sci. Technol*. 1998, 13, 207.

45 P. Garcia Parejo, M. Zayat and D. Levy, *J. Mater. Chem*., 2006, 16, 2165.

46www.corporate.basf.com/en/stories/wipo/col

48 L. Mascia, L. Prezzi, G. D. Wilcox and M. Lavorgna, *Progr. Org.Coatings*, 2006, 56(1), 13.

49 M. L. Zheludkevich, R. Serra, M. F. Montemor, K. A. Yasakau, I. M. Miranda Salvado and M. G. S. Ferreira, *Electrochimica Acta*, 2005, 51, 208.

50 B. Mahltig, C. Swaboda, A. Roessler and H. Shottcher, *J. Mater.Chem*., 2008, 18, 3180.

51 E. Bescher, F. Piquè, D. Stulik, J.D. Mackenzie, *J. Sol-Gel Sci. Technol*. 2000,19, 215.

CHAPTER III

MATERIALS CHARACTERIZATION

3.1. Introduction

The properties and improved performance exhibited by organic-inorganic hybrid materials are strongly dependent on their composition, size, surface structure, and interparticle interactions[1]. The heterogeneous nature of hybrid materials means that generally a variety of analytical techniques has to be used to investigate the structure–property relationships[2]. This requires the use of a range quite large of characterization methods used in the analysis of the composition, the molecular and nanometer structure as well as the physical properties of hybrid materials[3] .

A wide variety of spectroscopic, microscopic and other technique, may be used to obtain information on the identity, structure and properties of organic-inorganic hybrid materials

The electromagnetic spectrum covers an enormous span of frequencies, wavelength and, therefore, energy. Different spectroscopic techniques operate over different, limited frequency ranges within this broad spectrum, depending on the processes and magnitudes of the energy changes involved. The nuclear magnetic resonance (NMR) technique operates in the radiofrequency region at, for example, 400 MHz ($4x10^8$) and detects changes in nuclear spin state. At higher frequencies and shorter wavelengths, the energy increases and , for instance, vibrational motions of atoms in molecules or solids may be altered by absorption or emission of infrared (IR) radiation. For transitions involving outer (valence) shells, the associated energy usually lies in the visible and ultraviolet regions; for inner shell transitions, much larger energies are involved and fall in the X-ray region.

The spectroscopy gives information on *local* structure whereas diffraction is concerned primarily with *long range* order, then spectroscopic measurements on hybrid materials complement well the results obtained from X-ray diffraction

The main objective of this chapter is to discusses some important techniques used for characterization of organic-inorganic hybrid materials prepared in this work, and to indicate the kind of information that they can give about hybrid materials[2].

3.2. Vibrational spectroscopy

Atoms in solids vibrate at frequencies of 10^{12} to 10^{13} Hz. Vibrational modes can be excited to higher energy states by absorption of radiation of appropriate frequency[4]. Infrared and Raman spectrum both involve vibration and rotational energy levels, they are not duplicates of each other but rather complement each other. This is because the intensity of the spectral band depends on how effectively the photon energy transfer differs in the two techniques[56].

IR spectra and closely related Raman spectra are plots of intensity of absorption (IR) or scattering (Raman) as a function of frequency or wavenumber. In the IR technique, the frequency of the incident radiation is varied and the quantity of radiation absorbed or transmitted by the sample is obtained. In the Raman technique, the sample is illuminated with monochromomatic light, usually generated by a laser.

IR and Raman spectra of solids are usually complex with a large number of peaks, each corresponding to a particular vibrational transition. IR and Raman spectra are usually quite different since the two techniques are governed by different selection rules. The number of observed peaks is considerably less than the total number of vibrational modes and different modes may be active in the two techniques .For a mode to be *IR active*, the associated dipole moment must vary during the vibrational cycle. Consequently, centrosymmetric vibrational mode are IR inactive. For a vibrational mode to be made *Raman active*, the nuclear motions involved must be produce a change in polarizability.

IR and Raman spectra are much used to identify specific functional groups, especially in organic molecules. In organic solids, covalently bonded linkages such as hydroxyl groups, trapped water and oxyanions give rise to intense IR and Raman peaks.

Peaks that occur in the region ~ 3000 to 3500 cm^{-1} are usually characteristic of OH groups in some form: the peak frequencies depend on the O-H bond strength and give information on for instance the location of the OH group, whether it belongs to water molecule and whether or not hydrogen bonding is present.

Apart from uses in identification, vibrational spectra may be used to provide structural information; but a deeper understanding of the spectra and the assignment of peaks to specific vibrational modes is almost essential.

Vibrational spectroscopy of molecules can be relatively complicated. Quantum mechanics requires that only certain well-defined frequencies and atomic displacements are allowed. These are known as the *normal modes of vibration*[7] of the molecule. A linear molecule with N atoms has 3N - 5 normal modes, and a non-linear molecule has 3N - 6 normal modes of vibration. There are several types of motion that contribute to the normal modes. Some examples are: stretching motion between two bonded atoms;

bending motion between three atoms connected by two bonds; out-of-plan deformation modes that change an otherwise planar structure into a non-planar one.

3.2.1. Infrared spectroscopy

Infrared spectroscopy is one of the most important analytical techniques available today's scientists. One of the great advantages of infrared spectroscopy is that virtually any sample in virtually any state may be studied. Infrared spectroscopy provides a simple and rapid instrumental technique that can give evidence for the presence of various functional groups. IR spectroscopy, as all forms of spectroscopy, depends on the interaction of molecules or atoms with electromagnetic radiation[5,6].

Infrared radiation causes atoms and groups of atoms of organic compounds to vibrate with increased amplitude about the covalent bonds that connect them, the energy, of the radiation is not of sufficient energy to excite electrons. Since the functional groups of organic molecules include specific arrangements of bonded atoms, absorption of infrared energy by an organic molecule will occur in a manner characteristic of the types of bonds

and atoms present in the specific functional groups of that molecule. These vibrations are quantized, and as they occur, the compounds absorb IR energy in particular regions of the infrared portion of the spectrum. Infrared spectroscopy allows one to characterize vibrations in molecules by measuring the absorption of light of certain energies that correspond to the vibrational excitation of the molecule from v=0 v =1 (or higher) states. Not all of the normal modes of vibration can be excited by infrared radiation. There are *selection rules* that govern the ability of a molecule to be detected by infrared spectroscopy.

In their vibrations covalents bonds behave as if they were tiny springs connecting the atoms. When the atoms vibrate they can do so only at certain frequencies, as if the bonds were tuned. Because of this, covalently bonded atoms have only particular vibrational energy level i.e the levels are quantized. The excitation of a molecule from one vibrational energy level to another occurs only when the compound absorbs IR radiation of a particular energy, meaning a particular wavelength or frequency, since $\Delta E=h\nu$.

Molecules can vibrate in a variety of ways. Two atoms joined by a covalent bond can undergo a stretching vibration where the atoms move back and forth as if joined by a spring. Three atoms can also undergo a variety of stretching and bending vibrations:

The frequency of a given stretching vibration in an IR spectrum can be related to two factors. These are the masses of the bonded atoms, light atoms vibrate at higher frequencies than heavier ones, and the relative stiffness of the bond. Triple bonds are stiffer, and vibrate at higher frequencies than double bonds, and double bonds are stiffer, and vibrate at higher frequencies than single bonds.

The stretching frequencies of groups involving hydrogen such as C-H, N-H, and O-H all occur at relatively high frequencies. For a fundamental transition to occur by absorption of infrared radiation the transition moment integral must be nonzero. The transition moment integrals are of the form:

Equ. 3.1

a) $\int \psi_v^o x \psi_v^f d\tau$

b) $\int \psi_v^o v \psi_v^f d\tau$

c)

$$\int \psi_v^o z \psi_v^f d\tau$$

where v_o is the wave function for the initial state involved in the transition (the ground state), and v_f is the wave function for the final state involved in the transition (the excited state). The x, y and z involved in the integrals refers to the Cartesian components of the oscillating electric vector of the radiation. If any of these three integrals is nonzero, then the transition moment integral is nonzero and the transition is allowed. The symmetry representation for the excited state wave function, vf, depends on the symmetry of the normal mode vibration to be excited. If the product of the three terms in the transition moment integrals above are not the totally symmetric representation, then the integral will be zero.

An infrared spectrometer operates by passing a beam of IR radiation through a sample and comparing the radiation transmitted through the sample with a reference beam. Any frequencies absorbed by sample will be apparent by the difference between the beams. The spectrometer plots the results as a graph showing absorbance versus frequency or wavelength.

The location of an IR absorption band (or peak) can be specified in frequency-relateds units by its wavenumbers($\tilde{\nu}$) measured in reciprocal centimeters (cm^{-1}), or by its wavelength is the length of the wave, crest to crest[8].

$$\tilde{\nu} = \frac{1}{\lambda} \text{ (with } \lambda \text{ in cm)} \quad \text{or} \quad \tilde{\nu} = \frac{10000}{\lambda} \text{ (with } \lambda \text{ in } \mu\text{m)}$$

The most significant advances in infrared spectroscopy, however, have come about as a result of the introduction of Fourier-trasform spectrometers. This type of instrument employs an interferometer and exploits the well-established mathematical process of Fourier-trasformation. Fourier-trasform infrared (FTIR) spectroscopy has improved the quality of infrared spectra and minimized the time required to obtain data. The energy at which any peak in an absorption spectrum appears corresponds to the frequency of a vibration of a part of a sample molecule.

Fourier-transform infrared (FTIR) spectroscopy is based on the idea of the interference of radiation between two beams to yield and interferogram. The latter is a signal produced as a function of the change of pathlength between the two beams. The two domains of distance and frequency are interconvertible by the mathematical method of Fourier-transformation.

The radiation emerging from the source is passed through an interferometer to the sample before reaching a detector. Upon amplification of the signal, in which high-frequency contributions have been eliminated by a filter, the data are converted to digital form by an analog-to-digital converter and transferred to the computer for Fourier-transformation.

The essential equations for a Fourier-transformation relating the intensity falling on the detector, $I(\delta)$, to the spectral power density at a particular wavenumber, $\bar{\nu}$, given by $B(\bar{\nu})$, are as follows:

Equ. 3.2

$$I(\delta) = \int_0^{+\infty} B(\bar{\nu}) \cos(2\pi\bar{\nu}\delta) d\bar{\nu}$$

which is one half of a cosine Fourier-transform pair, with the other being[9]:

Equ. 3.3

$$B(\bar{\nu}) = \int_{-\infty}^{+\infty} I(\bar{\nu}) \cos(2\pi\bar{\nu}\delta) d\delta$$

These two equation are interconvertible and are know as a Fourier-transform pair. The first show the variation in power density as a function of the difference in pathlength, which is an interference pattern. The second shows the variation in intensity as a function of wavenumber. Each can be converted into the other by mathematical method of Fourier-trasformation.

The essential experiment to obtain an FTIR spectrum is to produce an interferogram with and without a sample in the beam and transforming the interferograms into spectra of (a) the source with sample absorptions and (b) the source without sample absorptions. The ratio of the former and the latter corresponds to a double-beam dispersive spectrum.

3.2.2. Raman spectroscopy

In the discussion of Raman spectroscopy, we can use language from particle theory [6,10] and we say that a photon is scattered by the molecular system. Most photons are elastically scattered, a process which is called Rayleigh scattering. In Rayleigh scattering, the emitted photon has the same wavelength as the absorbing photon. Raman spectroscopy is based on the Raman effect, which is the inelastic scattering of photons by molecules. The effect was discovered by the Indian physicist, C. V. Raman in 1928. The Raman effectcomprises a very small fraction, about 1 in 10^7, of the incident photons. In Raman scattering, the energies of the incident and scattered photons are different. A simplified energy diagram that illustrates these concepts is given in the scheme 3.1 .

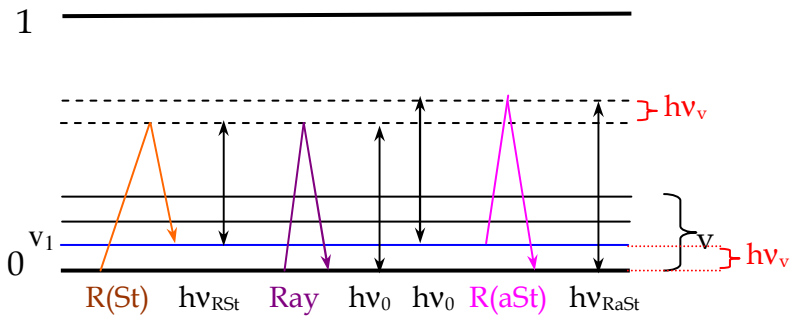

Figure 3.1- Energy diagram of the Raman effect.

The energy of the scattered radiation is less than the incident radiation for the Stokes line and the energy of the scattered radiation is more than the incident radiation for the anti-Stokes line. The energy increase or decrease from the excitation is related to the vibrational energy spacing in the ground electronic state of the molecule and therefore the wavenumber of the Stokes and anti-Stokes lines are a direct measure of the vibrational energies of the molecule.

We can describe the Raman effect also as an inelastic collision between the incident photon and the molecule where as a result of the collision the vibrational or rotational energy of the molecule is changed by an amount ΔE_m. In order that energy may be conserved, the energy of the scattered photon, $h\nu_s$, must be different from the energy of the incident photon $h\nu_i$, by an amount equal to ΔE_m:

Equ. 3.4

$$h\nu_i - h\nu_s = \Delta E_m$$

If the molecule gains energy then ΔE_m is positive and ν_s is smaller than ν_i, giving rise to Stokes lines in the Raman spectrum. If the molecule loses energy, then ΔE_m is negative and ν_s is larger than ν_i, giving rise to anti-Stokes lines in the Raman spectrum.

In the Raman scattering the frequency of the incident photon is usually much greater than ν_m. When the incident photon interacts with a molecule in the ground vibration state $\nu = 0$, the molecule absorbs the photon energy and is raised momentarily to some high level of energy which is not a stable energy level (figure 3.1).

Therefore, the molecule immediately loses energy and, most probably, returns to the ground vibration level, emitting a scattered photon (to make up for its energy loss) whose energy and frequency is the same as that of the incident photon. This is the Rayleigh scattering. However, a small proportion of the molecules in the unstable high level of energy may fall, not to the ground vibrational level but to the $\nu = 1$ energy level. The scattered photon in this case has less energy than the exciting photon, the difference being

$$h\nu_i - h\nu_s = \Delta E_m = h\nu_m$$

so

$$\nu_s = \nu_i - \nu_m \quad \text{when} \quad \Delta\nu = +1$$

This scattered photon gives rise to Stokes line in the Raman spectrum. According to quantum mechanic the allowed change in the vibrational quantum number for a Raman transition is $\Delta\nu = \pm 1$ for a harmonic vibration. The final possibility is that the molecule initially is in the excited state $\nu = 1$, absorbs the incident photon energy, and is raised to an unstable high level of energy. When the molecule falls to the ground vibrational level $\nu = 0$ the energy loss is made up for the emission of a photon whose energy is greater than that of the incident photon by $h\nu_m$. This scattered photon gives rise to an anti-Stokes line in Raman spectrum. According to the Boltzmann distribution function the ratio of the number of molecules in the $\nu = 0$ state for a given vibration is

Equ. 3.5

$$\frac{n_1}{n_0} = e^{-(h\nu_m / kT)}$$

At ordinary temperatures most of the molecules exist in the ground state and therefore Stokes lines have greater intensities than anti-Stokes lines which originate from an excited level with lower population. This difference increases as the vibrational frequency increases.

A schematic Raman spectrum may appear as:

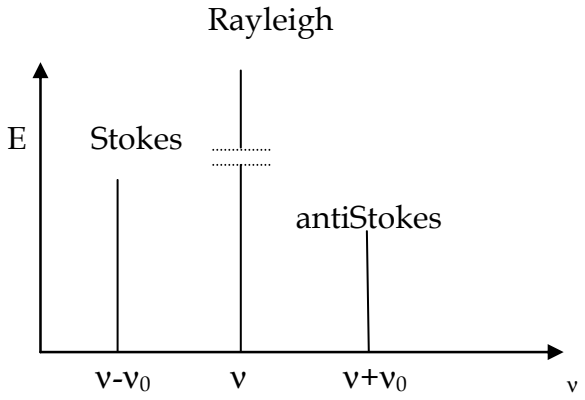

Figure 3.2- Schematic Raman spectrum.

In the figure 3.2 the Stokes and anti-Stokes lines are equally displaced from the Rayleigh line; this occurs because in either case one vibrational quantum of energy is gained or lost. The anti-Stokes line is much less intense than the Stokes line; this occurs because only molecules that are vibrationally excited prior to irradiation can give rise to the anti-Stokes line. Hence, in Raman spectroscopy, only the more intense Stokes line is normally measured. We only observe the Stokes shift in a Raman spectrum, the Stokes lines will be at smaller wavenumbers (or higher wavelengths) than the exciting light. Since the Raman scattering is not very efficient, we need a high power excitation source such as a laser. Also, since we are interested in the energy (wavenumber) difference between the excitation and the Stokes lines, the excitation source should be monochromatic For a

vibration to be Raman active, the polarizability of the molecule must change with the vibrational motion, thus, Raman spectroscopy complements IR spectroscopy.

The Raman effect can be describe also through the the interaction of the electromagnetic field of the incident radiation[11], $E_{i,}$ with a molecule. The electric field may induce an electric dipole in the molecule, given by $p = \alpha Ei$ where is referred to as the polarizability of the molecule and p is the induced dipole. The electric field due to the incident radiation is a time-varying quantity of the form $E_i = Eocos(2\pi it)$ For a vibrating molecule, the polarizability is also a time-varying term that depends on the vibrational frequency of the molecule, vib = o + vib cos(2 vib t)

Multiplication of these two time-varying terms, E_i and , gives rise to a cross product term of the form[7,12]:

Equ. 3.6
$$\frac{\alpha_{vib} E_o}{2}[\cos 2\pi t(\nu_i + \nu_{vib}) + \cos 2\pi t(\nu_i - \nu_{vib})]$$

This cross term in the induced dipole represents light that can be scattered at both higher and lower energy than the Rayleigh (elastic) scattering of the incident radiation. The incremental difference from the frequency of the incident radiation, i, are by the vibrational frequencies of the molecule, vib. These lines are the anti-Stokes and Stokes lines, respectively. The ratio of the intensity of the Raman anti-Stokes and Stokes lines is predicted to be[7]

Equ. 3.7
$$\frac{I_A}{I_S} = \left(\frac{\nu_i + \nu_{vib}}{\nu_i - \nu_{vib}}\right)^4 e^{\left(\frac{-h\nu_{vib}}{kT}\right)}$$

The Boltzmann exponential factor is the dominant term in equation 3.7 , which makes the anti-Stokes features of the spectra much weaker than the corresponding Stokes lines.

Infrared spectroscopy and Raman spectroscopy are complementary techniques, because the selection rules are different.

In a Raman spectrometer the sample is irradiated with an intense source of monochromatic radiation usually in the visible part of the spectrum. Generally this radiation frequency is much higher than the vibrational frequencies but is lower than the electronic frequencies. The radiation scattered by the sample is analyzed in the spectrometer. Two types of scattered light are produced. *Rayleigh scatter* emerges with exactly the same energy and wavelength as the incident light. *Raman scatter,* which is usually much less intense than Rayleigh scatter, emerges at either longer or shorter wavelength. This scattered light is detected in a direction perpendicular to the incident beam[13].

For a fundamental transition to occur by Raman scattering of radiation the transition moment integral must be nonzero. The transition moment integrals are of the form[7]:

Equ. 3.8 $$\int \psi_v^o \alpha \psi_v^f d\tau$$

where represents the polarizability of the molecule. The above integrals be nonzero means that there must be a change in polarizability of the molecule when the transition occurs.

3.3. Visible and ultraviolet spectroscopy

Transition of electrons between outermost energy levels are associated with energy changes in the range ~ 10^4 to 10^5 cm^{-1} or ~10^2 to 10^3 kJ mol^{-1}. These energies span the near IR through the visible to the UV, and are often associated with colour. Various types of electronic transition occur. The two atoms A and B are neighbouring atoms in some kind of solid structure; they may be an anion and cation in an ionic crystal. The inner electron shells are localized on the individual atoms.

The outermost shells may overlap to form delocalized bands energy levels. Four basic types of transition are indicated:

1) Promotion of an electron from a localized orbital on one atom to higher energy localized orbital on the same atom. The associated absorption band is sometimes know as an *exciton band*. Examples include (a) *d-d* and *f-f* transition in transition metal compounds, (b) outer shell transitions in heavy metal compounds, (c)

transitions associated with defects such as trapped electrons or holes, (d) transitions involving Ag atoms in photochromic glasses.

2) Promotion of an electron from localized orbital on one atom to higher energy localized orbital on an adjacent atom. The associated absorption bands are know ads *charge transfer spectra.* The transitions are usually allowed transitions according to the spectroscopic selection rules and hence the absorption bands are intense.

3) Promotion of an electron from a localized orbital on one atom to a delocalized energy band, the *conduction band*, which is characteristic of the entire solid. In many solids the energy required to cause such a transition is very high but in others, especially containing heavy elements, the transition occurs in the visible/ ultraviolet region and the materials are photoconductive.

4) Promotion of an electron from one energy band, the valence band, to another band of higher energy, the conduction band.

On the appearance of a typical UV and visible absorption spectrum we can found two principal features. Above a certain energy or frequency know as the *absorption edge*, intense absorption occurs; this places a high frequency limit on the spectral range that can be investigated. Transitions of types (2) and (3) lead to an absorption edge. In electronically insulating ionic solids the absorption edge may occur in the UV, but in photoconducting and semiconducting materials it may occur in the visible or near IR.

The second feature is the appearance of broad absorption peaks or bands at frequencies below that of the absorption cut-off. These are generally associated with type (1) transitions. Visible and UV spectroscopy has variety of application associated with the local structure of materials. This is because the positions of the absorption bands are sensitive to coordination environment and bond character.

3.4. Nuclear Magnetic Resonance Spectroscopy

The structure of a molecule determines its physical properties, reactivity and biological activity. Detailed information about molecular structure can be obtained by interpreting results from the interaction of energy with molecules.

In the study of nuclear magnetic resonance (NMR) spectroscopy the attention is on the energy absorption by molecules that have been placed in a strong magnetic field.

The nuclei of certain elements and isotopes behave as though they were magnets spinning about axis[14,15]. The nuclei of ordinary hydrogen (^{1}H) and carbon-13 (^{13}C) nuclei have this property. When one places a compound containing ^{1}H or ^{13}C atoms in a very strong magnetic field and simultaneously irradiates it with electromagnetic energy, the nuclei of the compound may absorb energy through a process called magnetic resonance.

This absorption of energy is quantized and produces a characteristic spectrum for the compound. Absorption of energy does not occur unless the strength of the magnetic field and the frequency of electromagnetic radiation are at specific values.

Instruments know as nuclear magnetic resonance (NMR) spectrometers allow to measure the absorption of energy by ^{1}H, ^{13}C, nuclei and by the nuclei of the other elements like for example ^{29}Si. These instruments use very powerful magnetes and irradiate the sample with electromagnetic radiation in the radio frequency (rf) region.

In a given molecule some hydrogen nuclei are in regions of greater electron density than others, and as a result, the nuclei (protons) absorb energy at slightly different magnetic field strengths. The signals for these protons consequently occur at different positions in the NMR spectrum; they are said to have different *chemical shifts*[11,12] . The actual field strength at which absorption occurs (the chemical shift) is highly dependent on the magnetic environment of each proton. This magnetic environment depends on two factors: on magnetic field generated by circulating electrons, and on magnetic fields that result from other nearby protons (or other magnetic nuclei). Chemical shifts are measured along the bottom of the spectrum on a delta (δ) scale (in units of parts per million); the externally applied magnetic field strength increases from left to right. The signal at δ 0, arises from a compound called tetramethylsilane (TMS)[11,12] that has been added to the

sample to allow calibration of the chemical shift scale. Exit a relation between the number of signals in the spectrum and the number of different types of hydrogen (carbon or silicon) atoms in the compound.

On the NMR spectrum the important is the area underneath it, these areas when accurately measured, are in the same ratio as the number of atoms causing each signal.

Sometimes we can observe the phenomena of signal splitting, this is arises from magnetic influences of hydrogens on atoms.

Liquid state NMR techniques are a well-known powerful tool in the characterization of solutions. Molecular liquids give NMR spectra composed of a number of sharp peaks. From their position and intensities it is possible to tell which atoms are bonded together, coordination numbers, next nearest neighbours etc.

The advantages of NMR spectroscopy is that it is a very sensitive technique for the chemical environment of specific nuclei and many nuclei can be investigated. On the solution NMR the spectra usually consist of a series of very sharp lines due to an averaging of all anisotropic interactions by the molecular motion in the solution, in the solid sample, broad peaks are observed due to anisotropic or orientation-dependent interactions.

An additional advantage of the technique is that it is nondestructive. There are a variety of nuclei that can be used as probes in solid state NMR because of their NMR activity, many of them are also interesting for hybrid materials such as H, C, Si, Al, Sn, and many others. The most investigated nucleus in the field of organic-inorganic hybrid materials is ^{29}Si and ^{13}C. ^{29}Si NMR is a powerful tool in the determination of the relative proportions of different silicon species in sol–gel derived materials; it offers the possibility to investigate into the kinetics of the process and the understanding of its fundamental parameters, such as precursor structure and reaction conditions. It is sensitive to the first and second nearest neighbors and therefore one can distinguish between different silicon atoms in the final material and their surroundings. Typical for hybrid materials is the nomenclature with letters and numbers. Four different species can be observed in hybrid materials derived by the sol–gel process depending on their

substitution pattern at the silicon. In principle one can have one, two, three or four oxygen atoms surrounding the silicon atom and respectively the number of carbon atoms is reduced from three to zero. The abbreviations for these substitution patterns are M (C_3SiO), D (C_2SiO_2), T ($CSiO_3$) and Q (SiO_4). Depending how many Si atoms are connected to the oxygen atoms 4 to 1 a superscript is added to the abbreviation. In addition these silicon species have different chemical shifts which helps to distinguish between them.

3.5. X-Ray diffraction

X-ray diffraction of a crystalline material is based on the principle of elastic scattering of X rays by a periodic lattice characterized by long-range order. It is a reciprocal space-based method (that is, it gives information about types of periodicity present in the material, rather than the real space distribution of individual atoms), and it gives an ensemble average information on the crystal structure and particles size of a nanostructured material[16].

X-ray are electromagnetic radiation of wavelength ~ 1 Å (10^{-10} m), they occur in that part of the electromagnetic spectrum between γ-ray and the ultraviolet. X-ray are produced when high- energy charged particles, e.g electrons accelerated through 30000 V, collide with matter[17]. The resulting X-ray spectra usually have two components, a broad spectrum of wavelengths knows as *white radiation* and a number of fixed or monochromatic wavelengths.

White radiation arises when the electrons are slowed down or stopped by the collision and some of their lost energy is converted into electromagnetic radiation. White radiation has wavelengths ranging upwards from a certain lower limiting value. This lower wavelength limit corresponds to the X-ray of the highest energy and occurs when all the kinetic energy of the incident particles is converted into X-rays. It may be calculated from the formula, λ_{min} (Å) =12400/V where V is the accelerating voltage.

The X-rays which are used in almost all diffraction experiments are produced by a different process that leads to *monochromatic X-rays.* A beam of electrons again accelerated through, say, 30 kV is allowed to strike a meal target, often Cu. The incident electrons have sufficient energy to ionize some of the Cu 1s (K shell) electrons. The transition energies have fixed values and so a spectrum of characteristic X-rays results. For Cu the 2p→1s transition, called Kα, has a wavelength of 1.5418 Å and the 3p→1s transition, called K_β, 1.3922 Å.; in fact the Kα is a doublet $K\alpha_1$= 1.54051 Å and $K\alpha_1$= 1.54433 Å, because the transition has a slightly different energy for the two possible spin state of the 2p electron.

The wavelength of the Kα line of the target metals and the atomic number Z of the metal are related by *Moseley's law:* $\lambda^{-1/2} = C(Z - \sigma)$; where C and σ are constants, the wavelength of the Kα line decreases with increasing of atomic number.

Historically two approaches have been used to treat diffraction by crystals: the Laue equation and Bragg's law[14,15].

The Bragg approach to diffraction is to regard crystals as built up in layers or planes such that each acts as a semi-trasparent mirror[14,15]. Some of the X-rays are reflected off a plane with the angle of reflection equal to the angle of incidence, but the rest are transmitted to be subsequently reflected by succeeding planes. The derivation of Bragg's law is shown in figure 3.2; two X-ray beams 1 and 2 are reflected from adjacent planes, A and B, within the crystal and we wish to know under what conditions the reflected beams $1'$ and $2'$ are in phase. The perpendicular distance between pairs of adjacent planes, the *d-spacing* , *d*, and the angle of incidence, or *Bragg angle*, ϑ ,are related to the distance xy by xy=yz=dsinθ.

Therefore

$$2d \sin\vartheta = n\lambda , \quad \textit{Bragg's law}$$

where n is an integer, λ is the X-ray wavelength, *d* is the spacing between crystallographic planes giving rise to a particular diffracted beam, and θ is the incidence angle. When Bragg's law is satisfied, the reflected beams are in phase and interfere

constructively. At angles of incidence other than the Bragg angle, reflected beams are out of phase and destructive interference or cancellation occurs. In the real crystals, which contain thousands of planes, Bragg'law imposes a stringent condition on the angles at which reflection may occur.

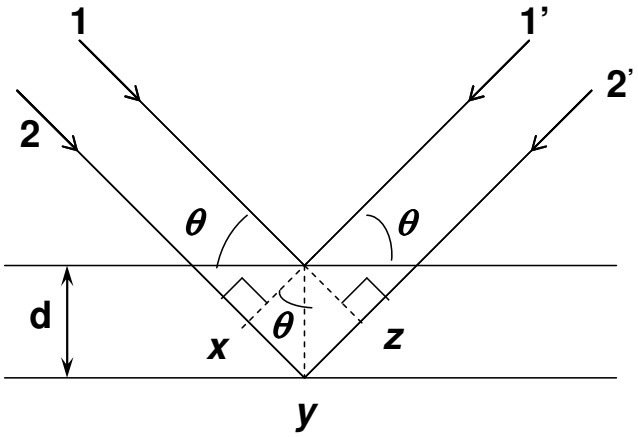

Figure 3.2- The derivation of Bragg's law.

Crystal structure, with their regularly repeating patterns, may be referred to a 3D grid and the repeating unit of the grid, the *unit cell*, can be found. The grid may be divided up into sets of planes in various orientations and it is these planes which are considered in the derivation of Bragg'law. In some cases with simple crystal structures, the planes also correspond to layers of atoms, but this is not generally the case.

X-ray diffraction is extensively used to characterize the crystalline state and to estimate the crystalline sizes of materials.

The diffraction pattern generated by constructive interference of the scattered X rays provides crystallographic information on the materials. In the case of nanomaterials, the sample can be in form of powder or as a thin film that is exposed to a beam of X-rays, where the angle of incidence is varied. For a sample consisting of polycrystalline

(powder) materials, the X-rays diffractogram is a series of peaks conforming to the 2θ values, where Bragg's law of diffraction is satisfied.

The observed line broadening can be used to estimate the average size of the nanocrystals (or crystalline domains). The size can be estimated from a single diffraction peak. The particle/grain size, *D*, is related to the X-ray line broadening by Scherrer's formula:

$$D = \frac{0.9\lambda}{\beta \cos \vartheta}$$

where λ is the wavelength, θ is the diffraction angle, and β is the full width (in radian) at half-maximum intensity. In those cases where stress may be present, a more rigorous method involving several diffraction peaks is required. However, Scherrer's formula should be used only as a rough guide for particle size.

X-ray diffraction is regularly used to identify the different phases in a polycrystalline sample. Two of its most important advantages for analysis of hybrid materials are that it is fast and nondestructive. When the positions and intensities of the diffraction pattern are taken into account the pattern is unique for a single substance. The X-ray pattern is like a fingerprint and mixtures of different crystallographic phases can be easily distinguished by comparison with reference data.

3.6. Electron microscopy

Electron microscopy is extremely versatile for providing structural information over a wide range of magnification. At one extreme, *scanning electron microscopy* (SEM), complements optical microscopy for studying the texture, topography and surface features of powders or solid pieces and, because of the depth of focus of SEM instruments the resulting picture have a definite 3D quality. Looking at electron micrographs one has always to be aware of some limiting points: (a) all specimens are in high vacuum and probably have another shape in a liquid or gel-like surrounding, (b) the images reveal only a small fragment of the whole sample raising the possibility that the

region analyzed may not be characteristic of the whole sample, and (c) the sample is treated with a high energy electron beam and it was probably changed by this beam

Electron microscopes operate in either transmission or reflection. For transmission, samples should usually be thinner than ~2000 Å because electrons interact strongly with matter and are completely absorbed by thick particles. Sample preparation may be difficult, especially if it is not possible to prepare thin foils. One possible solution is to use higher voltage instruments, e.g 1 MV. Thicker samples may then be used since the beam is more penetrating; in addition, the amount of background scatter is reduced and higher resolution may be obtained. Alternatively if the solid can be crushed into a fine powder the at least some of resulting particles should be thin enough to be viewed in transmission. The upper practical working limit of *transmission electron microscopy* (TEM) is ~ 0.1 μm.

3.6.1. Transmission Electron Microscopy (TEM)

In a TEM instrument electrons emitted from a tungsten filament (*electron gun*) are accelerated through a high voltage (50 to 100 kV). Their wavelength is related to the accelerating voltage is related to the accelerating voltage V[15] by

$$\lambda = h(2meV)^{-1/2}$$

where m and e are the mass and charge of the electron. At high voltage, as the velocity of the electrons approaches the velocity of light, m is increased by relativistic effects. The electron wavelength are smaller than X-ray wavelengths, e.g λ~0.04 Å at 90 kV accelerating voltage. Consequently, the Bragg angle for diffraction are smaller and the diffracted beams are concentrated into narrow cone centered on the on the undiffracted beam.

In order to use electrons, instead light, in a microscope it is necessary to be able to focus them; electrons may be focused by an electric or magnetic field. Electron microscopes contain several *electromagnetic lenses.* The condenser lenses control the size and angular spread of the incident electron beam. Transmitted electrons pass through a sequence of

lenses- objective, intermediate and projector- and form a magnified image of the sample on a fluorescent screen, photographic plate, or light sensitive sensor such as a CCD camera.. Photographs may be ; the region of the sample that is chosen for imaging is controlled by an aperture placed in the intermediate image plane.

It is often difficult in TEM to receive details of a sample because of low contrast which is based on the weak interaction with the electrons. Particularly samples that have a high content of organic components often reveal this problem, which can partially be overcome by the use of stains such as heavy metal compounds. The dense electron clouds of the heavy atoms interact strongly with the electron beam.

However, sometimes the organic components of the sample are not detected because they decompose in the electron beam; this can be avoided using cryogenic microscopy, which keeps the specimen at liquid nitrogen or liquid helium temperatures (cryo-TEM).

Additionally if the material observed is crystalline, diffraction patterns are obtained that give information about the crystal orientation and very powerful instruments can even investigate the crystal structure. Modern high-resolution TEM (HRTEM) goes down to a resolution <100pm. One of the major limitations of TEM is the extensive sample preparation, which makes TEM analysis a relatively time consuming process with a low throughput of samples.

3.7. Dynamic light scattering

Dynamic light scattering[18] the way in which light scatters off of particles in suspension, has the potential to yield a great deal of information about those particles, including their size and some notion of concentration. Such information is useful in many scientific fields, and the techniques of dynamic light scattering can provide such information relatively quickly and inexpensively, compared with other methods.

Brownian motion is a phenomenon that is fundamental to this measurements. It describes the way in which very small particles move in fluid suspension, where the fluid consists of molecules much smaller than the suspended particles. The motion of suspended particles is random in nature, and arises from the cumulative effect of bombardment by the suspending medium's molecules. Molecules in a liquid are, of course, constantly in motion, randomly jump one another. As these molecules move around in the liquid, they are also jump any suspended particles in a random manner, imparting a momentum to the suspended particles, the magnitude and direction of which fluctuate in time. It is the resulting 'random walk' behavior of the suspended particles that is called Brownian motion, and that randomness makes this measurements possible.

When a laser beam is shined through a liquid with suspended particles, the beam scatters off of those particles in all directions, resulting in a scattering-angle-dependent intensity pattern. When the particles are experiencing Brownian motion, the intensity pattern also fluctuates randomly. Measuring the intensity fluctuations at a given scattering angle can yield a great deal of information about the particles scattering the laser beam, including the hydrodynamic radius of the suspended particles. The hydrodynamic radius of a particle is the effective radius of an irregularly shaped particle that is used when describing the manner in which particles in suspension diffuse through the suspending medium.

References

1 P. N. Prasad, *Nanophotonics,* WILEY 2004.

2 G. Kickelbick, *Hybrid Materials. Synthesis, Characterization, and Applications*. WILEY-VCH, 2007**.**

3 G. Schotter *Chem. Mater*. 2001, 13, 3422-3435; C. Sanchez, B Lebeau, F. Chaput, J.P Boilot, *Adv. Mater.* 2003, 15, 1969.; C. Sanchez, B Lebeau, F. Chaput, J.P Boilot, *Adv. Mater.* 2003, 15, 1969.

4 A. R.West, *Basic Solid State Chemistry,* WILEY 1999.

5 N.B Colthup, L.H. Daly, S.E. *Introduction to Infrared and Raman Spectroscopy* Wiberley 1990.

6 R.L. McCreery, *Raman Spectroscopy for chemical Analysis,* WILEY 2000.

7 J.Chalmcrs, P.R. Griffiths, *Handbook of vibrational spectroscopy,*Vol. 1, Wiley 2002

8 G. Solomons, C. Fryhle, *Organic Chemistry*, *seventh edition*, WILEY 2000.

9 B. Stuard, *Infrared Spectroscopy: fundamentals and applications*, WILEY, 2004.

10 P.B. Bernath, *Spectra of Atoms and Molecules* , second edition, Oxford University Press 2005.

11 G. Turrel, J. Corset, *Raman Microscopy,* Elsevier 1996.

12 D.A. Skoog, J.J. Leary, *Chimica Analitica Strumentale*, EdisSES, 1995.

13 E.Smith, G. Dent, *Modern Raman Spectroscopy*, *a Practical Approach*, WILEY, 2005.

14 M.H. Levitt, *Spin Dynamics Basics of Nuclear Magnetic Resonance*, WILEY,2005.

15 J.K. M. Sanders, B.K. Hunter, *Modern NMR Spectroscopy*, Oxford University Press, 1988.

16 C. Kittel, *Introduction to Solid State Physics*, seventh edition, 1996, WILEY

17 N. W. Ashcroft, N. David Mermin, *Solid State Physics*, 1976, Harcourt.

18 http://mxp.physics.umn.edu/s05/Projects/s05lightscattering/introduction.html

CHAPTER IV

HYBRID ORGANIC-INORGANIC MATERIALS: FROM SELF-ORGANIZATION TO HYBRID NANOCRYSTALS

Introduction

3-Glycidoxypropyltrimethoxysilane (GPTMS) is one of the most common precursors for the preparation of hybrid organic–inorganic materials[1].Several important applications have been reported for these materials in many different fields, for instance as protective layers on organic polymers[2] antiscratch coatings[3] solid electrolytes[4] anticorrosion coatings and restoration materials[5]. GPTMS has been used also in the photonic field, for example to fabricate hybrid materials for optical waveguides[6] optical limiting[7] and second order non-linear optical materials[8] . GPTMS is also used as a grafting agent to functionalize silica surfaces[9].

The synthesis of hybrid materials through the precise structure control from the molecular to the macroscopic level is a key point for a variety of applications especially in photonics and optoelectronics[10,11] and for future development of advanced devices[12,13] Usually organic–inorganic hybrids commonly synthesized as amorphous but in few cases hybrid crystals can be obtained; the formation of hybrid crystals through self-organization[14] can be achieved by molecule-by-molecule self-assembly[15] or by specific molecular recognition through weak interactions[16]. The organic units within the hybrid material self-organize through van der Waals interactions or hydrogen bonding and different crystalline structures are obtained, such as helical fibres or lamellar crystals[17,18] .

In particular, the bridged organically modified alkoxides as been used to produce hybrid materials that consist of a bridging organic spacer and a trifunctional silyl group at both the ends of the spacer ($O_{1.5}Si–R–SiO_{1.5}$, with R the organic spacer)[19,20,2122] Besides that another important point is to control the dimension of the organic-inorganic nanocrystals because the dimensions of the hybrid crystals will affect the properties of the material. The controlling of the process is a crucial step to carry out this purpose. From the point of view of practical application like on photonics applications, require optically

transparent films and, therefore, the crystal dimensions should be smaller than the light wavelength. The presence of layered hybrid crystals of nanodimensions allows the fabrication of films with optically anisotropic photonic structures, such as birifrangent devices[23] . On the other hand the control of the hydrolytic reactions of GPTMS through the catalyst and the processing parameters [24,25,26]is the key to expand the structural design of the resultant materials.

The chemistry of GPTMS is quite complex and for several aspects not fully explored and understood[27].It has been shown, for instance, that in highly basic conditions (pH 14) GPTMS is able to self-organize to form crystalline layered structures[28] This is an important example of hybrid nano-crystals that could be obtained without employing bridged polysilsesquioxanes which are usually used to prepare hybrid layered crystals. GPTMS is an organically modified alkoxide containing an epoxy ring, whose opening allows the formation, under particular conditions, of a poly(ethylene oxide) chain. The organic polymerization is simultaneously achieved with the formation of the inorganic network; after opening of the epoxy ring, a large variety of possible reaction pathways and side reactions are possible. The epoxy group is capable of forming either glycol units by hydrolytic ring opening or polyethylene oxide chains (PEO) of different lengths by polymerization. Epoxy groups react to form poly(ethylene oxide) chains *via* photo[29]-or thermal[30]-induced polymerization or *via* basic[4,31]or acidic catalysts[3]. The final properties of GTPMS hybrid materials are, in any case, strongly dependent on the catalyst for epoxy reactions.

The simultaneous polymerization of the inorganic and organic network is a competitive process [32] ; a faster polycondensation rate of the inorganic network hinders the polymerization of the organic network and *vice versa*. This process can be controlled by the amount and nature of reaction promoter or catalyst employed[33]. From this description is clear as the control of the organic polymerization is a crucial step in the synthesis of these hybrid materials, because most of the final properties, such as mechanical[34] and optical characteristics, are affected by the length of the chains, the degree of interconnection between the organic polymers, and the homogeneity of the material. The

very fine control of the polymerization is, however, a more difficult task than in pure organic polymers, because the two covalently linked organic and inorganic networks are formed at different rates and yields.

In the present study we have investigated the reactions in highly basic conditions (pH 14) of GPTMS by liquid state nuclear magnetic resonance (NMR).We have studied the extent of the reactions as a function of aging time and we have presented the possible reaction pathways whose control is necessary to obtain a hybrid material of tunable properties.

Beside aging of basic catalysed solventless sols of (GPTMS), allowed the formation of crystals of some millimetres through opening of the epoxy and formation of organosilica lamellar crystals. This process is slow and is kinetically controlled, formation of crystals up to a millimetre scale can be observed during aging of the precursor sol. Because this self-organization is kinetically controlled and slow evaporation is necessary, the formation of hybrid crystals in thin films has been impossible to obtain up to now. In the present work we have tried to extend the formation of hybrid crystals to thin films, which are very important for applications, especially in photonics. This represents a quite challenging task because several requirements have to be fulfilled, such as optical transparency, and controlling of the properties that are added by nanocrystals.

We have also studied how we could achieve an efficient controlling and understanding of the kinetic process that allows formation of crystals in the films. We have varied some key processing parameters such as aging time and aging temperature, and we have studied how they affect the self-organization process through the study of the siloxane condensation and epoxy opening reactions.

Controlling the processing conditions of layered hybrid nanocrystals formation in hybrid coatings is an important step to produce new functional devices based on hybrid materials.

Finally we have demonstrate that the hybrid films prepared by sol-gel method employed GPTMS and DEPES as precursors in basic condition can be used for the microfabrication and this open the route to develop new functional materials.

NMR STUDY OF THE REACTION OF GPTMS IN HYGHLY BASIC CONDITION

Abstract

The multinuclear magnetic resonance is a powerful tool which allows to obtaining information about the reactions. We have used multinuclear magnetic resonance and light scattering techniques to study the reactions of 3-glycidoxypropyltrimethoxysilane in a highly basic aqueous solution. In this specific chemical environment the alkoxy groups of 3-glycidoxypropyltrimethoxysilane undergo a fast hydrolysis and condensation which favor the formation of open hybrid silica cages. The silica condensation reaches 90% at a short aging time but does not go to completion even after 9 days.

The highly basic conditions also slow down the opening of the epoxies which fully react only after several days of aging. The epoxy opening generates different chemical species and several reaction pathways have been observed especially the formation of polyethylene oxide chains, diols, termination of the organic chain by methyl ether groups and formation of dioxane species. These reactions are slow and proceed gradually with aging. The light scattering analysis has shown that clusters of dimensions lower than 20 nm are formed after two days of reactions, but their further growth is hindered by the highly basic conditions which limit full silica condensation and formation of organic chains.

4.1.1 Material preparation

3-Glycidoxypropyltrimethoxysilane (GPTMS 96% Aldrich) was used as the organically modified alkoxide, sodium hydroxide, NaOH, (Aldrich 98%) as the basic catalyst and distilled water for hydrolytic reactions; all the reagents were used as received without further purification.

The molar ratio of the components was GPTMS: H2O: NaOH = 1:5:0.1671; in a typical preparation GPTMS (20 cc) was added dropwise to a NaOH aqueous solution (8 cc, 1.85 M, pH >14) under stirring at 25 °C; the sol became transparent in a few minutes after the addition of GPTMS.

In-situ ^{13}C, ^{1}H and 29Si NMR measurements were carried out by using a Bruker AVANCE spectrometer, operating at a proton frequency equal to 400.13 MHz; chemical shifts were referenced towards dissolved tetramethylsilane (0 ppm). D_2O, instead of water, was used as solvent to acquire the NMR spectra in a 5 mm diameter capillary tube. The capillary tube was sealed and maintained closed during the full duration of the experiment. ^{29}Si-NMR spectra were recorded with a 300 ppm spectral width using a 90° excitation pulse and ^{1}H decoupling. The number of scans was between 500 and 1000 depending on the signal-to-noise ratio, the recycling delay was 45 s to ensure complete longitudinal relaxation, which was estimated to be around 20 s for the different samples. ^{13}C-NMR spectra were recorded by using a 240 ppm spectral width, centred at 115 ppm, using between 1 k to 8 k scans depending on the signal-to-noise ratio; the sequence was a 90° excitation pulse for ^{13}C and ^{1}H decoupling. The recycling delay was set at equal to 15 s to ensure complete longitudinal relaxation which was estimated to be in the range of 5–8 s for the different samples. Lorentzian functions were chosen for spectra modelling; the amount of each species was obtained from the areas of the deconvoluted signals.

Light scattering measurements were carried out by a LB-500 Dynamic light-scattering (DLS) particle size analyzer operating with a diode laser. The measurements were performed at room temperature and the working range for the determination of particle size is from 2 nm to 6 nm.

4.1.2 NMR Characterization

The NMR spectroscopy is a powerful instrument to investigate the mechanism of reaction of the GPTMS in a highly basic aqueous solution. We followed the reactions of the

GPTMS at a pH around 14 and in a closed vessel during several days of reactions by *in-situ* ^{29}Si, ^{13}C and ^{1}H NMR. The experiments were performed by recording the spectra from the GPTMS solution kept in the silica capillary tube for increasing aging times. After the addition of GPTMS to the aqueous NaOH solution, the sol turns opaque, but within a few minutes of reaction it becomes transparent. Even after several months of aging, if the sol is kept in a sealed container, it remains transparent without gelation

^{29}Si NMR spectroscopy

We at first followed the reactions of the triethoxysilane moieties at a pH around 14 and in a closed vessel during several days of reactions.

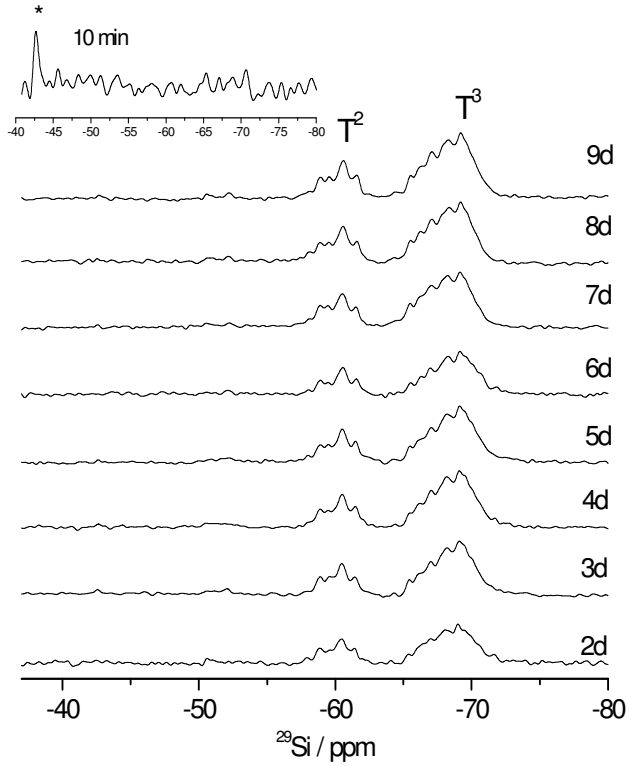

Figure 4.1- The ^{29}Si NMR spectra of the GPTMS in a highly basic solution system during the

Figure 4.1 shows the ^{29}Si NMR spectra of the GPTMS system over 10 min, and from 2 to 9 days of aging. From the spectrum taken from a 10 min aged solution we have observed only one sharp signal at −42.7 ppm, these signal is assigned to silicon in R-Si-$(OH)_3$ moieties[34] derived from GPTMS which appears fully hydrolyzed immediately after mixing with water.

^{29}Si NMR spectroscopy yields information on the connectivity of the siloxane bonds. The tri-functional silicon sites are labeled with the conventional T^n notation, where the superscript n denotes the number of siloxane bonds. During the aging we have observed a broad peaks located in two regions centred around = −60 and −68 ppm, assigned to T^2 and T^3 species, respectively. We have studied the overlapped peaks in this two regions after Lorentzian deconvolution of these broad peaks.

The degree of condensations were determined by the integration of each T^n species with the equation: $(T^1+2T^2+3T^3)/3(T^0+T^1+T^2+T^3)$[35] The condensation degree of siloxane exceeds 90% after 2 days whilst epoxy opening and polymerization resulted much slower. The several peaks in the T2 and T3 regions are sharp and overlapped indicating the presence of different types of well defined siloxane environments. The simulated Lorentzian curves obtained from the 9 days aged sol are shown in Figure 4.2a (T^2) and 2b (T^3). We have resolved 4 Lorentzian components for T2 and 6 Lorentzian components for T^3 siloxane units and we have tentatively assigned these signals on the basis of the literature[36,37,38,39,40,41] .

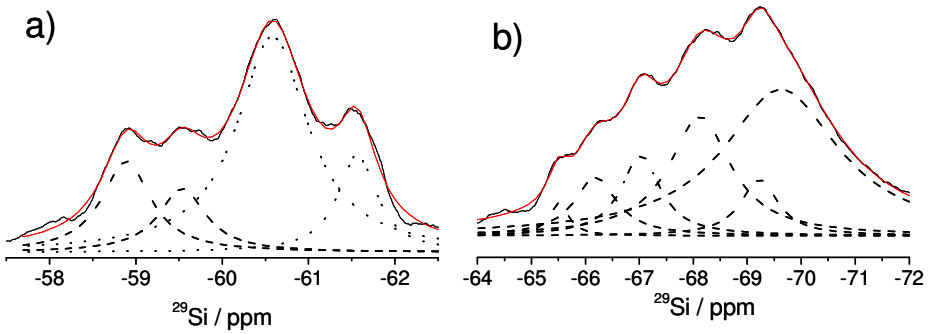

Figure 4.2- The deconvoluted ^{29}Si NMR spectrum of the GPTMS system with 9 days of aging.

From these spectra we have obtained some information about the formation of several types of cyclic or even ladder like structures. The signals at −65.4, −66.2, −67, −68.1, −69.2 ppm are assigned to T^3 units in cubic T^8 cage structures[41], and the signal at −69.6 ppm to condensed siloxane species not in cyclic units. T^2 signals are resolved at −58.9, −59.5, −60.6 and −61.6 ppm and are an indication that a significant part of the T^8 cages are not completely condensed, with one of the bonds between silicon atoms not formed, leaving an open cage[40]. This is in accordance with the reaction conditions that are expected at very high pH; the cyclization of organically modified alkoxides[38] is a known phenomenon that can be observed in highly acidic or basic conditions. Epoxy functional polyhedral oligomeric silsesquioxanes (POSS) are used to build up different types of hybrid nanocomposites[39] and are commercially available (Glycidil POSS of formula $(C_6H11O_2)n(SiO_{1.5})n$ (with n = 8, 10, 12). Some authors (Matijeka 40 *et al*) has showed the formation of cages for GPTMS during hydrolytic reactions catalyzed by benzyldimethylamine, dibutyltin dilaurate or *p*-toluenesulfonic acid. In the present work, we observe that the hydrolysis of silicon alkoxy groups is completed in 10 min of reaction while condensation of siloxane is estimated at around 91% after two days of aging and does not change even in sols aged at longer times (figure 4.1). This means that at the high pH of the sol a fast hydrolysis is accompanied by a relatively fast and extended siloxane condensation which, however, does not go to completion, even at long aging times; in a closed environment we do not observe, in fact, gelation of the sol. This situation promote the formation of highly hydrolyzed species that are pushed to form cyclic structures but on the other hand can not be fully condensed and tend to form open cubic cages[32,42] .

^{13}C NMR spectroscopy

In the scheme 1 is showed the different carbon atoms in GPTMS, these are marked from 1 to 6 .We have followed the reactions of the epoxy group at a pH around 14 and in a closed vessel during several days of reactions, like for the ^{29}Si NMR spectroscopy.

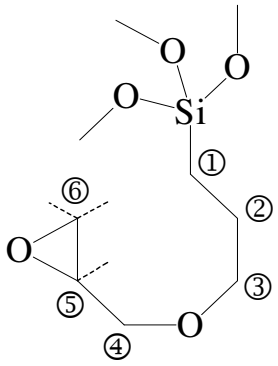

Scheme 4.1- The GPTMS molecule

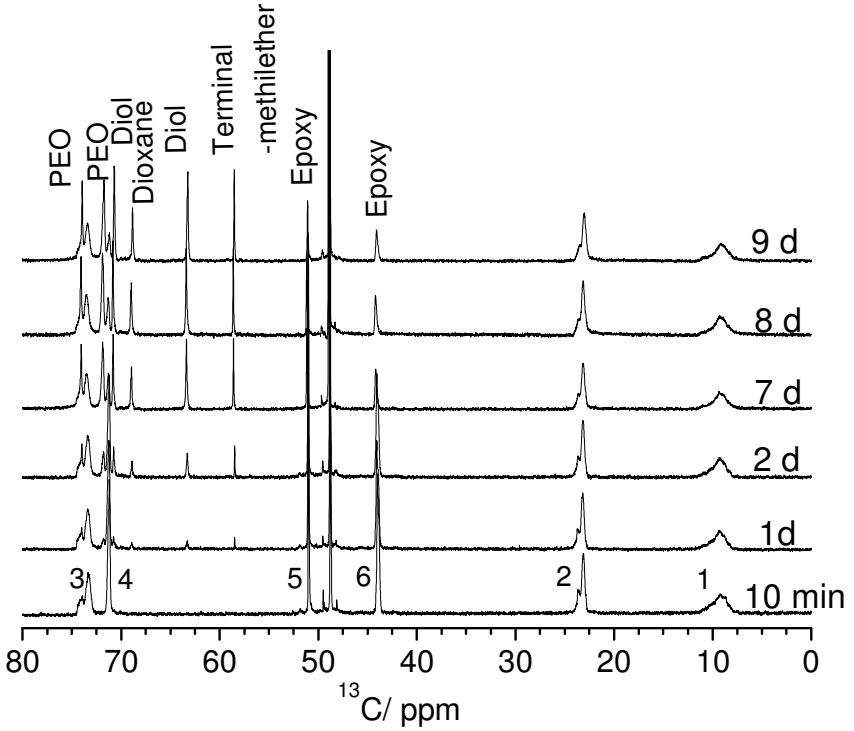

Figure 4.3 – ^{13}C NMR spectra of GPTMS in a highly basic solution at different aging times.

Figure 4.3 shows the ^{13}C NMR spectra of the sol aged up to 9 days. On the basis of our previous work[29,32-34,43,44] we have attributed the different ^{13}C NMR signals presented on the figure 4.3.

Table 4.1. Assignment of the chemical shifts observed by ^{13}C NMR experiments in the liquid precursor sol with aging.

δ (^{13}C) (ppm)	**Assignment**	**Comment**	**References**
10	≡Si-**C**H_2-CH_2-	**1**	**[36] ,[37], [32], [33],**
24	≡Si-CH_2-**C**H_2-	**2**	**[36] ,[37], [32], [33],**
73	-CH_2-**C**H_2-O-CH_2-	**3**	**[36] ,[37], [32], [33],**
71	-CH_2-CH_2-O-CH_2-	**4**	**[37], [32], [33**
52	CH_2(-O-)-**C**H-	**5** in epoxy ring	**[36] ,[37], [32], [33],**
45	**C**H_2(-O-)-CH-	**6** in epoxy ring	**[36] ,[37], [32], [33],**
59	-O-CH_2-C(OH)-CH_2-O-**C**H_3	Terminal methyl ether group	**[28] , 36] ,[37], [32], [33],**
74	-[CH_2-**C**H(R)-O]$_n$--CH_2-O-**C**H(R)- (R :- CH_2-O-)	**5** in the PEO chains and in dioxane	**[[28] , 36] ,[37], [32], [33],44],[45]**
72	-O-[**C**H_2-CH(R)-O]$_n$--O-**C**H_2-CH(R)-O- (R :- CH_2-O-)	**6** in PEO chains and **4** in propyl group	**[28] , [36] ,[37], [32], [33],44],[45]**
70	-O-CH_2-C(OH)H-**C**OH	**6** in diols	**[37], [42]**
49	Si-O**C**H_3 H-O**C**H_3	Carbons in residual methanol or methoxy groups	**[36],[37], [32],**
64	-O-CH_2-C(OH)H-COH	**5** in diols	**[36], [37], [42],**
69	-**C**H_2-O-CH-	**6** in dioxane	**[28]**

Carbons in positions 5 and 6 are assigned to the epoxy group; we have used these signals to trace the evolution of the opening reactions during aging.

From these data we can observe that the ring opening is not a fast process under highly basic conditions and appears to proceed with an almost constant rate with the aging time; this is confirmed by the decrease of epoxy signals 6 (43 ppm) and 5 (52 ppm).

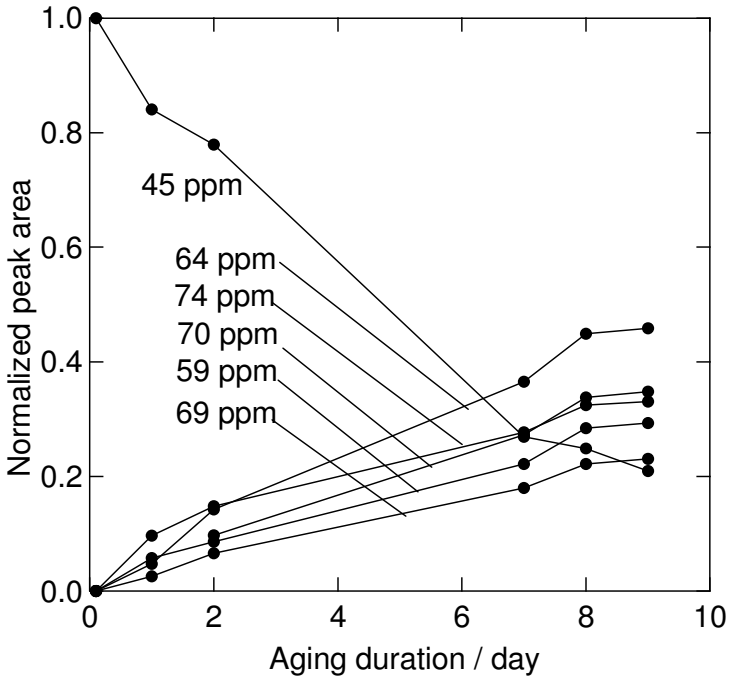

Figure 4.4 – Normalized peak intensity as a function of aging time of peaks 45 ppm, 59 ppm, 64 ppm, 69 ppm, 70 ppm, 74 ppm observed in ^{13}C NMR spectra of GPTMS.

Figure 4.4 shows the change of the normalized areas of the different carbon signals as a function of aging time of the sol. The opening reaction of the epoxy groups is accompanied by the appearance and increase of different signals; these are an indication that several side reactions and reaction pathways of epoxy groups in GPTMS can be activated in the Table 4.1 are reported the signals and the respective assignments.

Carbons in positions 3 and 4 in GPTMS (Scheme 4.1) are found at 73 and 71 ppm, respectively. We observe the rise of a peak at 59 ppm after one day of reaction which gradually increases in intensity with aging time (Figs. 4.3 and 4.4); we assign this signal to the carbon in the terminal methyl ether groups (Table 4.1). These species are formed upon reaction of open epoxy with methyl alcohol that is a by-product of the hydrolysis of the methoxy groups. A similar trend is observed for carbon signals at 64, 69, 70 ppm, they start to appear after one day of reaction and steadily increase in intensity with aging time (Figures 4.3 and 4.4). These signals indicate that different reaction pathways of the

epoxy in the basic aqueous environment are activated. The couple of signals at 64 and 70 ppm are assigned to diols formed by hydrolytic opening of the epoxy[44]; this reaction proceeds with time as soon as more epoxies react. The other carbon signal at 69 ppm has a similar trend and is due to the formation of dioxane species by the reaction of diols[28]. The slow formation of this chemical species gives linear compounds that have been observed to generate hybrid layered crystals through self-organization[28].With the increase of aging time we also observe the rise of sharp peaks in the 70–75 ppm range; the carbon signals at 72 and 74 ppm are the typical signature of the formation of ethylene oxide chains in GPTMS based hybrids[45].These signals are characteristic of C atoms in oligo- or poly(ethylene oxide) (PEO) derivatives (-[-CH_2-CH(R)-O]*n*-; R: organic functional group) formed from a ring-opening reaction of the epoxy groups[46]. The sharp character of the signal indicates that the ethylene oxide chains are not extended and oligomeric species are formed.

^{1}H NMR spectroscopy

We have also used ^{1}H NMR analysis to follow the GPTMS reactions during aging in the aqueous basic conditions, the assignments of the observed signals were based on previous work[32,22] and the database[47]. On the figure 5 are showed the ^{1}H NMR of the sol during 9 days of aging.

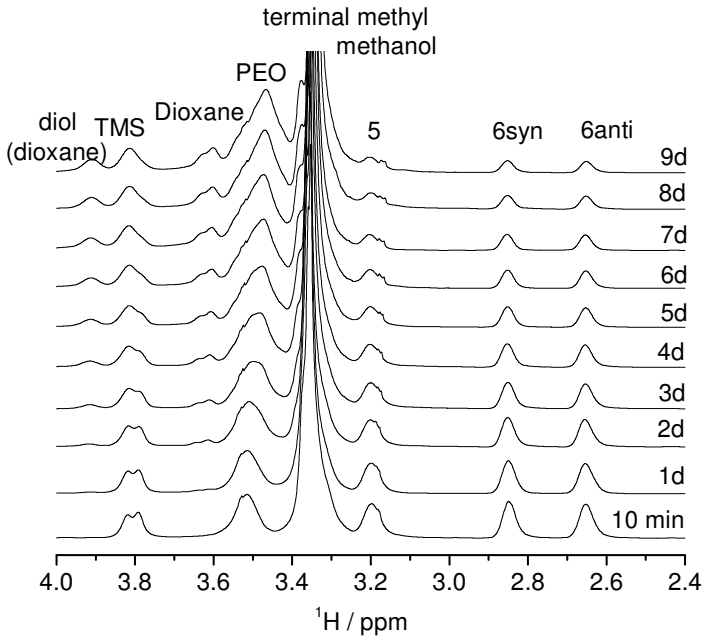

Figure 4.5 - ^{1}H NMR spectra of GPTMS in a highly basic solution at different aging times.

The two unequivalent protons bonded to carbon in position 6 give wide bands peaking at 2.65 ppm (6anti) and 2.85 ppm (6syn), while the proton bonded to carbon in position 5 gives a signal at 3.2 ppm. The relationship between the signal of carbon 6 in the epoxy ring and the signal of the proton 6anti is shown in Figure 4.8 were we have normalized the 6anti and carbon 6 signals to the peak of the spectrum after 10 min of aging.

The peak around 3.33 ppm is attributed to protons in methanol and the shoulder at 3.37 ppm to hydrogen in terminal methyl ether groups (-O-CH_2-C(OH)-CH_2-O-CH_3). At 3.51 ppm the band assigned to protons bonded to carbon 4, is observed; this signal broadens in the samples aged for more than two days. This effect is due to the rise of a new overlapped signal at 3.46 ppm which increases in intensity with aging and is attributed to

protons bonded to carbons in polyethylene oxide chains formed upon reaction of epoxies. We have observed in these spectra some peaks which indicate the formation of new species during the opening of epoxy groups. ^{1}H NMR spectra show peaks around 3.62 ppm and around 3.90 ppm, both these peaks increase during aging time, and are due to protons in the dioxane ring (O-C*H*$_2$-CH-) and diol species, respectively. As observed from ^{13}C NMR data the epoxy ring opening is not a fast process and has an almost constant rate with the aging time (Figure 4.5). These processes are accompanied by the appearance and increase of different signals indicating that several side reactions and reaction pathways of epoxy groups in GPTMS can be activated as described (Scheme 4.3). The signal at 3.81 is assigned to the proton bonded to carbon 4, 4*b*.

4.1.3. Dynamic light scattering characterization

We have also obtained some information about the reaction of GPTMS in highly basic aqueous solution at pH 14 by light scattering measurements. This technique allows monitoring the dimension of the species in solution.

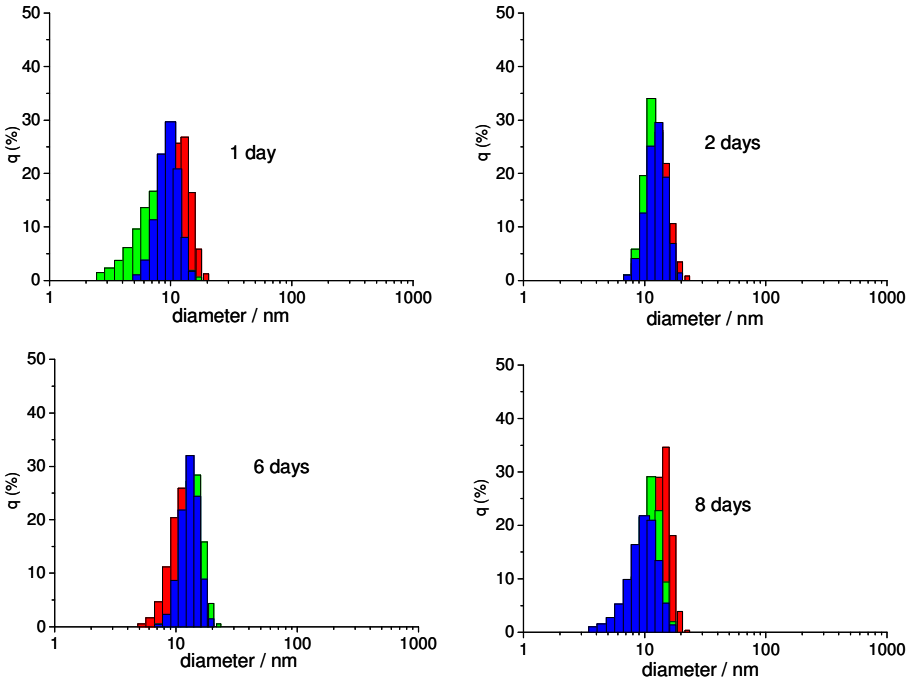

Figure 4.6 – Light scattering analysis of aged GPTMS sols. The colours indicate the different sampling of each solution.

We have made a series of measurements over 10 days (figure 4.6) to evaluate the formation of small particles and to monitor the dimensional changes during aging.

The appearance of the sol during aging in a sealed glass bottle is homogeneous and transparent; from light scattering measurements we have evaluated a particle size of 10 nm after 2 days of reaction (Figure 6). After this time we have not observed any other change; the size of the aggregates remains around 10 nm, we observe a small change in distribution with increasing aging time but not changes in the average size.

4.1.4. The reaction of GPTMS on highly basic aqueous solution

The hydrolytic reactions of GPTMS under highly basic conditions are realized in a very peculiar environment which is expected to affect in a significant way the sol–gel reactions of the hybrid organic–inorganic material. GPTMS is an organically modified alkoxide bearing an epoxide, the final material will be a hybrid resulting from the siloxane polycondensation (the inorganic network) and the polycondensation reactions upon opening of the epoxide (the organic chains). The highly basic conditions are expected to slow down the polycondensation of silica and the epoxy opening reactions.

The relative rate of these reactions is the key parameter to be controlled to obtain a hybrid material with a tailored final structure.

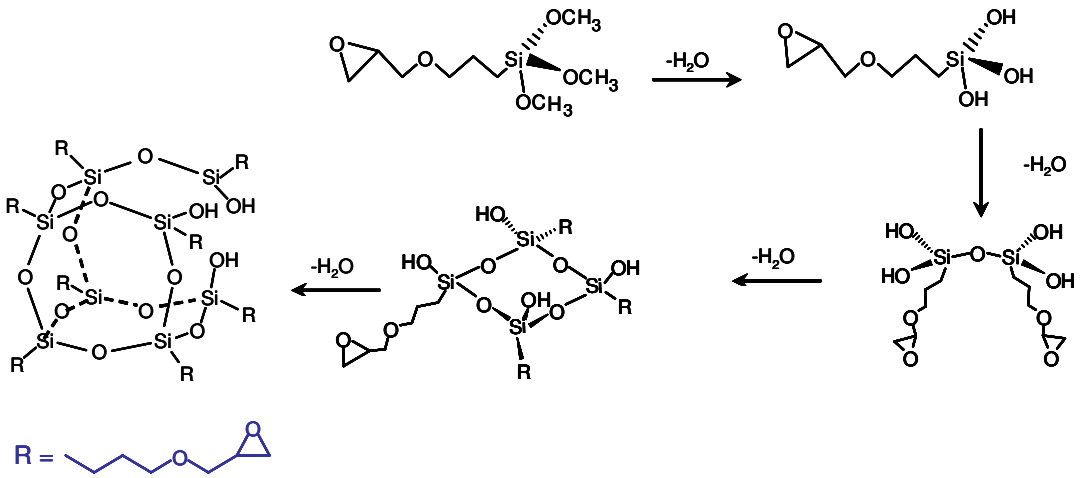

Scheme 4.2- Open Silica hybrid cage formation

The information obtained from the analysis of the ^{29}Si NMR spectra, permit to understood the mechanism of reaction of the GPTMS in a highly basic aqueous solution.

A simplified scheme of the open silica hybrid cage formation is shown in Scheme 4.2.

The hydrolysis of GPTMS produces silica nano-building units resembling silsesquioxane species. In Scheme 4.2 we have not shown the reaction pathway of the ladder like structures, whose presence is however indicated by ^{29}Si NMR.

The formation of the hybrid organic–inorganic structure is very much dependent on the relative rates of inorganic condensation and polymerization of the epoxy after opening. We have seen that in highly basic conditions the fast hydrolysis and the peculiar condensation conditions promote the formation of cubic open cages, which do not fully condense. This indicates that the inorganic silica structure is not closely interconnected and there is enough room to accommodate the organic chains that could be formed by the epoxy opening reactions.

We have sketched the different reaction pathways of epoxy in the present synthesis conditions in Scheme 4.3.

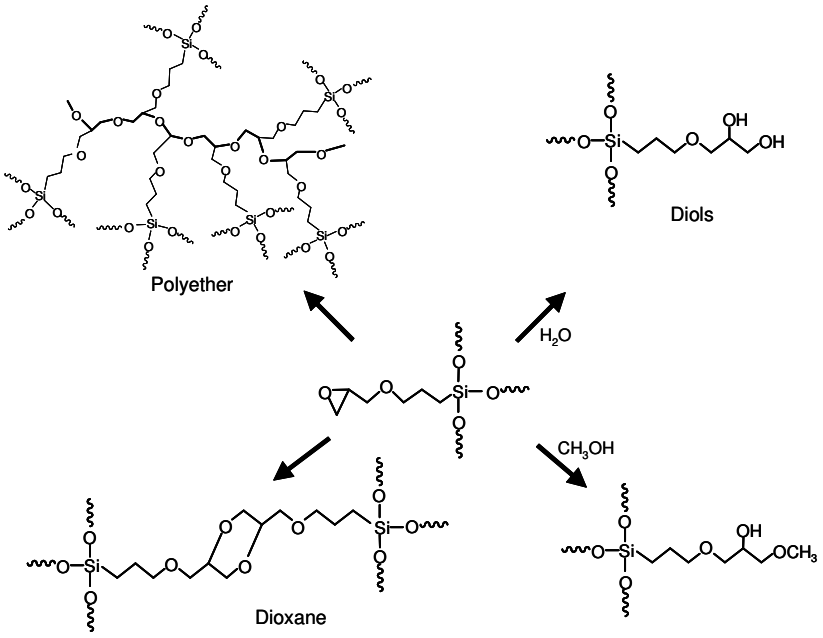

Scheme 4.3- Formation of different moieties from the opening reaction.

Epoxy ring opening is a slow process that proceeds with aging time. After epoxy opening we can observe the formation of different chemical species: diols; dioxane rings by reaction of opened epoxies; formation of terminal methyl ether species by reaction of an open epoxy with methanol and finally polyaddition reactions to form polyether chains.

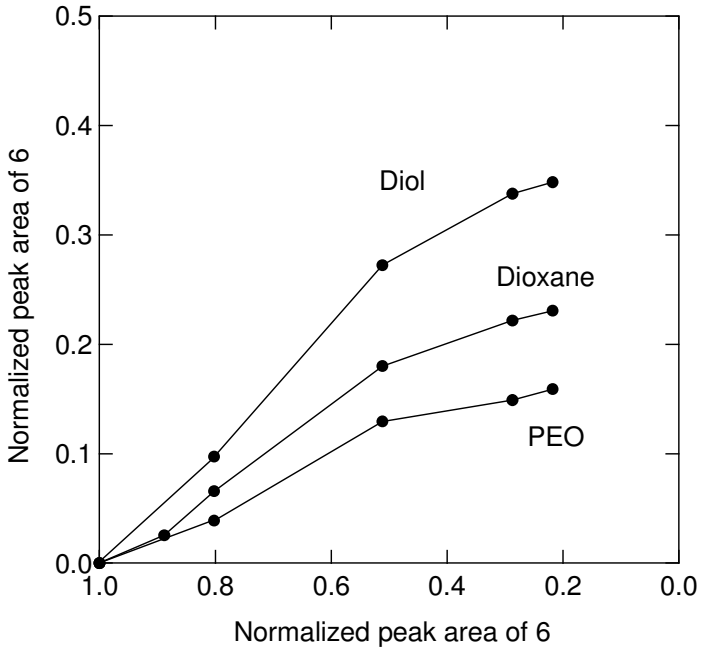

Figure 4.7– Correlation between the peak intensity normalized to the spectra taken after 10 minutes of carbon 6 in epoxy ring and that in products such as diols, dioxane, and PEO.

Figure 4.7 shows the correlation between the decrease of carbon 6 in the epoxy ring and the increase of that signal in the products.From this figure we can see that the dominant product of the epoxy reactions is diols while the formation of PEO chain seems less effective than the one of other products.

This is explained by the advanced siloxane condensation at short aging times which hinders both the intra- and intermolecular condensation of epoxy rings through the steric effect.

The plot in Figure 4.8 shows that there is very good agreement between the NMR data from the ^{13}C and ^{1}H spectra.

We have evaluated from the integrated intensity of these ^{1}H signals that around 90% of the epoxies are opened after 9 days of reaction. As observed from ^{13}C NMR data the

epoxy ring opening is not a fast process and has an almost constant rate with the aging time; these processes are accompanied by the appearance and increase of different signals indicating that several side reactions and reaction pathways of epoxy groups in GPTMS can be activated as described in Scheme 3.

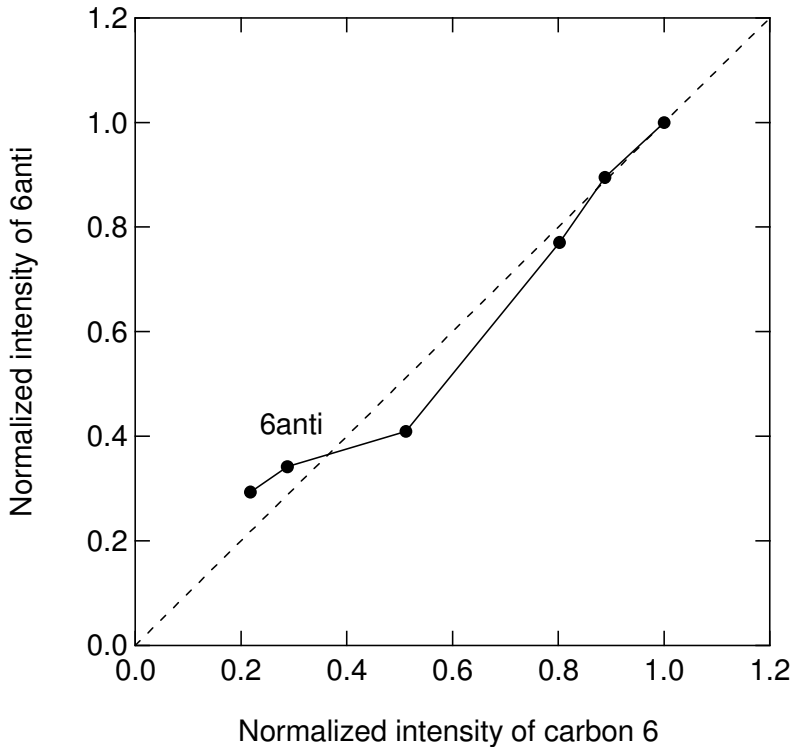

Figure 4.8 - Correlation between normalized peak intensity of carbon 6 and proton bonded to carbon 6 at 2.6 ppm (6_{anti}).

The DLS measures give a direct indication that the sol does not gel after several days of aging and that after the first stage of fast hydrolysis and condensation the silica clusters stop to grow. From ^{29}Si NMR spectra we have observed after 2 days the formation of open cyclic siloxane species, the light scattering measures indicate that there is a critical dimension of these organic-inorganic hybrid clusters which is around 20 nm. The organic-inorganic hybrid clusters they stop growing beyond this dimension because polycondensation reactions are strongly hindered by the highly basic conditions. From these NMR study we have observed the important role played by the organic chains that

are formed with the opening of the epoxies; they reduce the interactions between silica clusters and the condensation.

4.1.5. Conclusions

3-Glycidoxypropyltrimethoxysilane in a highly basic aqueous environment shows condensation reactions that are kinetically controlled. The reaction of alkoxy in GPTMS forms preferentially open cages structures and the silica condensation does not go to completion even after long times of aging even if a high condensation degree, up to 90%, is observed after two days. On the other hand formation of siloxane bonds affects the epoxy opening kinetics, which is much slower in comparison with the silica condensation. The opening reactions of epoxies form different chemical species: diols; dioxane rings by reaction of opened epoxies; formation of terminal methyl ether species by reaction of an open epoxy with methanol and finally polyaddition reactions form polyether chains of short length. Controlling the complex reactions of 3-glycidoxypropyltrimethoxysilane will allow us to obtain advanced hybrid materials with engineered structures, such as self-organized hybrid crystals described in the next section.

FORMATION OF HYBRID NANOCRYSTALS BY SELF-ORGANIZATION PROCESS

Abstract

Organic-inorganic hybrid films containing organosilica nano-crystals have been obtained by an alcohol-free hydrolytic sol-gel process from a mono-functionalized organically modified alkoxide. To design this organic-inorganic hybrid nanocomposite films a kinetically controlled self-organization has been used. Nanocrystals of around 100 nm in diameter and 4 nm in thickness have been formed in transparent hybrid films prepared from the aged sol. From measurements of refractive index we have observed that the films exhibit an optical anisotropy ($\Delta n > 10^{-3}$); these measurements and from TEM observation indicating that the layered nanocrystals are oriented within the hybrid film.

4.2.1. Materials preparation

All the regents were used as received without further purification. All the preparation processes were carried out at ambient atmosphere. 3-glycidoxyproplytrimethoxysilane (GPTMS, 96% Aldrich) and sodium hydroxide (98%, Aldrich) were used as a hybrid precursor and the basic catalyst, respectively. The molar ratio of the components was GPTMS : H_2O : NaOH = 1 : 5 : 0.1671. The prescribed amount of GPTMS (20 cc) was added dropwise to NaOH aqueous solution (8 cc, 1.85 M, pH13) under vigorous stirring for 45 minutes without lid. Then the reaction container was sealed with a lid and the solution was stirred for one night. The obtained sols were aged in an ambient temperature with a lid. To control the viscosity of the sol, 5 cc of the NaOH aqueous solution was added to the solution aged for 10 days. It was confirmed that IR and XRD spectra did not show any apparent change between films obtained before and after the addition of NaOH

aqueous solution. The hybrid films were deposited on silicon or silica substrate by spin coating (Mikasa MA-10) with 5000 rpm rotation speed for 20 seconds.

4.2.2. Material characterization

The infrared analyses were performed with a Nicolet Nexus FTIR spectrometer in a transmission mode in the range 400-4000 cm^{-1}; the data were collected over 256 scans with a resolution of $4cm^{-1}$. FTIR spectra were recorded using KBr pellets prepared by powder obtained by scratching the film surface.

The low-angle x-ray diffraction patterns were collected in the angular range from 2 to 15° in 2θ, using a Bruker D8 instrument in the Bragg-Brentano geometry with a copper tube (λ = 1.54056 A). The X-ray generator was working at a power of 40 kV and 40 mA. The patterns were scanned several times and averaged at each data points until minimizing the counting error to a satisfactory level. The spectra were normalized respect to the peak at 22^{o}.

Transmission electron microscopy (TEM) images were obtained on a JEOL 200CX microscope equipped with a tungsten cathode operating at 200 kV. Prior to observation, the sample was removed from the glass substrate and deposited on a carbon-coated copper grid after gentle grinding on an agate mortar.

The refractive index was measured by using a prism coupling method (Metricon 2010) by a using 633 nm radiation from a He-Ne laser.

In-situ ^{13}C and ^{29}Si NMR measurements were carried out by using Bruker AVANCE spectrometer, operating at a proton frequency equal to 400.13 MHz. Chemical shifts were estimated in ppm with respect of the reference tetramethylsilane (0 ppm). NMR spectra were acquired by dissolving the correct amount in 0.7 mL deutered solvent (D_2O) in a 5 mm NMR tube. ^{29}Si-NMR spectra were recorded with a 300 ppm spectral width using a 90° excitation pulse and 1H decoupling. Number of scans were between 500 and 1,000 depending upon signal-to-noise ratio, delay between scans was 45 seconds to ensure complete longitudinal relaxation. ^{13}C-NMR spectra were recorded by using a 240 ppm

spectral width, centered at 115 ppm, using between 1k to 8k scans depending upon signal-to-noise ratio. Sequence was a 90° excitation pulse for ^{13}C and 1H decoupling. Delay between scans was set equal to 15 seconds to ensure complete longitudinal relaxation.

4.2.3. FTIR characterization

In the previous section we have describe the evolution of the sol during aging monitored by nuclear magnetic resonance (NMR). We have obtained information about the reaction also from the Fourier transform infrared (FTIR) spectroscopy. Figure 4.9 show the FTIR spectra of the organic-inorganic hybrid film prepared from the sol whit different aging time in the region 3600-400 cm^{-1}.

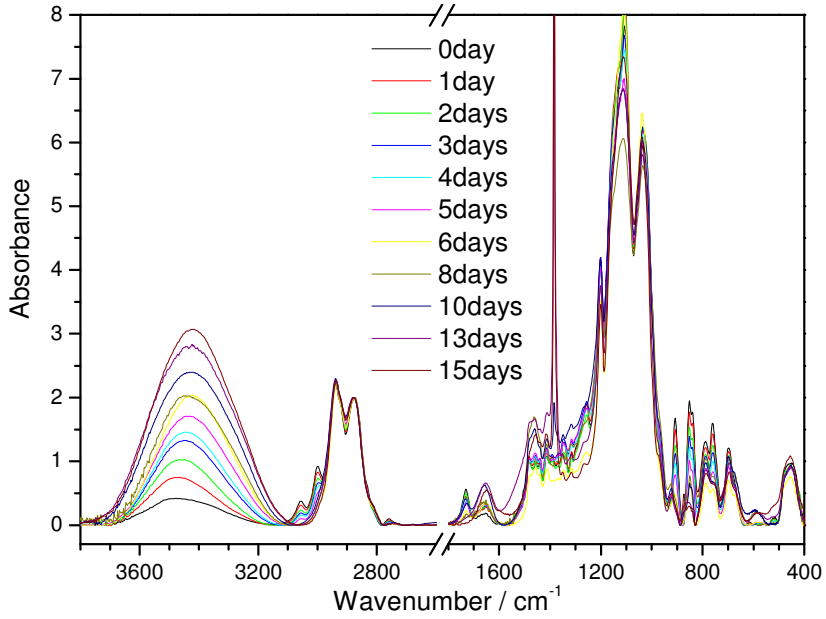

Figure 4.9- The FT-IR absorption spectra prepared from the sols with different aging time.

In the figure 4.10 is showed in particular the FTIR absorption spectra of hybrid films obtained from sols of different aging times in the range 3800-2600 cm^{-1}. In this region we can see two bands 3000 and 3055 cm^{-1} bands assigned to C-H stretching in the epoxy ring[48]. These two bands decrease during the aging indicating the decrease of epoxy ring with the sol aging. After 15-days aging the epoxy ring signals disappear, and we observe

the formation of hydrolyzed species, glycol and polymerized one, poly/oligo(ethylene oxide).

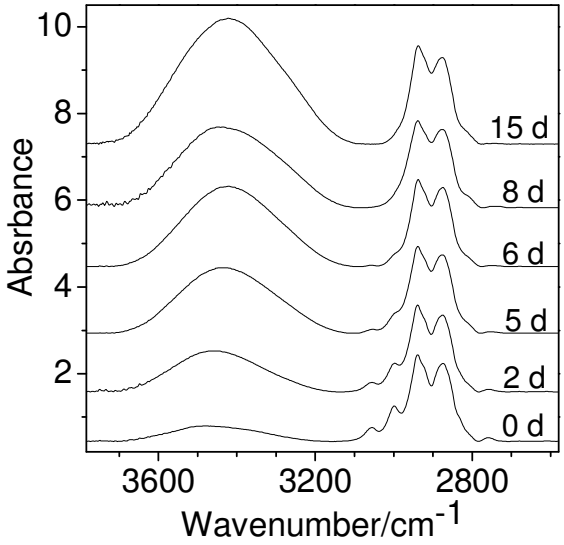

Figure 4.10- FT-IR spectra of the hybrid films in the region 3800-2600 cm^{-1}

From these spectra we can observe the different behaviour of the band 3400 cm^{-1} . This bands, the wide O-H stretching band peaking, shows an opposite trend with respect to the epoxy and increases with aging time. This band is formed by the overlapping of several species that we can identify in silanols and adsorbed water (~3200 cm^{-1})[49]. To separate the two contributions as a function of aging time we have done 2D correlation analysis [50] . In the figure 4.11 the synchronous and asynchronous spectra are showed. From these spectra we can obtain several information: the asynchronous spectra allow identification of two contributions of different sign; comparison with the synchronous spectra indicates that the component at lower wavenumber (adsorbed water) has the same sign of the synchronous diagonal peak, while the other asynchronous component (silanols) has a negative sign.

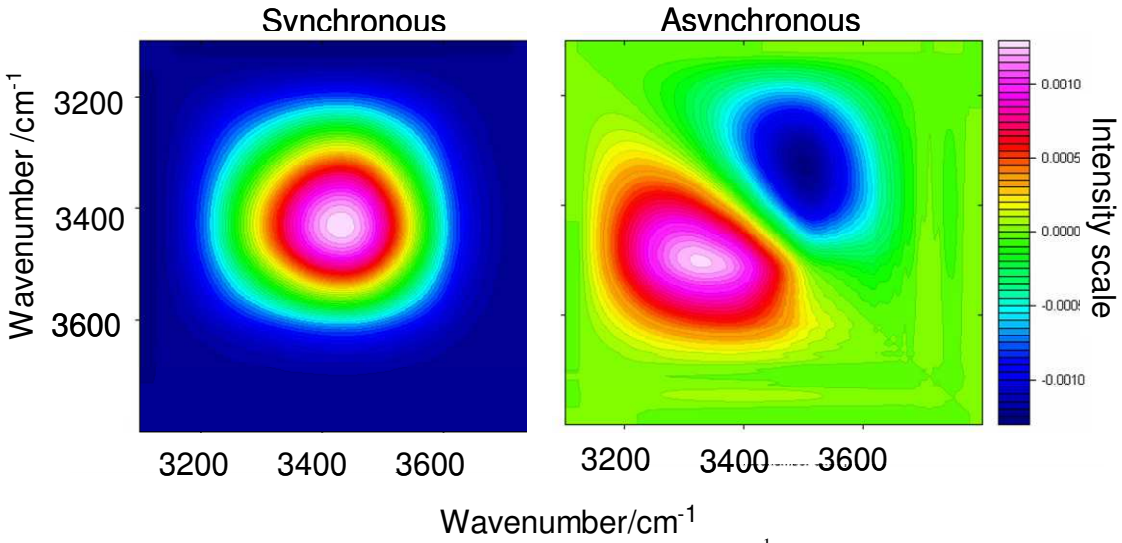

Figure 4.11- 2D correlation analysis in the region 3800-3000 cm^{-1}

4.2.4. XRD characterization

The evolution of the organic-inorganic hybrid films prepared from the sol whit different aging time was studied also by XRD diffraction. Figure 4.12 shows the X-ray diffraction (XRD) spectra of the hybrid films obtained from the sols of different aging times.

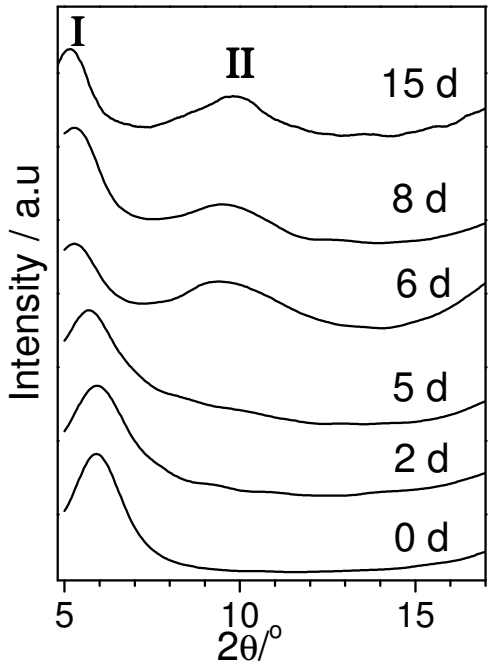

Figure 4- XRD spectra of the hybrid film prepared from the sol with different aging time.

The hybrid film deposited from the as-prepared sol (0 aging day) shows a signal at 5.95° (d = 1.48 nm), which is due to intermolecular correlation of siloxane chains in an amorphous state[51].

The correlation length (peak I) increases with the aging time of the coating sol from d = 1.48 nm (0 day) to 1.66 nm (15 days) lake showed on the figure 4.13 indicating the formation of poly/oligo(ethylene oxide) as side chains of the siloxane framework.

After 5-days aging, a new XRD peak is observed at 9.61° (d = 0.923 nm) (peak II), the diffraction angle of the peak does not show any dependence on sol aging as we can see from the figure 4.12.

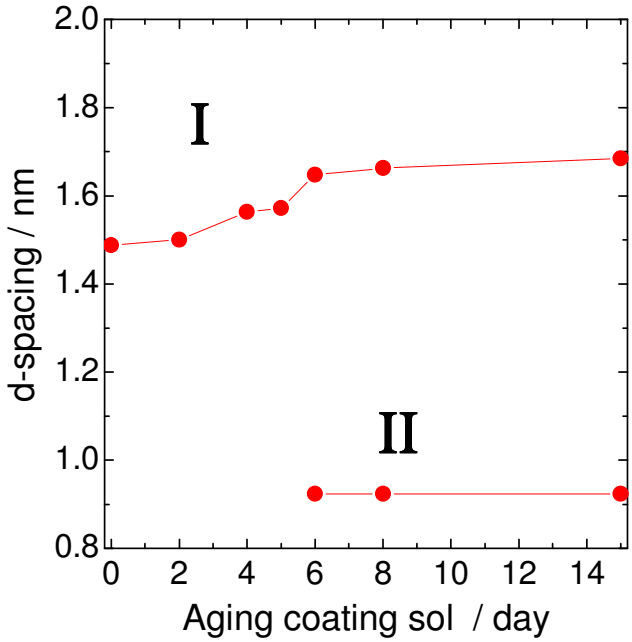

Figure 4.13- Evolution of d-spacing evolution of the peak I and II with the aging time

This signal, so-called a basal peak [52], is the signature of the formation of a long-range ordered lamellar structure. The thickness of the layered crystals has been calculated to be around 4 nm applying the Scherrer equation to the basal peak in figure 4.13.

4.2.5. TEM characterization

The formation of organic-inorganic nano-crystals within the hybrid film has been confirmed from a direct observation by transmission electron microscopy (TEM).

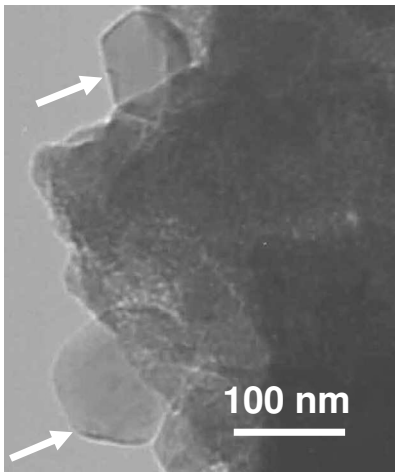

Figure 4.14- TEM images of the htbryd nanocrystals embedded in the hybrid matrix.

The images taken from scratched fragments of the 15-days aged sol films show nanocrystals of 103 ± 24nm in diameter. The TEM observation indicate that the organic-inorganic hybrid crystals show a preferential orientation parallel to the substrate, like also indicate from the mesueraments of refractive index discuss in the next paragraph.

4.2.6. Optical properties

An optically transparent silica-based hybrid films have been obtained from the GPTMS sol after aging at different times in controlled conditions (up to 15 days). The GPTMS sol was spin-coated on glass or silicon substrates. In the figure 4.15a) is showed the

appearance of the organic-inorganic hybrid films deposited on glass substrate from the sol with 15 days of aging.

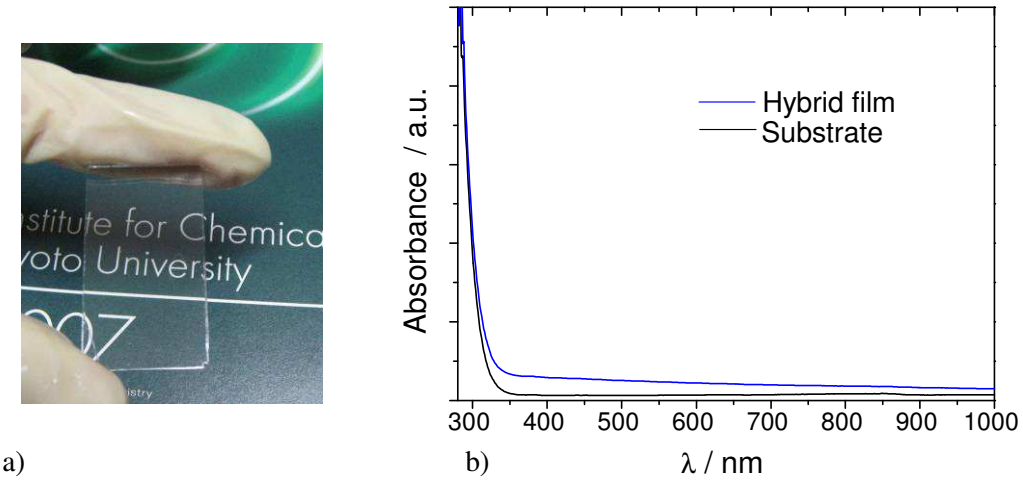

Figure 4.15- Image of the hybrid film (a) and Optical absorption spectra (b) of hybrid film and substrate

The appearance of the film is homogeneous and optically transparent (Figure 4.15), indicating that the nano-crystals are well dispersed and their dimensions are smaller than visible light.

Figure 4.15b) shows the optical absorption spectra of hybrid films containing the nano-crystals, the films appear highly transparent, the formation of the self-organized crystalline structure do not change the optical transparency of the material. Refractive indices of two different polarizations of light, TE and TM modes (λ = 632.9 nm (He-Ne laser)), have been estimated by using a prism coupling equipment. The measured values are summarized in Table 4.3.

Table 4.3. Refractive index, n, of the hybrid films prepared from sols of different aging times. The difference, Δn, in refractive index between the value obtained in TM mode and TE mode is reported in the last column on the right.

Sol aging time (days)	**n (TM mode)**	**n (TE mode)**	**Δn**
0	1.48107	1.48090	0.00017
15	1.49564	1.49376	0.00188

TE mode: polarization parallel to the film surface

TM mode: polarization normal to the film surface

The refractive indices of the organic-inorganic hybrid film with nanocrystals prepared from the sol whit 15 days of aging were ~1.4×10^{-2} larger than those of amorphous hybrid film prepared from the sol whit 0 day of aging, indicating the existence of a denser crystalline phase in the material. The amorphous hybrid film showed isotropic optical property whilst the hybrid film with nano crystals exhibited an optical anisotropy, $\Delta n = 1.88\times10^{-3}$, due to the orientation of the plate shaped crystallites.

4.2.7. Contact angle measurements

The formation of hydrophilic species like glycol from the opening of the epoxy group was confirmed also from the measurements of the contact angle.

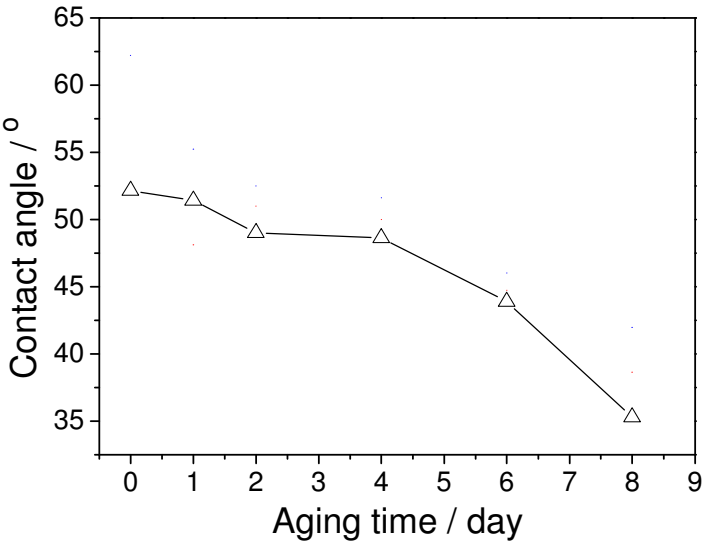

Figure 4.16- Contact angle measurements of the hybrid films prepared from sol with different aging time

In the figure 8 is showed evolution on the value of the contact angle for the films prepared from the sols with different aging time. The contact angle decrease from 52° (0day) to 32° (after 10 days).

4.2.8. Nanocrystal formation obtained by chemical design: a proposed model

Controlling sol-gel synthesis of GPTMS based hybrids is quite complex due to the large variety of possible reaction pathways and side reactions after opening of the epoxy ring[53,54,55,56] .On the other hand, this type of hybrid sol-gel chemistry allows tuning on a very fine level the final material structure. The GPTMS has been used as the precursor to form organosilica layered nanocrystals in organic-inorganic thin films. A faster inorganic condensation with respect to the organic polymerization hinders the formation of extended organic ethylene oxide chains, while an extended organic polymerization could limit the inorganic polycondensation[57]. An alcohol-free hydrolytic sol-gel reaction of GPTMS has been carried out in highly basic conditions using NaOH as a catalyst (~pH14). The GPTMS sol after aging at different times in controlled conditions (up to 15 days) has been spin-coated on glass or silicon substrates and optically transparent silica-based hybrid films have been obtained. Controlled aging of the sol is a key strategy to obtain self-organized nano-crystals within the organic-inorganic hybrid films. To obtain that, several parameters have to be controlled because the viscosity of the sol should be not too high in order to allow deposition of a homogeneous and transparent film. In the previous section we have describe the evolution of the sol during aging monitored by nuclear magnetic resonance (NMR), were we have showed like We have obtained information about the reaction also from the Fourier transform infrared (FTIR) spectroscopy. From the X-ray diffraction (XRD) spectra of the hybrid films we can see a signal at 5.95° (d = 1.48 nm), which is due to intermolecular correlation of siloxane chains in an amorphous state[58], the correlation length increases with the aging time of the coating sol from d = 1.48 nm (0 day) to 1.66 nm (15 days) indicating the formation of poly/oligo(ethylene oxide) as side chains of the siloxane framework. After 5-days aging, a new XRD peak is observed at 9.61° (d = 0.923 nm), the diffraction angle of the peak does not show any dependence on sol aging. The formation of organic-inorganic nano-crystals within the hybrid film has been confirmed from a direct observation by transmission electron microscopy (TEM).

From the FTIR absorption spectra of hybrid films we observe the decrease of epoxy ring with the sol aging , indicating the formation of hydrolyzed species, glycol and polymerized one, poly/oligo(ethylene oxide) like showed from the sol aging process followed in-situ by ^{29}Si, ^{13}C and ^{1}H NMR analysis (previous section) The condensation degree of siloxane exceeds 90% after 2 days whilst epoxy opening and polymerization resulted much slower. The adsorption of water in the hybrid film from the aged sol indicates the increase of hydrophilicity due to the formation of glycol group, which is also confirmed by ^{13}C NMR measurements (previous section) and contact angle measurement. The formation of layered silicates gives optical anisotropy which is usually observed by polarization microscopy to see differences in colour of particles or domains due to the retardation of light, because, in most cases, the layered silicates are prepared in powder shape. Corriu et al. observed gel fragment of some micrometers[59,60] but it was impossible to have a quantitative evaluation of the optical anisotropy of the hybrids. In the present case, we can estimate the optical anisotropy of the film as an average of crystalline and amorphous parts because the hybrid is transparent and homogeneous to visible light. The formation of crystalline hybrid structure by bridged silsesquioxane is explained by the sol-gel condensation of a non-mesomorphous precursor (heterogeneous nucleation and growth mechanism by molecule-by-molecule assembly).

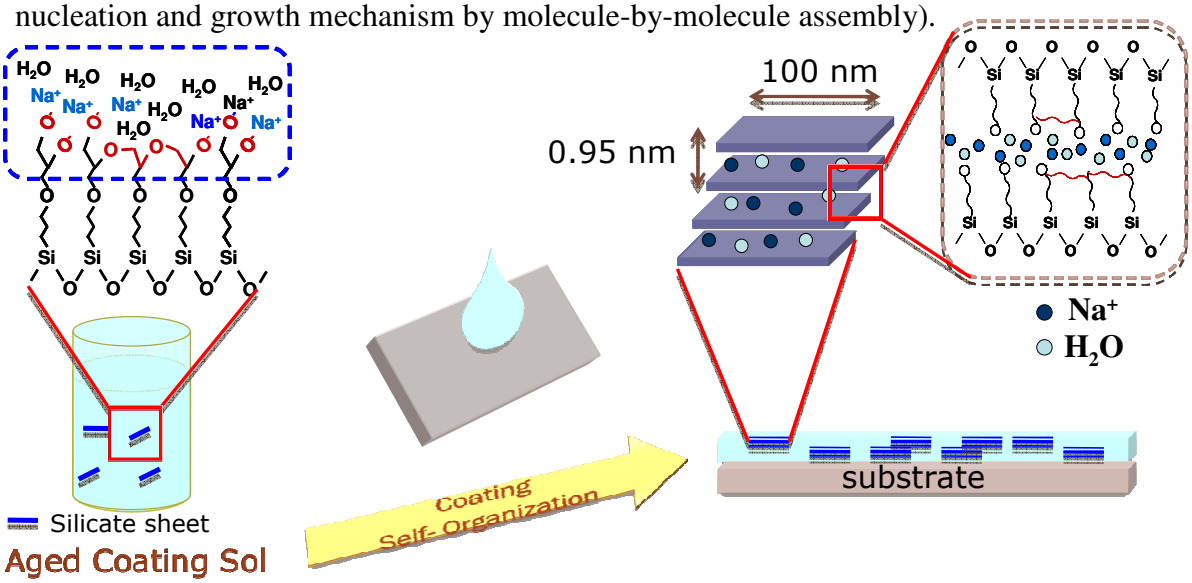

Scheme 4.4- Chemical design of the organic-inorganic hybrid films whit hybrid nanocrystals

In the present case of hybrid films containing hybrid nano-crystals, however, the optical anisotropy measurement and TEM observation suggest the formation of organosiloxane sheets as a structure directed intermediate that is formed during sol aging. Controlled epoxy opening, which is realized through sol aging in highly basic conditions (scheme 4.4), is the key for mastering the self-organization of the nano-crystals. In the scheme 4.4 is showed the chemical design strategy employed to obtain the formation of the organic inorganic hybrid materials, were from the aged solution with the silica sheet we obtain the formation of hybrid nanocrystals in the hybrid films by a self-organization process during coating.

4.2.9. Conclusions

Layered organosilicate nano-crystalline have been produced, for the first time to our knowledge, in hybrid organic inorganic films through a self-organization process. The organosilicate nano-crystals formation is kinetically controlled the different condensation kinetics of silica backbone and organic polymerization trigger the process. The simple and facile preparation method that we have reported in the present work allows obtaining organosilicate layered nano-structures in curable epoxy-silica hybrid films. The hybrid films after deposition show a good combination of properties and show an possibility to be used to allow for microfabrication technique (see last section). This approach is opening the route to new applications in electronics, photonics, and bio-chemistry in combination with micro/nanolithography techniques.

EFFECT OF THE TEMPERATURE ON THE HYBRID NANOCRYSTALS FORMATION

Abstract

We have evaluate the effect of the temperature during the sol-gel processing on the formation of organic–inorganic films containing hybrid nanocrystals obtained from the GPTMS like precursor. In particular we have studied the effect of the temperature on the siloxane condensation and on the epoxy opening reaction. For this purpose we have systematically changed the temperature and the aging time of a precursor sol containing an organically modified alkoxide bearing an epoxy group, 3-glycidoxypropyltrimethoxysilane, to obtain a controlled crystallization of hybrid layered structures in hybrid films. To evaluate the effect of the temperature, the precursor sol has been aged at different temperatures, from 5 to 60 ^{o}C, and for 1, 2 or 3 days. The films have been deposited from the aged sol and then after characterized by X-ray diffraction, Fourier transform infrared spectroscopy and Raman spectroscopy. From this study we have observed that the formation of the hybrid crystals can be obtained only when at least 50% of the epoxies are opened and a larger silica condensation is achieved. These conditions are reached after aging at 60 ^{o}C for 1 day, or at longer aging times when the sol is aged at lower temperatures.

The formation of the organic-inorganic hybrid nano-crystals was confirmed by transmission electron microscopy and by optical polarized images .

4.3.1 Materials Preparation

3-glycidoxypropyltrimethoxysilane (GPTMS) and sodium hydroxide (Aldrich 98%) were used as received without further purification. The molar ratio of the components was set to GPTMS:H2O:NaOH = 1:5:0.1671. The precursor sol was prepared by dropwise addition of GPTMS (20 cc) to a NaOH aqueous solution (8 cc, 1.85 M, pH14) under stirring. Immediately after the preparation the precursor sol was left in an open vessel at 25 ^{o}C and 40% RH for 45 min to allow the evaporation of methanol which is a by-

product of the sol–gel reactions; after this time the sol container was sealed and the sol left under stirring for 12 h at 25 ^{o}C. At the end of this first preparation step the sol was aged for 3 days at 5, 20, 30 or 60 ^{o}C; hybrid films were deposited by spin-coating on soda lime glass or silicon substrates using a rotation speed of 3000 rpm for 20 s. The substrates were cleaned with water, acetone and EtOH.

4.3.2 Materials Characterization

The systems aged at different temperature and with different aging time was characterize by different tecniques: XRD, FT-IR and Raman spectroscopy. X-ray diffraction (XRD) patterns were collected in the angular range from 1 to 30^{o} in 2h, using a Bruker Discovery- 8 instrument in the Bragg–Brentano geometry with a copper tube (λ = 1.54056 A°); the X-ray generator worked at a power of 40 kV and 40 mA. The infrared absorption analysis was done on films deposited on silicon substrates with a Bruker Vertex70 FT-IR spectrometer in a transmission mode in the range 400–4,000 cm-1; the data were collected over 128 scans with a resolution of 4 cm-1 and silicon was used as the background. Raman analysis was performed on the films by using a Bruker Senterra at λ= 532 nm, with a 20X objective, collecting the data by averaging 10 acquisitions each one lasting for 5 s with a resolution range of 9–15 cm^{-1}. The analysis was done on the film deposited on a silicon substrate. Microscopic analysis was performed by an Olympus microscope equipped with a polarizer. Transmission electron microscopy (TEM) images were obtained by a JEOL 200CX microscope equipped with a tungsten cathode operating at 200 kV. For the analysis some fragments of the sample were removed from the substrate and deposited on a carbon-coated copper grid after grinding in an agate mortar.

4.3.3 XRD characterization

The X-ray diffraction (XRD) patterns of the films prepared from solutions aged at different temperatures 5 ^{o}C (Figure 4.17a), 20 ^{o}C (Figure 4.17b), 30 ^{o}C (Figure 4.17c) and 60 ^{o}C (Figure 4.17 d) are showed on the Figure 4.17 a–d for different aging times

precisely 1 day 2 and 3 days . We have observed in a previous work showed in the previous section that the formation of layered organic– inorganic crystals in the hybrid films is characterized by the appearance of a wide diffraction peak around 9^o (d = 0.9 nm) and by a more intense peak around 5^o. The 5^o peak has been observed to shift to lower angles with aging and this effect has been correlated to the increase of the average intermolecular distance due to the formation of polyethylene oxide (PEO) chains by epoxy opening and polycondensation and intermolecular correlation of siloxane chains in an amorphous state.

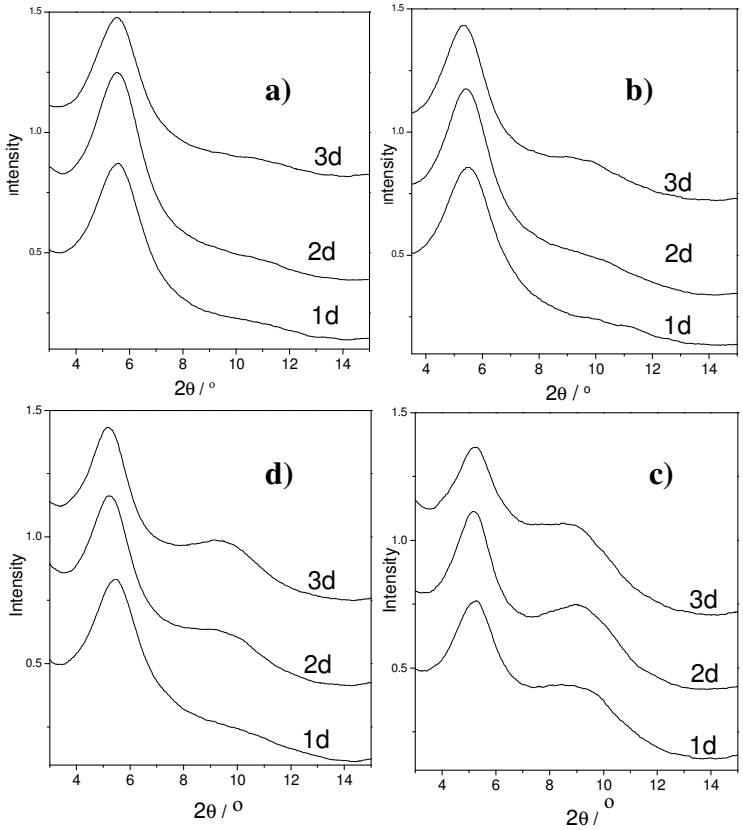

Figure 4.17- XRD spectra of hybrid films prepared from sols aged at different temperature.

The 5^{o} peak shifts from 5.61^{o} (5 ^{o}C, 1 day aged sol sample) to 5.15^{o} (60 ^{o}C, 3 days aged sol sample) while we observe that only the film prepared from the sol aged at 60 ^{o}C shows the appearance of the 9.5^{o} diffraction peak, which is the signature of the formation of crystalline layered structures, even after 1 day of aging[61] In the sample aged at 5 ^{o}C there is no appearance of the 9^{o} peak, which is observed after 3 days of aging at 20 ^{o}C, and after 2 and 3 days of aging at 30 ^{o}C. The XRD data show, therefore, that crystallization in the films is directly correlated with temperature and time of aging.

4.3.4 TEM characterization

The formation of the organic-inorganic hybrid nano-crystals was confirmed by transmission electron microscopy like showed in the figure 4.18. Then we have an agreement between observations of crystals by TEM with the presence of the 9^{o} peak, which well supports the attribution.. The figure 4.18 shows the TEM image of a fragment taken from a hybrid film aged at 60 ^{o}C for 3 days. The hybrid nanocrystals appear to be formed and homogeneously distributed within the matrix.

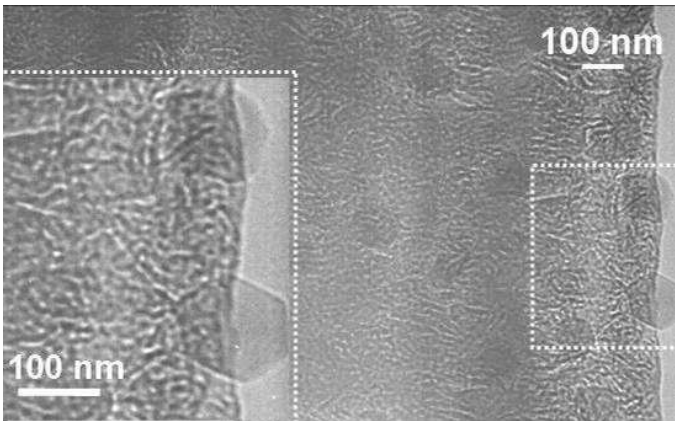

Figure 4.18- TEM image of a fragment taken from a hybrid film aged at 60 ^{o}C for 3 days.

The nanoscrystals with dimeter around 103 nm are well dispersed on the organic-inorganic hybrid materials as observed on the figure,and in the enlargement on the left.of the image are showed two hybrid crystals with hexagonal shape.

4.3.5 FTIR Characterization

The hybrid films prepared from the sols aged at different temperature was characterized by FTIR to evaluate the effect of the temperature on the mechanism of reaction. Figure 4.19 a–d shows the infrared absorption spectra in the 3700–2650 cm^{-1} range of hybrid films obtained from sols aged at different temperatures: 5 ^{o}C (Figure 4.19a), 20 ^{o}C (Figure 4.19 b), 30 ^{o}C (Figure 4.19 c) and 60 ^{o}C (Figure 4.19 d) for different times 1 day , 2 days and 3 days. In the CH_2 stretching region (3100–2800 cm^{-1}), the two main bands around 2920 and 2880 cm^{-1} are attributed to CH_2 anti-symmetric and CH_2 symmetric stretching, respectively[62] and we have used these absorption bands for normalization of the infrared spectra.

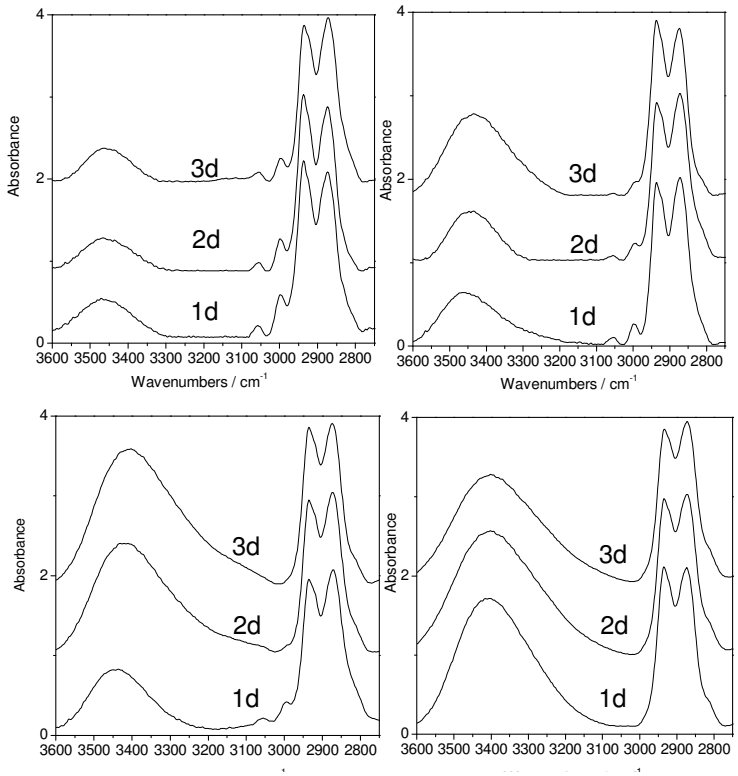

Figure 4.19 –FTIR of the hybrid film prepared from sols aged at different temperature.

Two other absorption peaks of smaller intensity at 3057 and 2997 cm^{-1} are attributed to stretching modes of terminal CH_2 groups of the epoxy in GPTMS[6364] .From the figure 4.19 we can see that the epoxy absorption bands completely disappear in the films

prepared from the 60 °C aged sol and 3 days 30 °C aged sol while in the other samples are still well detected, indicating as the temperature increase the reaction opening of the epoxy group.

In the same figure we can observe the behavior of the –OH group. The wide -OH stretching band peaking around 3400 cm^{-1}, shows an opposite trend with respect to the epoxy; this band is formed by the overlapping of different species that we can identify as silanols around 3300 cm^{-1} and water around 3200 cm^{-1}.

The -OH stretching band increases in intensity and shifts to lower wavenumbers in the sample prepared at the highest aging temperature. This effect is mainly due to waterwhich has been detected in all the samples except those prepared with the sol aged longer than 1 day at 5 °C or 2 days at 20 °C.

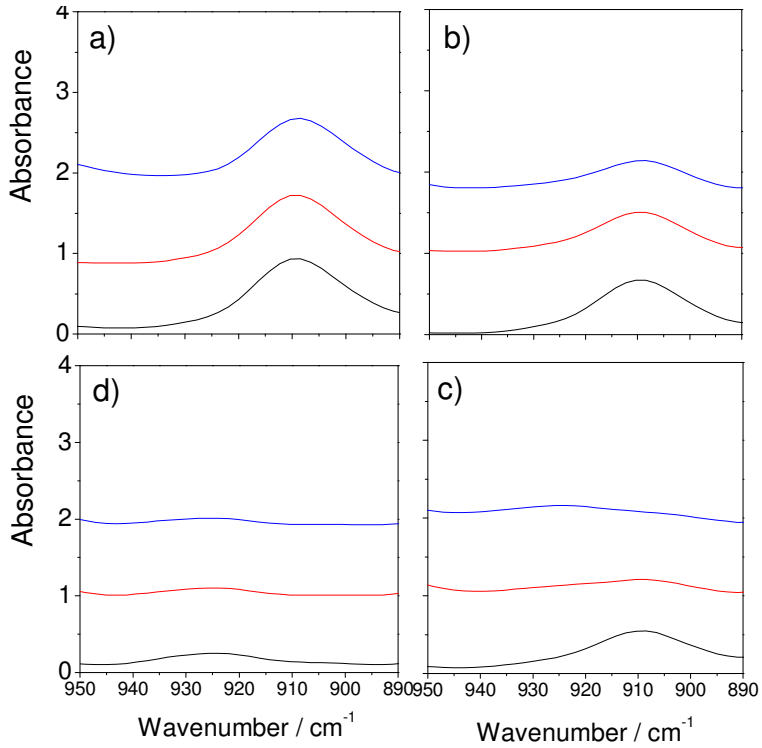

Figure 4.20 - FTIR spectra in the in the 950–890 cm^{-1} range of hybrid films obtained from sols aged at different temperatures

Figure 4.20 shows the infrared absorption spectra in the 950–890 cm^{-1} range the spectra are characterized by the presence of an absorption band peaking around 910 cm^{-1}, which is assigned to Si–OH [63] .In the figure are reported in particular the spectra of hybrid films obtained from sols aged at different temperatures: 5 ^{o}C (Figure 4.20 a), 20 ^{o}C (Figure 4.20b), 30 ^{o}C (Figure 4.20c) and 60 ^{o}C (Figure 4.20d) for different times 1 day (black line), 2 days (red line) and 3 days (blue line). We have used the band around 910 cm^{-1}, to evaluate the effect of aging on silica condensation (figure 4.25).

4.3.6 Raman characterization

From the Raman spectroscopy we can obtain some information about the reaction of the GPTMS in highly basic condition at different temperatures Figure 4.21 show the Raman spectra of the GPTMS (bottom) and the reaction after 45 minutes from the mixing of the GPTMS with the basic aqueous solution, the peaks around at 640 cm^{-1} are assigned to the $Si(OCH_3)_3$, and we can observe after 45minutes the completely absence of this signals indicating that the hydrolysis is very fast, on the other hand the signals ~ 750 cm^{-1} and 1250 cm^{-1} assigned to the epoxy group is not changed. We can use the signals to monitored the epoxy opening.

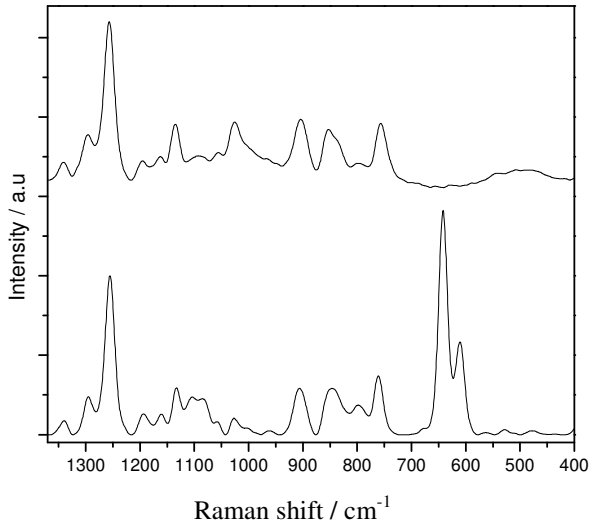

Figure 4.21- Raman Spectra of the GPTMS (bottom) and GPTMS in the basic aqueous solution after 45 minutes from the mixing (up).

Figure 4.22 a–b shows the Raman spectra around at 750 cm^{-1} of the hybrid films obtained from sols aged at different temperatures: 5 ^{o}C (Figure 4.22a), 20 ^{o}C (Figure 4.22b), 30 ^{o}C (Figure 4.22c) and 60 ^{o}C (Figure 4.23d) for different times (1 day (black line), 2 days (red line) and 3 days (blue line)) obtained from sols aged strongly decreases in the film prepared from the 60 ^{o}C aged sol. We clearly observe that in the 60 ^{o}C aged sol films the signal of epoxy is not detected while in the other samples the intensity of the band decreases with sol aging and with the aging temperature

To obtain a quantitative evaluation of the epoxy opening as a function of the sol aging parameters we have used the 760 cm-1 Raman band, which is assigned to the symmetric ring stretching of the epoxy group[65,66]. We have calculated the change in the area of the epoxy Raman band and the results are shown in Figure 9 for 1 day, 2 days and 3 days; there is an almost linear dependence on aging temperature of epoxy opening.

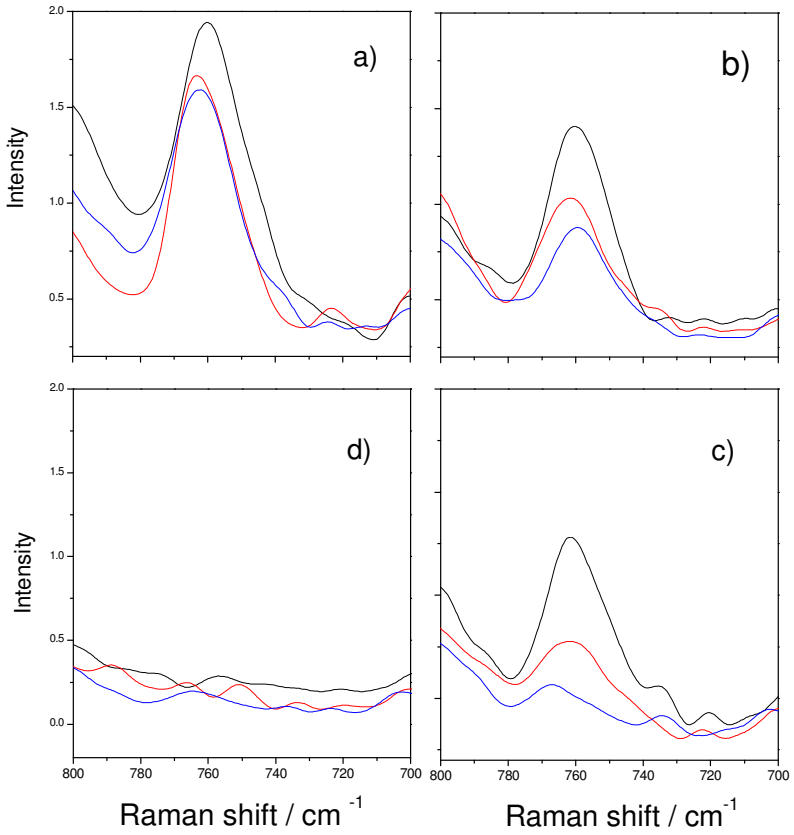

Figure 4.22- Raman spectra in the 800-700 cm^{-1} range of the hybrid films prepared from sols aged at different temperatures.

4.3.7 NMR characterization

From the NMR spectroscopy we have obtained some information about the reaction of the GPTMS at different temperatures, in the figure 4.23 are reported the ^{29}Si NMR data (a) and ^{13}C (b) NMR spectra of sols at 5 and 60°C whit one day of aging.

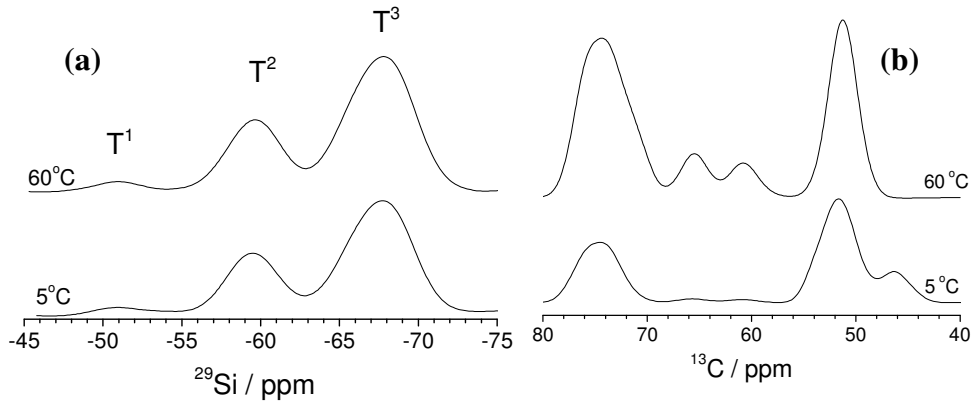

Figure 4.23- ^{29}Si (a) and ^{13}C (b) NMR spectra of sols at 5 and 60°C whit one day of aging

The spectra indicate that the temperature don't change the inorganic reaction, but on the other hand affect the opening reaction of the epoxy groupe and favored the formation product of the reaction like PEO and Glycol.

4.3.8 The effect of the temperature on the nanocrystals formation

The formation of hybrid crystals within an organic–inorganic film is a kinetically driven process which can be controlled through the processing parameters. Aging conditions of the precursor sol, such as temperature, relative humidity and atmosphere in the storage room affect the self-organization of the hybrid crystals. We have studied the effect of the temperature during the aging time on the formation of self-ordered hybrid crystals keeping constant the other parameters, like pH, amount of water and catalyst. The sols appeared optically transparent after the preparation and remained transparent after different days of aging; the films resulted also optically transparent independently of the precursor sol. We have used FTIR data to correlate the formation of hybrid crystals,

observed by XRD analysis, with structural changes upon aging in the films. In general we observe that longer aging times and higher temperatures of aging are correlated with a more efficient epoxy opening and the presence of water. We have used Raman analysis to obtain a more quantitative evaluation of the epoxy content with sol aging; in some cases, when in FTIR spectra the bands result strongly overlapped, Raman spectra are an alternative for quantitative evaluations [64] .The FTIR absorption bands at 3057 and 2997 cm^{-1}, in fact, are well resolved and can give a good qualitative indication but are strongly overlapped with the C–H stretching modes at lower wavenumbers; data processing results therefore difficult because baseline calculation and deconvolution of the spectra is necessary [63-67] .Then we have calculated the change in the area of the epoxy Raman band and the results are shown in Figure 4.24 (1 day (black line), 2 days (red line) and 3 days (blue line)); there is an almost linear dependence on aging temperature of epoxy opening. The region of crystallization, which is obtained correlating the epoxy opening with XRD data for crystal formation, is coloured in blue; when around 60% of the epoxy are opened crystallization appears in the films. The sol aging parameters, time and temperature, affect the kinetics of epoxy opening reactions but have also a direct influence on the polycondensation reactions of silica species.

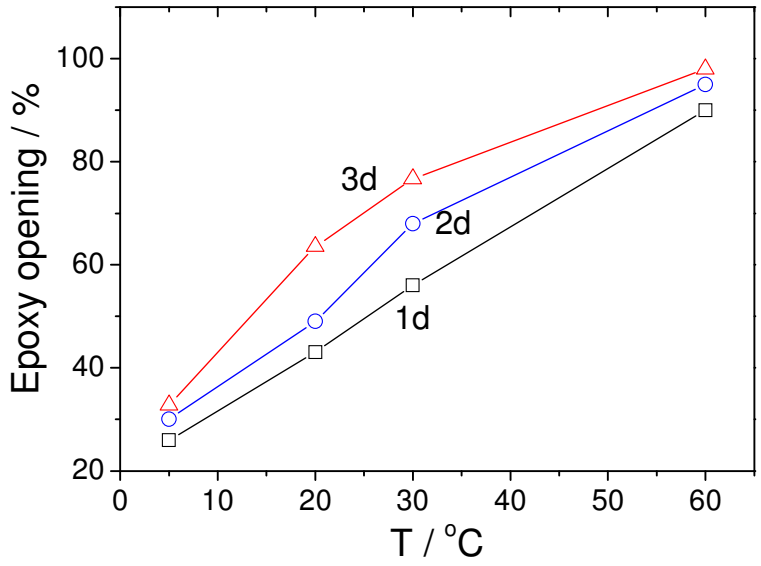

Figure 4.24- Evolution of the area of the signal of epoxy group .

We have used the band in the 950–890 cm^{-1} range to evaluate the effect of aging on silica condensation; the change of Si– OH band area as a function of aging time and aging temperature is shown in Figure 4.25 (1 day (black line), 2 days (red line) and 3 days (blue line).

Higher aging temperatures induce a stronger silica condensation, which is reflected by a decrease of silanol content; if we take as reference the silanol area of the film prepared by a fresh sol, we observe that when the reduction of silanols in the other samples is around 50% with respect to the reference film we observe formation of hybrid crystals. The crystallization region is shown in light blue such as in figure 9; the condensation is also well correlated to the presence of water detected in the samples that is a by product of the reaction.

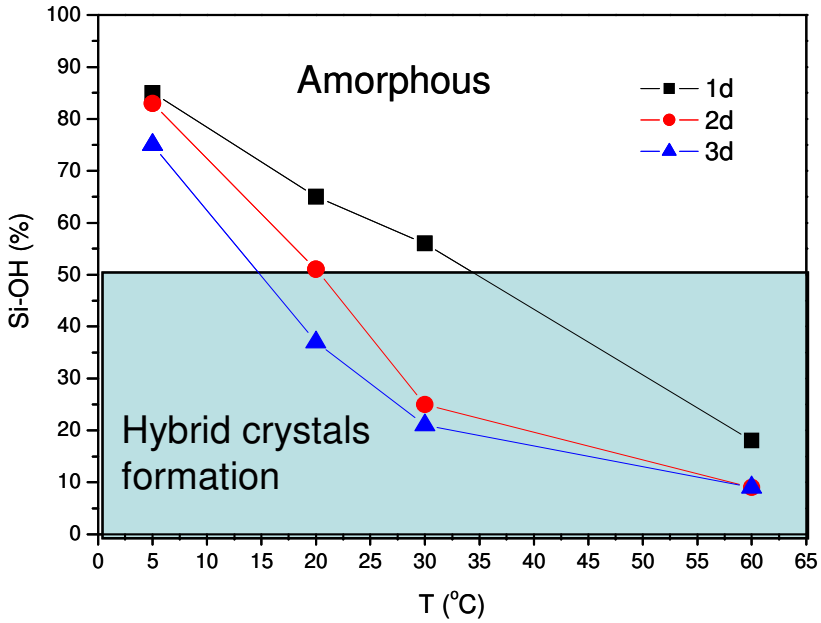

Figure 4.25- the change of Si– OH band area as a function of aging time and aging temperature

The results show that a strong correlation between opening reaction of the epoxy groups and the layered nanocrystals formation exists; the experimental data show that there is a specific region, which is represented by a critical epoxy opening and silica condensation,

for crystallization of the hybrid films. The overall process appears kinetically controlled, on the other hand only a good balance of the opening and condensation reactions of the epoxy and hydrolysis and condensation of silica alkoxy allows the formation of hybrid crystal. In general, in fact, the two condensation processes, the organic and the inorganic, are in competition and an extended polymerization of organic chains in GPTMS is allowed only if the silica condensation is not so advanced[67] . The process induce a slow condensation of silanols and epoxy allows the formation by controlled aging of layered structures. It should be also underlined that this reaction can evolve in different pathways, because several side reactions are possible [64-66] and small changes in the synthesis can give different products .

4.3.9 Conclusions

Crystallization in hybrid materials obtained by reaction of GPTMS in highly basic conditions is a kinetically controlled process which is controlled by the processing parameters of sol–gel reactions. Temperature which was aged the sol and not only the aging time of the sol like showed on the previous section affect the siloxane condensation and the epoxy opening reaction and then the crystal formation. From these studies we have observed that exist a critical threshold of epoxy opening and silica condensation that allows self-organization into hybrid crystals in the films.

EFFECT OF DIETHOXYDIPHENYLSILANE ON THE CONDENSATION PROCESS AND EPOXY OPENING OF THE GPTMS IN BASIC CONDITION

Abstract

We have employed on the preparation of hybrid materials a new precursor with the GPTMS. We have varied the amount of DEDPES to evaluate the effect during the sol-gel processing on the formation of organic–inorganic films containing hybrid nanocrystals obtained from the GPTMS like precursor. In particular we have studied the effect on the siloxane condensation and on the epoxy opening reaction. For this purpose we have changed the amount of the DEDPES on the precursor sol containing an organically modified alkoxide bearing an epoxy group, 3-glycidoxypropyltrimethoxysilane, to obtain a controlled siloxane condensation and opening reaction in hybrid films for develop future application especially in microfabbrication. To evaluate the effect of the DEDPES, we have prepared two sol with 10% and 20% of DEDPES. The films have been deposited from the aged sol and then after characterized by X-ray diffraction, Fourier transform infrared spectroscopy and Raman spectroscopy. From this study we have observed that the siloxane condensation increase and epoxy opening increase with the increase amount of DEDPES .The formation of hybrid nanocrystals on the hybrid films is indicate from the appearance of the peak at 10^{o}C in XRD spectra, that show as the formation of nanocrystals is obtained also in presence of DEDPES.

4.4.3 Materials preparation

3-glycidoxypropyltrimethoxysilane (GPTMS, Aldrich 98%), sodium hydroxide (Carlo Erba pellets 98%) and diethoxydiphenylsilane (DEDPS, Aldrich 97%) were used as received without further purification. Two solutions indicated like sol 10% and sol 20%, were prepared by replacing on the standard solution with only GPTMS the 10% (sol 10%) and 20% (sol 20%) respectively of volume of GPTMS with the DEDPS. The precursor sol A was prepared by addition of GPTMS (9 cc) to a NaOH aqueous solution (4 cc, 1.85 M, pH14) under stirring and adding after few second DEDPS (1 cc). The precursor sol B was prepared by addition of GPTMS (8 cc) to a NaOH aqueous solution (4 cc, 1.85 M, pH14) under stirring and adding after few second DEDPS (2 cc). The molar ratio of the components was set to GPTMS: DEDPS = 1:0.09 for the sol A and GPTMS: DEDPS = 1:0.2 for the sol B. Immediately after the preparation the precursor sol was left in an open vessel at 25 ^{o}C and 40% RH for 45 min to allow the evaporation of methanol which is a by-product of the sol–gel reactions; after this time the sol container was sealed and the sol left under stirring for 12 h at 25 ^{o}C. At the end of this first preparation step the sol was aged for 8 days 25 ^{o}C; hybrid films were deposited by spin-coating on s glass or silicon substrates using a rotation speed of 5000 rpm for 20 s. The substrates were cleaned with water, acetone and EtOH.

4.4.2 Materials Characterization

The systems aged at different temperature and with different aging time was characterize by different tecniques: XRD, FT-IR and Raman spectroscopy. X-ray diffraction (XRD) patterns were collected in the angular range from 1 to 30^{o} in 2h, using a Bruker Discovery- 8 instrument in the Bragg–Brentano geometry with a copper tube (λ = 1.54056 A°); the X-ray generator worked at a power of 40 kV and 40 mA. The infrared absorption analysis was done on films deposited on silicon substrates with a Bruker Vertex70 FTIR spectrometer in a transmission mode in the range 400–4000 cm^{-1}; the data were collected over 128 scans with a resolution of 4 cm^{-1} and silicon was used as the background. Raman analysis was performed on the films by using a Bruker Senterra at λ

= 532 nm, with a 20x objective, collecting the data by averaging 5 acquisitions each one lasting for 5 s with a resolution range of 9–15 cm^{-1}. The analysis was done on the film deposited on a silicon substrate. Wettability characteristics of the hybrid films were performed on the films by using a Dataphysics Contact Angle System OCA. A sessile drop method was used to measure a contact angle (θ) of a 5 μL distilled water drop, which was applied to the surface by means of syringes.

4.4.3 FTIR characterization

.The hybrid films prepared from the sols with different amount of DEDPES was characterized by FTIR to evaluate the effect of the DEDPES on the mechanism of reaction. Figure 4.26 shows the infrared absorption spectra in the 930–880 cm^{-1} range of hybrid films obtained from sols aged) for different times 1 day , to 8 days. The spectra are characterized by the presence of an absorption band peaking around 910 cm^{-1}, which is assigned to Si–OH .

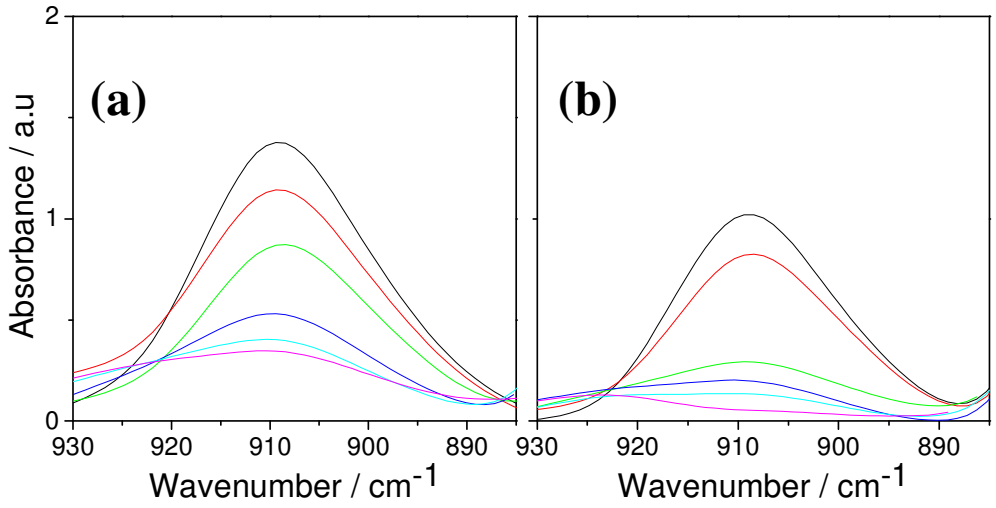

Figure 4.26- FT-IR spectra (a) and (b) of hybrid films in the range 930-880 cm^{-1} deposited from sol 20% and sol 10% of different aging time.

We have used this band to evaluate the effect of aging on silica condensation (figure 4.31a). From the figure 4.26 we can see that the silanol absorption bands (~910 cm^{-1})

completely disappear in the films prepared from the sol 20% and 3 days of aging , while in the other samples are still well detected, indicating as the high presence of DEDPES increase the silanol condensation.

4.4.8 Raman characterization

The Raman spectroscopy get information about the reaction of the GPTMS in highly basic condition with different amount of DEDPES Figure 4.27 show the Raman spectra of the sol with GPTMS and 10 % of DEDPES (a) and the sol with GPTMS and 20 % of DEDPES (b). The signals ~ 750 cm^{-1} is assigned to the epoxy group. We can use the signals to monitored the epoxy opening . We clearly observe that in the films prepared from the sol with 20% of DEDPES the signal of epoxy decrease faster then that of the films prepared from the sol with 10% of DEDPES ; the intensity of the band decreases with sol aging .

From the figure we observe that the increase of the amount of DEDPES affect the reaction of the epoxy group; the increase of the opening of the epoxy group is observed. We can observe for the sol 20% the almost completely opening of the epoxy group already after 3 days of aging.

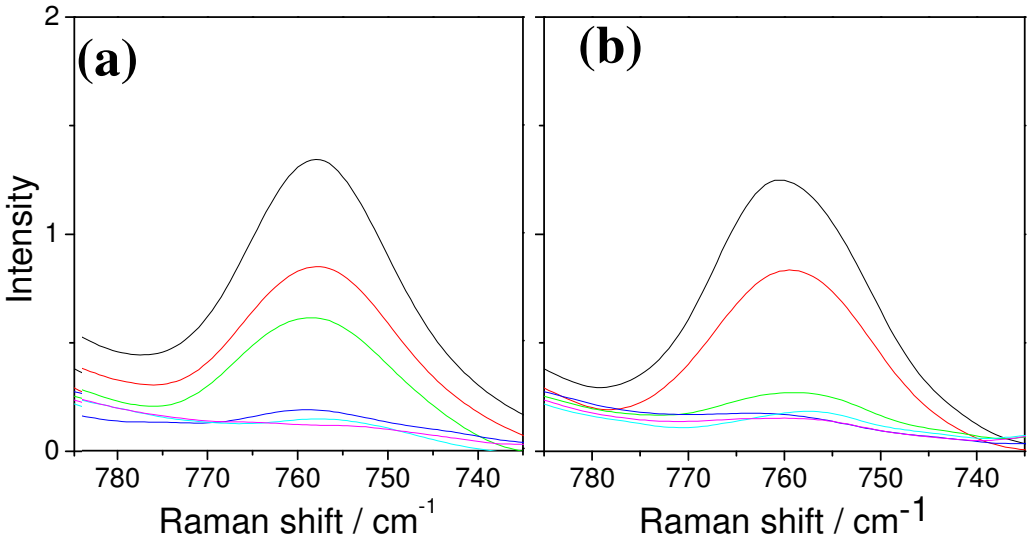

Figure 4.27- Raman spectra (a) and (b) of hybrid films in the range 790-710 cm^{-1} deposited from sol 20% and sol 10% of different aging time.

4.4.8 XRD measurements

The X-ray diffraction (XRD) patterns of the films prepared from solutions with different amount of DEDPES (10% and 20%) are showed on the Figure 4.28 for different aging times (from 1 day to 8 days).

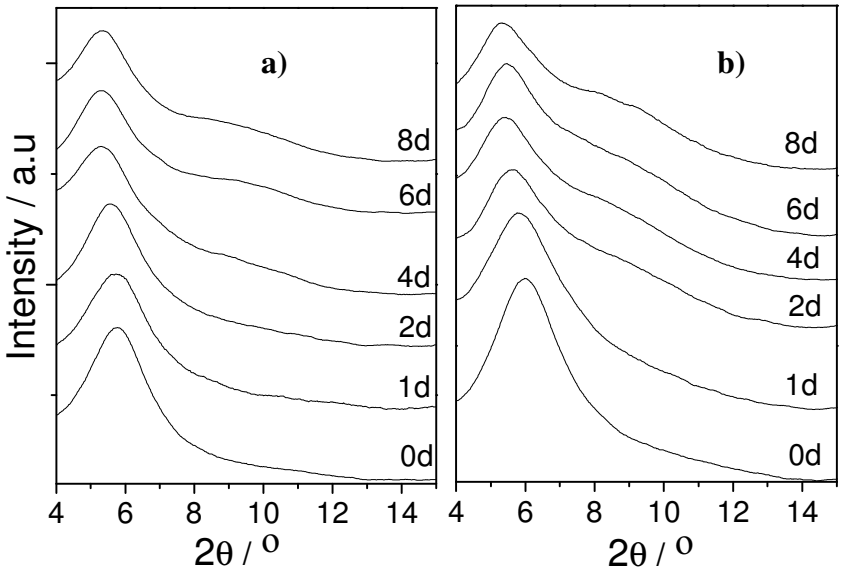

Figure 4.28- XRD spectra of the hybrid films deposited from (a) sol 10% and (b) sol 10% of different aging time.

We have reported in the previous sections that the formation of layered organic–inorganic crystals in the hybrid films is characterized by the appearance of a wide diffraction peak around 9^o (d = 0.9 nm) and by a more intense peak around 5^o. The 5^o peak has been observed to shift to lower angles with aging and this effect has been correlated to the increase of the average intermolecular distance due to the formation of polyethylene oxide (PEO) chains by epoxy opening and polycondensation and intermolecular correlation of siloxane chains in an amorphous state.

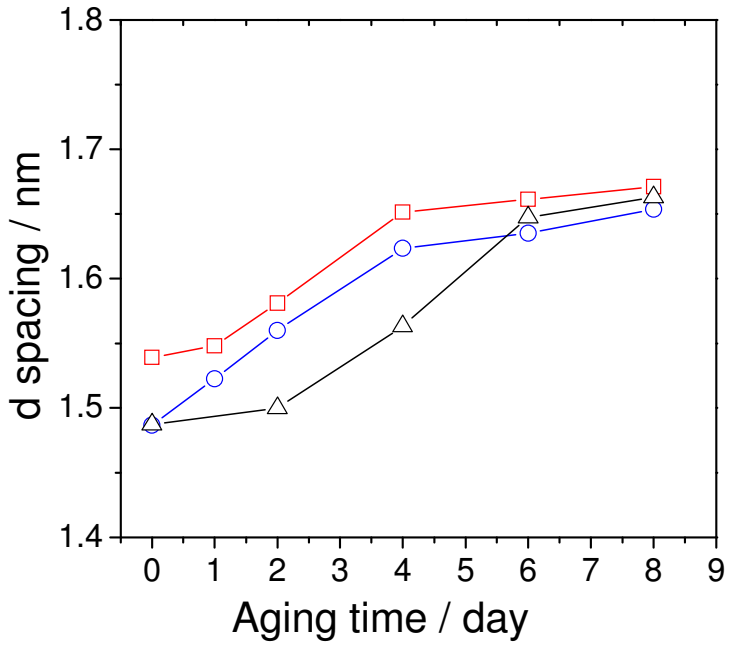

Figure 4.29- The variation of *d*-spacing of the signal around 6° as a function of sol aging time for the sol 10% (*red line*) sol 20%*(blue line*) and standard sol (*dark line*).

Figure 4.29 show the variation of the d-spacing of the signal around 6° as a function of the sol aging time for the sol 10% and sol 20% compared with the sol standard.

4.4.8 Contact angle measurements

The formation of hydrophilic species like glycol from the opening of the epoxy group was confirmed also from the measurements of the contact angle.

In the figure 4.30 is showed evolution on the value of the contact angle for the films prepared from the sols with different amount of DEDPES at different aging time. The contact angle decrease from 52° (0day) to 34°(after 10 days) for the films prepared with 10 % of DEDPES, and from 62° (0day) to 42°(after 10 days) for the films prepared from the sol with 20% of DEDPES.

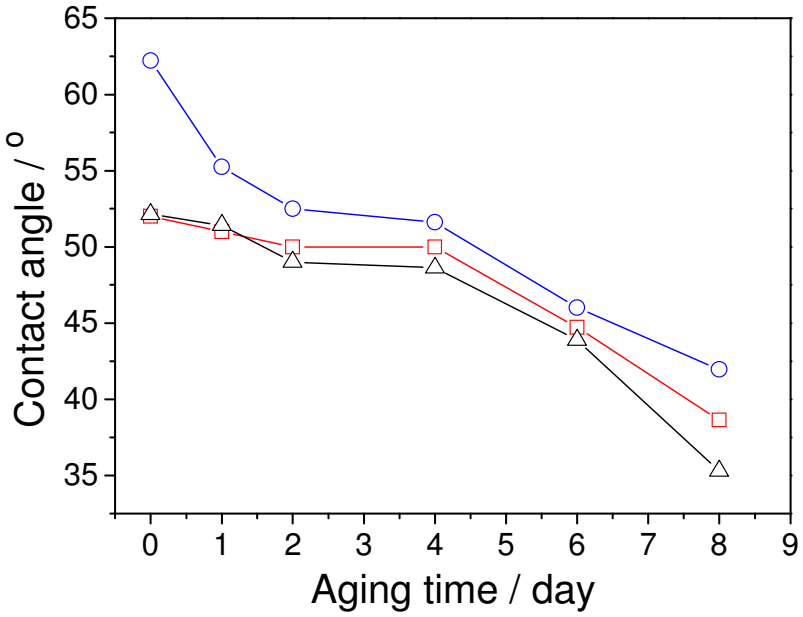

Figure 4.30. Contact angle of the hybrid films deposited from sol 10% (*red line*) sol 20% (*blue line*) sol standard (*dark line*) of different aging time.

4.4.8 Effect of the DEDPES on the inorganic condensation and epoxy opening

The formation of hybrid crystals within an organic–inorganic film is a kinetically driven process which can be controlled through the processing parameters. We have used FTIR data to correlate the formation of hybrid crystals, observed by XRD analysis, with structural changes upon aging in the films. In general we have evaluated the effect of the presence of DEDPES, on the inorganic condensation and opening epoxy of the GPTMS in basic condition. From FTIR and Raman spectroscopy we have investigate the change in the silanol content and the the epoxy opening. The sols appeared optically transparent after the preparation and remained transparent after different days of aging; the films resulted also optically transparent.

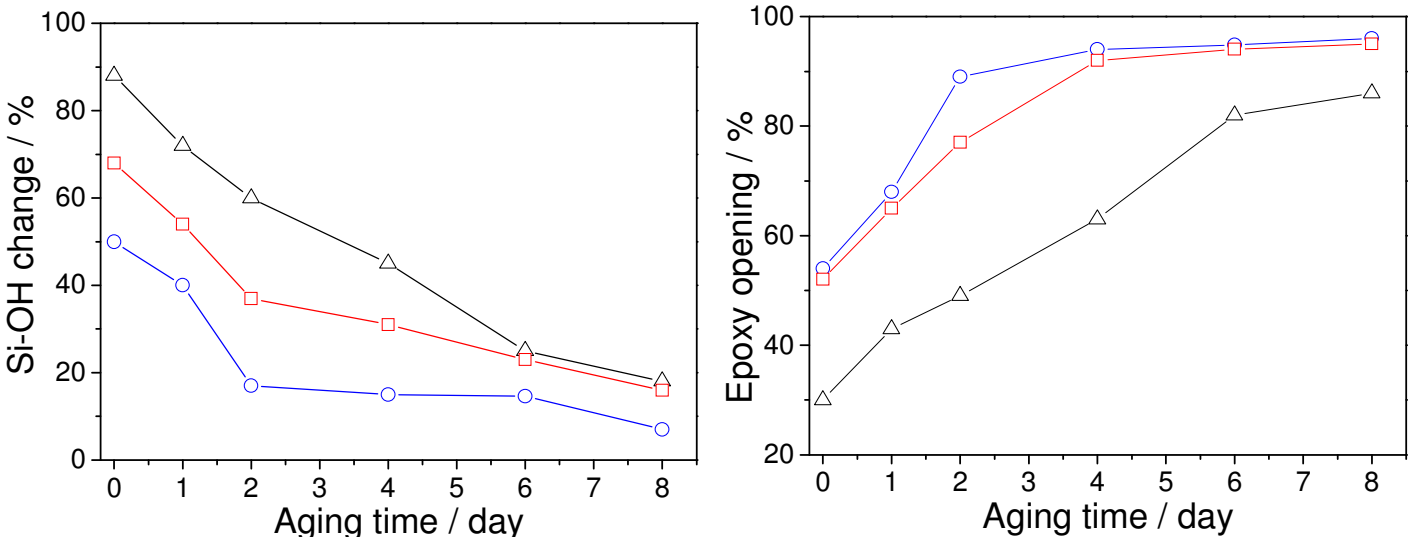

Figure 4.31. Change in silanol content (variation of the Si-OH band area at ~ 910 cm^{-1}) and **(b)**Epoxy opening (%) as a function of time and different amount of DEDPS for the sol 10% (*red line*), the sol 20% (*blue line*) and the standard sol (*dark line*) .

The change in silanol content is reported in the figure 4.31 a) through a variation of the Si-OH band area at ~ 910 cm^{-1} calculated with respect to area measured in a sample prepared from a fresh sol as a function of time and different amount of DEDPS. The data have been obtained from FTIR spectra of Figure 4.26. From these analysis we can observe that the silanol content depend from the amount of DEDPES.

Also the epoxy opening show a dependence from the amount of DEDPS ; in the figure 6b) is presented the variation of the epoxy opening (%) as a function of time and different amount of DEDPS at aging days calculate from the peaks at 750 cm^{-1} of the Raman spectra of Figure 4.27.

Also the XRD spectra show a similar trend, indicating the faster condensation reaction and formation of PEO for the presence of DEDPS, then this affect also the formation of the hybrid nanocrystals indicating by appearance of the peak at 10^{o}. The surface of this films became much hydrophobic with the increase of the amount of DEDPES, as indicate from measurements of contact angle. The optical quality of the films appear improved, the films remain transparent for long especially when employed on the microfabbrication.

4.4.8 Conclusions

We have studied the effect of different parameter on the reaction of GPTMS and on the formation of the hybrid nanocrystals. Crystallization in hybrid materials obtained by reaction of GPTMS in highly basic conditions is a kinetically controlled process which is controlled by the processing parameters of sol–gel reactions. The presence of other reagent which was added to the sol and not only the aging time of the sol like showed on the previous section affect the siloxane condensation and the epoxy opening reaction and then the crystal formation. From these studies we have observed that exist a critical threshold of epoxy opening and silica condensation that allows self-organization into hybrid crystals in the films. The added of DEDPES increase the hydrophobic character of the surface and this character can be tuned and employed for future application application.

SOFT-LYTHOGRAPHY: AN APPLICATION

Abstract

The hybrid nanocomposite material has shown to be suitable for micro/nanofabrication by soft lithography and different patterned structured containing the hybrid nanocrystals have been obtained.

We have exploited the possibility of using the organic-inorganic films containing the layered nano-crystals for micro fabrication; the possibility of patterning the films is, in fact, a key property for developing functional applications. A polydimethyl siloxane (PDMS) mold has been used as the master to produce different types of patterned structures on the hybrid film. This is an additional important property exhibited by this hybrid material.

4.5.1 Soft-Lithography

The patterning required in microfabrication is usually carried out with photolithography but this technique show some disadvantages[68] : the sizes it can produce are limited by optical diffraction, and the high-energy radiation required complex facilities and technologies, in addition is expansive and it cannot be easily applied to nonplanar surfaces; and it almost no control over the chemistry of patterned surface, especially when complex organic functional groups of the sorts needed in chemistry, biochemistry, and biology are involved. The soft-lithography[1,69], that they use patterned elastomer as the mask, stamp o mold, provide routes to high-quality patterns and structures with lateral dimensions of about 30 nm to 500nm in systems presenting problems in topology, materials, or molecular-level definition that cannot easily be solved by photolithography.

A combination of self-assembly and pattern transfer using elastomeric stamps, molds, or mask constitutes the basis of soft lithographic methods[2]. It complements photolithography in a number of aspects and provides a wide range of new opportunities for micro and nanofabrication.

An elastomeric stamp, mold or mask having relief structures on its surface is the key element of soft lithography[70,71,72].

It is usually prepared by replica molding by casting the liquid prepolymer of an elastomer against a master that as a patterned relief structure in its surface, in most of case is used as elastomer a poly(dimethylsiloxane) (PDMS)[73]. Several properties of PDMS are instrumental in the formation of high quality patterns and structures in soft lithography, (see the section about the soft-lithography)

Is reported in literature application of the soft lithography in many field from the optics to microbiology[74], that demonstrate way is important produce materials employable in this area of the microfabrication[75].

We have demonstrate that the hybrid films prepared by sol-gel method employed GPTMS and DEPES as precursors in basic condition can be used for the microfabrication and this open the route to develop new functional materials.

4.5.2 Film preparation

3-glycidoxypropyltrimethoxysilane (GPTMS, Aldrich 98%), sodium hydroxide (Carlo Erba pellets 98%) and diethoxydiphenylsilane (DEDPS, Aldrich 97%) were used as received without further purification. Three solutions indicated like standard sol , and sol 10% and sol 20%, were prepared by replacing on the standard solution with only GPTMS the 10% (sol A) and 20% (sol B) respectively of volume of GPTMS with the DEDPS. The precursor sol 10% was prepared by addition of GPTMS (9 cc) to a NaOH aqueous solution (4 cc, 1.85 M, pH14) under stirring and adding after few second DEDPS (1 cc). The precursor sol 20% was prepared by addition of GPTMS (8 cc) to a NaOH aqueous solution (4 cc, 1.85 M, pH14) under stirring and adding after few second DEDPS (2 cc). Immediately after the preparation the precursor sol was left in an open vessel at 25 ^{o}C and 40% RH for 45 min to allow the evaporation of methanol which is a by-product of the sol–gel reactions; after this time the sol container was sealed and the sol left under stirring for 12 h at 25 ^{o}C. At the end of this first preparation step the sol was aged for 8

days 25 °C; hybrid films were deposited by spin-coating on s glass or silicon substrates using a rotation speed of 5000 rpm for 20 s. The substrates were cleaned with water, acetone and EtOH. Fresh films were used for the microfabrication.

4.5.3 Mold preparation

A nano-imprinting mold of quartz (NTT-AT, NIM-PH350) was used as a master for fabricating polydimethyl siloxane PDMS molds. Thermally curable PDMS (Toray-Daw Corning, Silpot 184) was poured onto the master and cured at 100°C for an hour on a hot plate. After the solidification, the PDMS mold was removed from the master and used for the soft-lithography.

In the scheme 1 is showed the preparation method of the mold employed for the patterning of the hybrid films; each mastes can be used to fabricate more than 50 PDMS replicas. Representative range of values for h, d, and l, are 0.2-20, 0.5-200, and 0.5-200 μm.

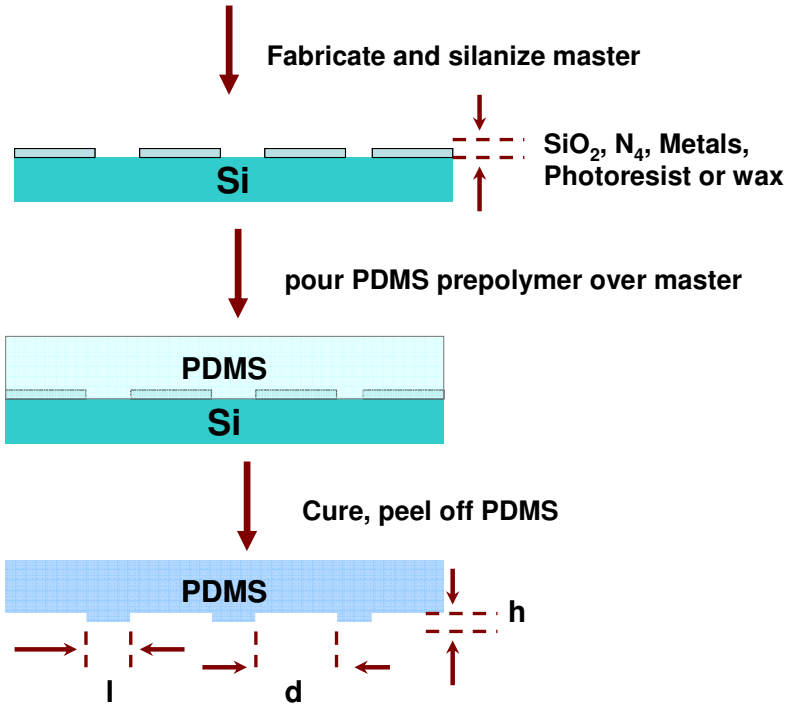

Scheme 4.5- Schematic procedure for casting PDMS replicas from a master having relief structures on its surface. Each master can be used to frabricate more than 50 PDMS replicas.

In the figure 4.32 is showed the appearance of the mold f good quality after cure at 100°C for 1 h on the hot plate.

Figure 4.32- Appearance of the PDMS mold after cure at 100°C for 1 h.

4.5.4 Patterning by soft-lithography

We have exploited the possibility of using the organic-inorganic films containing the layered nano-crystals for micro fabrication; the possibility of patterning the films is, in fact, a key property for developing functional applications. A polydimethyl siloxane (PDMS) mold has been used as the master to produce different types of patterned structures[76]. The microfabrication has been performed on freshly deposited hybrid films, they exhibited a good combination of properties to allow patterning trough molding. The films were enough viscous to be patterned but at the same time maintained the pattern after removal of the mold. This is an additional important property exhibited by this hybrid material.

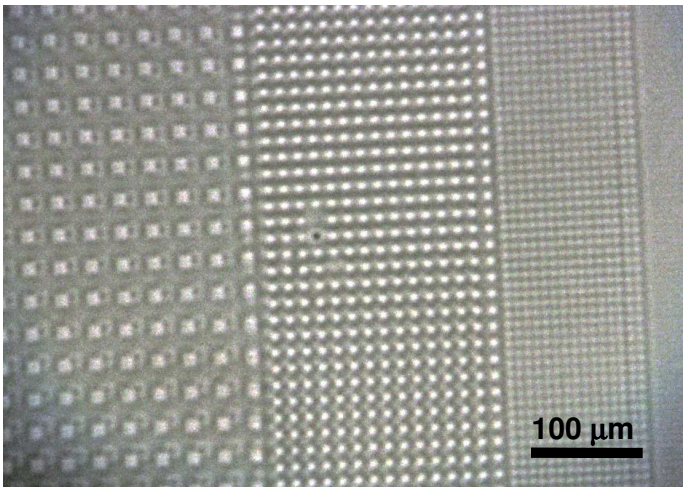

Figure 4.33- Optical microscope image of the patterned hybrid film containing the layered organosilica nanocrystals that has been micro-fabricated by soft-lithography.

The mold prepared as described was employed to produce patterning on the hybrid films depositede from the standard solution (only GPTMS in basic aqueous solution) and GPTMS with DEDPES. The presence of DEDPES affect the viscosity of the sol ad the results is a better film patterned. We have observed the pattern by a microscope. In the figure 2 is reported the image of a patterned film prepared with standard solution, square structures with excellent spatial resolution, as high as 350 nm, have been obtained. This type of fabrication technique should allow to produce anisotropic photonic structures by

controlling the optical axis direction of the nanocrystals in order to modulate the birefringence.

4.5.5 Conclusions

We have exploited the possibility of using the organic-inorganic films containing the layered nano-crystals for micro fabrication; the possibility of patterning the films is, in fact, a key property for developing functional applications. A polydimethyl siloxane (PDMS) mold has been used as the master to produce different types of patterned structures. A patterned film prepared with standard solution, square structures with excellent spatial resolution, as high as 350 nm, have been obtained.

This type of fabrication technique should allow to produce anisotropic photonic structures.

REFERENCE

1 M. Popall, J. Kappel, M. Pilz, J. Schulz and G. Feyder, *J. Sol-Gel Sci. Technol.*, 1994, **2**, 157; H. Schmidt, *J. Non-Cryst. Solids*, 1994, **178**, 302 ; Y. Sorek, R. Reisfeld and R.Tenne, *Chem. Phys. Lett.*, 1994, **227**, 235 .

2 R. Nass, E. Arpac, W. Glaubitt and H. Schmidt, *J. Non-Cryst. Solids*, 1990, **121**, 370; J.D. Watling and D. A. Lewis, *J. Sol-Gel Sci. Technol.*, 2003, **28**, 167.

3 G. Philipp and H. Schmidt, *J. Non-Cryst. Solids*, 1984, **63**, 283.

4 M. Popall and H. Durand, *Electrochim. Acta*, 1992, **37**, 1593.

5 P. Cardiano, S. Sergi, M. Lazzari and P. Piratino, *Polymer*, 2002, **43**, 6635 .

6 P. Innocenzi, A. Martucci, M. Guglielmi, L. Armelao, G. Battaglin, S. Pelli and G. C. Righini, *J.Non-Cryst. Solids*, 1999, **259**, 182 ; G. Brusatin, M. Guglielmi, P. Innocenzi, A. Martucci,G. Battaglin, S. Pelli and G. Righini, *J. Non-Cryst. Solids*, 1997, **220**, 202 .

7 P. Innocenzi, G. Brusatin, M. Guglielmi, R. Signorini, M. Meneghetti, R. Bozio, M. Maggini, G.Scorrano and M. Prato, *J. Sol-Gel Sci. Technol.*, 2000, **19**, 263 ; P. Innocenzi, G. Brusatin,M. Guglielmi, R. Signorini, R. Bozio and M. Maggini, *J. Non-Cryst. Solids*, 2000, **265**, 68; R. Signorini, M. Meneghetti, R. Bozio, M. Maggini, G. Scorrano, M. Prato, G. Brusatin, P. Innocenzi and M. Guglielmi, *Carbon*, 2000, **38**, 1653 .

8 P. Innocenzi, E. Miorin, G. Brusatin, A. Abbotto, L. Beverina, G. A. Pagani, M. Casalboni, F.Sarcinelli and M. Pizzoferrato, *Chem. Mater.*, 2002, **14**, 3758 ; G. Brusatin, A. Abbotto, L.Beverina, G. A. Pagani, M. Casalboni, F. Sarcinelli and P. Innocenzi, *Adv. Funct. Mater.*, 2004,**14**, 1160; G. Brusatin, P. Innocenzi, L. Beverina, G. A. Pagani, A. Abbotto, F. Sarcinelli and M. Casalboni, *J. Non-Cryst. Solids*, 2004, **345–346**, 575.

9 J.A.A. Sales and C. Airoldi, *J. Non-Cryst. Solids*, 2003, **330**, 142 ; J.A.A. Sales, A.G.S. Prado and C. Airoldi, *J. Therm. Anal. Calorim.*, 2002, **70**, 135.

10 Innocenzi, P. & Lebeau, B., Organic–inorganic hybrid materials for non-linear optics. J. Mater. Chem., 2005, 15, 3821-3831.

11 Sanchez, C., Julian, B., Belleville, P. & Popall, M., Applications of hybrid organic–inorganic nanocomposites. J. Mater. Chem., 2005, 15, 3559- 3592.

12 Innocenzi, P., Brusatin, G., Guglielmi, M., Signorini, R., Bozio, R., Maggini, M., 3-(glycidoxypropyl)-trimethoxysilane-TiO2 Hybrid Organic-Inorganic Materials for Optical Limiting. J. Non-Cryst. Solids 2000, 265, 68-73.
13 Innocenzi, P., Brusatin, G., Guglielmi, M., Signorini, Meneghetti, M., Bozio, R., Maggini, M., Scorrano, G. & Prato, M., Optical limiting devices based on C60 derivatives in sol-gel hybrid organic-inorganic materials. M. J. Sol-Gel Sci. Technol. 2000, 19, 263-267.
14 Lerouge, F., Cerveau, G., & Corriu, R.J.P., Supramolecular self-organization in non-crystalline hybrid organic–inorganic nanomaterials induced by van der Waals interactions. New J. Chem. 2006, 30, 1364-1376.
15 Fujita, S. & Inagaki, S., Self-Organization of Organosilica Solids with Molecular-Scale and Mesoscale Periodicities. Chem. Mater. 2008, 20, 891-908.
16 Arrachart, G., Carcel, C., Moreau, J. J. E., Hartmeyer, G., Alonso, B., Massiot, D., Creff, G., Bantignies, J.-L., Dieudonne, P., Wong Chi Man, M., Althoff, G., Babonneau, F., Bonhomme, C., J. Mater. Chem. 2008, 18, 392
17 Moreau, J.J.E., Vellutini, L., Wong Chi Man, M. & Bied, C. New Hybrid Organic−Inorganic Solids with Helical Morphology via H-Bond Mediated Sol−Gel Hydrolysis of Silyl Derivatives of Chiral (*R*,*R*)- or (*S*,*S*)-Diureidocyclohexane. J. Am. Chem. Soc. 2001, 123, 1509-1510.
18 Ogawa, M. & Kuroda, K., Photofunctions of Intercalation Compounds. Chem. Rev. 1995, 95, 399–438.
19 Boury, B., Corriu, R.J.P., Le Strat, V., Delord, P. & Nobili, M., Nanostructured Silica-Based Organic-Inorganic Hybrid Materials - Evidence for Self-Organization of a Xerogel Prepared by Sol-Gel Polymerization. Angew. Chem. Int. Ed. 1999, 38, 3172-3175.
20 Moreau, J.J.E., Pichon, B.P., Wong Chi Man, M., Bied, C., Prizkow, H. J.-Bantignies, L., Dieudonne, P. & Sauvajol, J.-L., A Better Understanding of the Self-Structuration of Bridged Silsesquioxanes. Angew. Chem. Int. Ed., 2004, 43,

203-206.
21 Okamoto, K., Kapoor, M.P. & Inagaki, S., Organosilicate–surfactant lamellar mesophase with molecular-scale periodicity in the silicate layers. Chem. Comm. 2005, 1423-1425.
22 Moreau, J.J.E., Pichon, B.P., Arrachart, G., Wong Chi Man, M. & Bied, C. Nanostructuring organo-silicas: combination of intermolecular interactions and molecular recognition properties to generate self-assembled hybrids with phenylene or adenine thymine bridging units. New J. Chem. 2005, 29, 653.
23 Takahashi, M., Figus, C., Kichob, T., Enzo, S., Casul,a M., Valentini, M. & Innocenzi, P., Self-Organized Nanocrystallyne Organosilicates in Organic-Inorganic Hybrid Films. Adv. Mater. 2009, 21, 1-5.

24 Innocenzi, P., Brusatin, G., Guglielmi M. & Bertani, R., A new synthetic route to 3-(glycidoxypropyl)-trimethoxysilane based hybrid organic-inorganic materials. Chem. Mater., 1999, 11, 1672-1680.
Innocenzi, P., Esposto, M. & Maddalena, A., Mechanical properties of 3-glycidoxypropyltrimethoxysilane based hybrid organic-inorganic materials. J. Sol-Gel Sci. & Technol., 2001, 20, 293-299.
[25] Alonso, B., Massiot, D., Babonneau, F., Brusatin, G., Della Giustina, G., Kidchob, T. & Innocenzi, P., Structural Control in Germania Hybrid Organic-Inorganic Materials. Chem. Mater. 2005, 17, 3172-3180.
26 Hou, X., Kirkpatrick, R.J., Struble L. J.& Monteiro, P. J. M. Structural Investigations of Alkali Silicate Gels. J. Am. Ceram. Soc., 88 (2005) 943-949.
[27] Alonso, B., Massiot, D., Valentini, M., Kidchob, T. & Innocenzi, P., Design of hybrid organic-inorganic materials through their structure control: the case of epoxy bearing alkoxides. J. Non-Crystal. Solids, 2008, 354, 1615-1626.
Brusatin, G., Innocenzi, P., Guglielmi, M. & Babonneau, F., Basic catalysed synthesis of hybrid sol-gel materials based on 3-glycidoxypropyltrimethoxysilane. J. Sol-Gel Sci. Technol, 2003, 26, 303–306,

28 B. Menaa, M. Takahashi, P. Innocenzi and T. Yoko, *Chem. Mater.*, 2007, **19**, 1946.

29 G. Brusatin, G. Della Giustina, M. Guglielmi and P. Innocenzi, *Prog. Solid State Chem.*, 2006, **34**,223.

30 R. Kasemann, S. Bruck and H. Schmidt, *Proc. SPIE–Int. Soc. Opt. Eng.*, 1994, **2288**, 321.

31 B. Riegel, S. Blittersdorf, W. Kiefer, S. Hofacker, M. Muller and G. Schottner, *J. Non-Cryst. Solids*, 1998, **226**, 76.

32 P.Innocenzi, G.Brusatin, F. Babonneau, *Chem. Mater.* 2000, 12, 3726; P.Innocenzi, G.Brusatin, M. Guglielmi, R. Bertani, *Chem. Mater.* 1999, 11, 1672.

33 Alonso, D. Massiot, F. Babonneau, G. Brusatin, G. Della Giustina, T. Kidchob and P.Innocenzi, *Chem. Mater.*, 2005, **17**, 3172

34 P. Innocenzi, M. Esposto and A. Maddalena, *J. Sol-Gel Sci. Technol.*, 2001, **20**, 293B

35 K.H Nam · T.H Lee, B. Bae, M. Popall *J Sol-Gel Sci Techn.* ,2006, *39*:255.

36 M. Templin, U. Wiesner and W. H. Spiess, *Adv. Mater.*, 1997, **9**, 814.

37 D. Hoebbel, M. Nacken, H. Schmidt, *J.Sol Gel Sci. Technol.*, 1998, 12, 169

38 F. Brown, L.H. Vogt and P. I. Prescott, *J. Am. Chem. Soc.*, 1964, **86**, 1120 .

39 A. Strachota, P. Whelan, J. Kr z, J. Brus, M. Urbanova, M. S. Louf and L. Matejka, *Polymer*,2007, **48**, 3041.

40 L. Matejka, O. Dukh, J. Brus Jr, W.J. Simonsick and B. Meissner, *J. Non-Cryst. Solids*, 2000, **270**, 34.

41 J.V. Crivello and R. Malik, *J. Polym. Sci., Part A: Polym. Chem.*, 1997, 35, 407 ; A.Tsuchida, C. Bolln, F. G. Sernetz, H. Frey and R. Mulhaupt, *Macromolecules*, 1997, 30, 2818; M.C. Gravel and R. M. Laine, *Polym. Prepr.*, 1997, 38, 155 .

42 F. J. Feher, D. Soulivong and A. E. Eklund, *Chem. Commun.*, 1998, 399 ; F. J. Feher, D.Soulivong and F. Nguyen, *Chem. Commun.*, 1998, 1279; F. J. Feher, F. Nguyen, D.Soulivong and J. W. Ziller, *Chem. Commun.*, 1999, 1705; F. J. Feher, R. Terroba and J.W. Ziller, *Chem. Commun.*, 1999, 2309.

43 B. Alonso, D. Massiot, M. Valentini, T. Kidchob and P. Innocenzi, *J. Non-Cryst. Solids*, 2008, **354**, 1615.

44 S. R. Davis, A. R. Brough and A. Atkinson, *J. Non-Cryst. Solids*, 2003, **315**, 197

45 P. Innocenzi, A. Sassi, G. Brusatin, M. Guglielmi, D. Favretto, R. Bertani, A. Venzo and F.Babonneau, *Chem. Mater.*, 2001, **13**, 3635

46 G. Schottner, *Chem. Mater.*, 2001, **13**, 3422 .

47 ^{1}H NMR data of the precursor alkoxide and solvents are available at the SDBS data base:http://www.aist.go.jp/RIODB/SDBS/.

48 a) B.; Alonso, D.; Massiot, M.; Valentini, T.; Kidchob, P.Innocenzi, *J.Non-Cryst Solids*, **2008**, 354,1615. b) B. Alonso, D. Massiot, F.Babonneau, G. Brusatin, G. Della Giustina, T. Kidchob, P. Innocenzi, *Chem. Mater.* **2005**, *17,* 3172.

49 P. Innocenzi, *J. Non-Cryst. Solids* **2003**, *316*, 309.

50 I. Noda, Y. Ozaki, *Two-Dimensional Correlation Spectroscopy Applications I Vibrational and Optical Spectroscopy*, Wiley, New York, 2004.

51 a) H.B. Park,J. K. Kim, S.Y. Nam, Y. M. Lee, *J. Membr. Sci.* **2003**, *220*, 59. b) H.Han, C.C. Gryte, *Polymer,* **1995,** *63*, 1663. c) C. Joly, M. Smaihi, L. Porcar, \ and R. D. Noble, *Chem. Mater.* **1999**, *11*, 2331

52 X. Hou, R.J. Kirkpatrick, L.J. Struble, P.J.M. Monteiro, *J. Am. Ceram. Soc.*, **2005**, *88*, 943.

53 P. Innocenzi, G. Brusatin, M. Guglielmi, R. Bertani, *Chem. Mater.* **1999**, *11*, 1672.

54 P. Innocenzi, G. Brusatin, F. Babonneau, *Chem. Mater.* **2000**, *12*, 3726.

55 P. Innocenzi, A. Sassi, G. Brusatin, M. Guglielmi, D. Favretto, R. Bertani, A. Venzo F. Babonneau, *Chem. Mater.* **2001**, *13*, 3635.

56 P. Innocenzi, G. Brusatin, S. Liccocia, M.L. DiVona, F. Babonneau, B. Alonso, *Chem. Mater.* **2003**, *15*, 4790.

57 P. Innocenzi, *J. Non-Cryst. Solids* 2003,316, 309.

58 a) H.B. Park,J. K. Kim, S.Y. Nam, Y. M. Lee, *J. Membr. Sci.* **2003**, *220*, 59. b) H.Han, C.C. Gryte, *Polymer,* **1995,** *63*, 1663. c) C. Joly, M. Smaihi, L. Porcar, and R. D. Noble, *Chem. Mater.* **1999**, *11*, 2331

59 J.J. Moreau, L. Vellutini, M.W.Chi Man, C. Bied, *J. Am. Chem. Soc*. 2001,123,1509.

60 F. Lerouge, G. Cerveau, R.P.J. Corriu, *J. Mater. Chem.* **2006**, *16*, 90.

61 Takahashi, M., Figus, C., Kichob, T., Enzo, S., Casul,a M., Valentini, M. & Innocenzi, P., Self-Organized Nanocrystallyne Organosilicates in Organic-Inorganic Hybrid Films. Adv. Mater. 2009, 21, 1-5.

62 Brusatin, G., Innocenzi, P., Guglielmi, M. & Babonneau, F., Basic catalysed synthesis of hybrid sol-gel materials based on 3-glycidoxypropyltrimethoxysilane. J. Sol-Gel Sci. Technol, 2003, 26, 303–306,

63 Sapic, I. M., Bistricic, L.. Volovseka, V., Dananica, V., Furi, K., DFT study of molecular structure and vibrations of 3-glycidoxypropyltrimethoxysilane. Spectrochim. Acta Part A, 2009, 72, 833–840

64 Innocenzi, P., Infrared spectroscopy of silica sol-gel films: a spectramicrostructure overview. J. Non-Cryst. Solids, 2003, 316, 309-320.

65 Riegel, B., Kiefer, W., Hofacker, S. & Schottner, G. J., FT-Raman Spectroscopic Investigations on the Organic Crosslinking in Hybrid Polymers Part II: Reactions of Epoxy Silanes. Sol-Gel Sci. Technol., 2002, 24, 139-145;

66 Riegel, B., Blittersdorf, S., Kiefer, W., Hofacker, S., Müller, M., & Schottner, G. G., Kinetic investigations of hydrolysis and condensation of the Glycidoxypropyltrimethoxysilane aminopropyltriethoxy-silane system by means of FT-Raman spectroscopy I. J. Non-Cryst. Solids, 1998, 226, 76-84

67 Hou, X., Kirkpatrick, R.J., Struble L. J.& Monteiro, P. J. M. Structural Investigations of Alkali Silicate Gels. J. Am. Ceram. Soc., 88 (2005) 943-949.

68 Y. Xia, G. M. Whitesides, *Angew. Chem. Int.Ed.***1998,** *37*,550-575.

2 X.M, Zhao, Y. Xia, G. M. Whitesides, *J.Mater. Chem.***1997**, 7, 1069-1074.

70 A. Kumar, G. M. Whitesides, *Appli. Phys. Lett.* **1993,** 63, 2002-2004.

71 X.M, Zhao, Y. Xia, G. M. Whitesides, *Adv. Mater*. **1996**.8, 837-840.

72 E.Kim, Y. Xia, G. M. Whitesides, *Nature*, **1995**, 376, 581-584.

73 J.F. Kunzler, *Trends Polym. Sci.* **1996**, 4, 52-59.

74 D.B. Weibel, W. R. Diluzio and G. M. Whitesides, *NATURE REVIEWS*, **2007**, *5,* 209.

75 E.S. Kang, M.Takahashi, Y. Tokuda, T. Yoko, *J. Mater. Res.* **2006**, *21*, 2186.

CONCLUSIONS

Hybrid organic-inorganic films, as amorphous films or with hybrid nanocrystals, have been successfully prepared and opportunely studied for future applications.

The organic-inorganic hybrid materials was prepared through the sol-gel process of an organically modified alcoxide bearing with an functional group (epoxy group) using NaOH as catalyst.

The reaction process of the 3-glycidoxypropyltrimethoxysilane and the self-organization on nanocrystals of these system was studied using XRD, FTIR, NMR, Raman and UV-Vis spectroscopies; the formation of the nanocrystals through TEM observation. The wettability of the surface of hybrid films was studied by contact angle measurements and information about the optical anisotropy of the films was obtained by refractive index measurements.

From fresh and aged sol films by spin and dip-coating were deposited on different substrate (glass, silicon, silica) and organic-inorganic hybrid transparent films were obtained.

The formation of silica species in the sol during the aging and the organic products was studied by NMR spectroscopy. NMR spectroscopy shows condensation reactions that are kinetically controlled. The reaction of alkoxy in GPTMS forms preferentially open cages structures and the silica condensation does not go to completion even after long times of aging even if a high condensation degree, up to 90%, is observed after two days. On the other hand formation of siloxane bonds affects the epoxy opening kinetics, which is much slower in comparison with the silica condensation. The opening reactions of epoxies form different chemical species: diols, dioxane rings by reaction of opened epoxies, formation of terminal methyl ether species by reaction of an open epoxy with methanol and finally polyaddition reactions form polyether chains of short length. The slow formation of this chemical species gives linear compounds that have been observed to generate hybrid layered crystals through self-organization.

XRD diffraction which show after 5-days aging, a new peak observed at 9.61° (d = 0.923 nm) the diffraction angle of the peak does not show any dependence on sol aging. This

peak, is the signature of the formation of a long-range ordered lamellar structure. The formation of organic-inorganic nano-crystals of around 103 nm within the hybrid film has been confirmed from a direct observation by TEM. The amorphous hybrid film showed isotropic optical property whilst the hybrid film with nano crystals exhibited an optical anisotropy, $\Delta n = 1.88\times10^{-3}$, due to the orientation of the plate shaped crystallites.

We have studied the effect of different parameter (aging and temperature) on the reaction of GPTMS and on the formation of the hybrid nanocrystals. From these studies we have observed that exist a critical threshold of epoxy opening and silica condensation that allows self-organization into hybrid crystals in the films.

Besides the added of other species like DEDPES affect the inorganic condensation and the epoxy opening reaction, besides increase the hydrophobic character of the surface and this character can be tuned and employed for future application.

Finally we have exploited the possibility of using the organic-inorganic films containing the layered nano-crystals for micro fabrication. A polydimethyl siloxane (PDMS) mold has been used as the master to produce different types of patterned structures. This type of fabrication technique should allow to produce anisotropic photonic structures.

In conclusion, layered organosilicate nano-crystalline have been produced, for the first time to our knowledge, in hybrid organic inorganic films through a self-organization process. The organosilicate nano-crystals formation is kinetically controlled the different condensation kinetics of silica backbone and organic polymerization trigger the process. Controlling the complex reactions of 3-glycidoxypropyltrimethoxysilane allow to obtain advanced hybrid materials with engineered structures, such as self-organized hybrid crystals.

The simple and facile preparation method that we have reported in the present work allows obtaining organosilicate layered nano-structures in curable epoxy-silica hybrid films. This approach is opening the route to new applications in electronics, photonics, and bio-chemistry in combination with micro/nanolithography technique.